Robust time spectral methods for solving fractional differential equations in finance

by

Claude Rodrigue, Bambe Moutsinga

Submitted in partial fulfillment of the requirements

for the degree Philosophiae Doctor

Department of Mathematics and Applied Mathematics

Faculty of Natural and Agricultural Sciences

University of Pretoria

Supervisor: Pr. Eben Maré

Co-Supervisor: Dr. Edson Pindza

February 26, 2021

Abstract

In this work, we construct numerical methods to solve a wide range of problems in finance. This includes the valuation under affine jump diffusion processes, chaotic and hyperchaotic systems, and pricing fractional cryptocurrency models. These problems are of extreme importance in the area of finance. With today's rapid economic growth one has to get a reliable method to solve chaotic problems which are found in economic systems while allowing synchronization. Moreover, the internet of things is changing the appearance of money. In the last decade, a new form of financial assets known as cryptocurrencies or cryptoassets have emerged. These assets rely on a decentralized distributed ledger called the blockchain where transactions are settled in real time. Their transparency and simplicity have attracted the main stream economy players, i.e, banks, financial institutions and governments to name these only. Therefore it is very important to propose new mathematical models that help to understand their dynamics. In this thesis we propose a model based on fractional differential equations.

Modeling these problems in most cases leads to solving systems of nonlinear ordinary or fractional differential equations. These equations are known for their stiffness, i.e., very sensitive to initial conditions generating chaos and of multiple fractional order. For these reason we design numerical methods involving Chebyshev polynomials. The work is done from the frequency space rather than the physical space as most spectral methods do.

The method is tested for valuing assets under jump diffusion processes, chaotic and hyperchaotic finance systems, and also adapted for asset price valuation under fraction Cryptocurrency. In all cases the methods prove to be very accurate, reliable

and practically easy for the financial manager.

Declaration

I, the undersigned, declare that this thesis, which is submitted for the degree Philosophiae Doctor at the University of Pretoria, is my own independent research. This work has not been submitted, in whole or in part, at any other university.

Signature:

Name: Claude Rodrigue Bambe Moutsinga

Acknowledgement

First and foremost, I would like to acknowledge the Lord Jesus Christ for his mercy and favour upon me through my journey of my PhD studies. Let me express my gratitude to the University of Pretoria for allowing me the opportunity to pursue my studies with them. I also thank Dr Edson Pindza for his expertise and guidance availablility, specially for his great patience and understanding. What a wonderful supervisor! I am also grateful to Prof Maré for his directions and leardership. Always ready to find solutions. A word of gratitude goes to my colleagues Dr Chin, Dr Adem, Dr Tesfalem, Dr Aphane, Prof Gopalraj, Mrs Deepa V, Dr Tabane , for their support. A word of gratitude also to my pastor S.O. Orefuwa, Pastor G.O. Mbazaboua and all my church fellow brothers and sisters in Christ for their prayers. To my wife Prisca, my children Greg, Guillian, Josias, thank you so much for your patience with me, when I spent long hours at work as though I had deserted you. A special thank you to my brother Dr C. Achille Mbickou Moutsingue for always believing in me, and his ongoing encouragements.

Dedication

This thesis is dedicated to my family for their continuous emotional support.

Contents

List of Tables

List of Figures

List of Symbols

Γ	Gamma function
$B(z, w)$	Beta function
E_α	One-parameter Mittag-Leffler function.
$E_{\alpha,\beta}(z)$	Two-parameter Mittag-Leffler function
J^α	Fractional integral operator of order α
${}_a^{RL}D_t^q f(t)$	Riemann-Liouville fractional derivative of order q of $f(t)$
${}_a^{C}D_t^q f(t)$	Caputo fractional derivative of order q of $f(t)$
${}_a^{ABR}D_t^q f(t)$	Atangana-Baleanu fractional derivative Riemann-Liouville sense of order q of $f(t)$
${}_a^{ABC}D_t^q f(t)$	Atangana-Baleanu fractional derivative Caputo sense of order q of $f(t)$
${}_a^{ABR}I_t^q f(t)$	Atangana-Baleanu fractional integral Riemann-Liouville sense of order q of $f(t)$
$\mathcal{L}$	Laplace transform operator
$T_k(x)$	Chebyshev polynomial of order k
$\mathbf{\Lambda}$	Chebyshev matrix transform representation.
$\mathbf{A^{(i)}}$	Matrix representation of differential operator over the interval $[t_i, t_{i+1}]$

$\mathcal{P}_{M_n}$	Set of polynomials of order at most M_n
(J_{nm})	Integration matrix operator.
W_t	Wiener process
Z_t	Jump process
S_t	Stock price process
X_t	State process
μ_t	Drift process
σ_t	Volatility process
λ_t	Jump arrival rate
r_t	Interest rate process
V_t	Variance process
$\Psi(t, X_t)$	Payoff process
$\mathcal{A}$	General differential operation

List of Publications

Part of this thesis has been submitted in the form of the following research papers submitted to international journals for publications.

1. Claude Rodrigue Bambe Moutsinga, Edson Pindza, and Eben Maré. Homotopy perturbation transform method for pricing under pure diffusion models with affine coefficients. *Journal of King Saud University-Science*, 30(1): 1-13, 2018.

2. Claude Rodrigue Bambe Moutsinga, Edson Pindza, and Eben Maré. A time multidomain spectral method for valuing affine stochastic volatility and jump diffusion models. *Communications in Nonlinear Science and Numerical Simulation*, 84: 105-159, 2020.

3. Claude Rodrigue Bambe Moutsinga, Edson Pindza, and Eben Maré. A robust spectral integral method for solving chaotic finance systems. *Alexandria Engineering Journal*, 59(2): 601-611, 2020.

4. Claude Rodrigue Bambe Moutsinga, Edson Pindza, and Eben Maré, Comparative performance of time spectral methods for solving hyperchaotic finance system, submitted for publication.

5. Claude Rodrigue Bambe Moutsinga, Edson Pindza, and Eben Maré, Fractional spectral integral methods for valuing cryptocurrency asset flow fractional differential equations., submitted for publication.

Part I

Introduction and Background Materials

Chapter 1

General Introduction

The innovation brought by the digital world has affected the financial sector, bringing along new concepts such as digital money or cryptocurrencies [65]. This new ecosystem comes with its challenges when it comes to pricing of assets. Adding the fact that processes in this new environment do not loose memories, this suggests the use of fractional derivatives in the modelling. In this context asset pricing problems gets more complicated and trying to find an analytical solution would be an obsolete task. Thus the need for reliable numerical methods for solving such problems is of great importance.

As most problems arising finance center around ODEs and PDEs, various numerical methods have been introduced. They range from classical finite difference methods (FDM), finite element method (FEM) to spectral methods. In FDM the idea to approximate the solution function by local polynomials of lower order resulting from the Taylor expansion. Actually, one simply replaces the derivatives with finite-difference expressions and demands that the resulting algebraic equations be satisfied exactly at the grid points. Thus finite-difference formulations can be interpreted as collocation methods without a trial solution [34]. However, difficulties arise in imposing boundary conditions, and low-order finite-difference formulations are often inaccurate, particularly on coarse grids.

Spectral methods on the other hand offer the route of approximating the solution

globally by high order polynomials. Because of being extremely accurate, spectral methods have been intensively studied in the past decades. Depending on trial functions, we can have Fourier spectral method, or Legendre type of Chebyshev type and many more. While Fourier types cater for periodic boundary conditions problems the Chebyshev tends to suit for non-periodic boundary conditions. In this last case the solution is approximated by a finite series of Chebyshev polynomials. However, the questions is how to get the coefficients of the series.

Two main approaches are commonly used. The Chebyshev spectral methods could be implemented as spectral collocation (or pseudospectral) methods, where the work is carried in the physical space of the values at a specific grid or as Galerkin and tau methods, where the work is done in the spectral space of the coefficients.

One main disadvantage of working in the physical space in order to find coefficients is that the matrices resulting in the discretization process have an increased condition number, and thus computational rounding errors deteriorate the expected theoretical exponential accuracy. Moreover, the discretization matrices are in general fully populated, making efficient algebraic solvers hard to apply. These disadvantages are more obvious when solving from fourth order problems onwards, where stability and numerical accuracy are lost when applying higher order approximations. Several attempts were made in order to try to circumvent these inconveniences of this approach but most of them are based on the fairly large flexibility in the choice of trial and test functions in order to reduce the condition number and the bandwidth of the matrices. For more on this approach the reader is referred to Boyd [14], Dongarra et al. [26], Driscoll [27], Hiegemann [48], Trefethen [93], Weideman and Reddy [101] to mention a few.
Working in the space of coefficients on the other hand takes advantage of the spectral properties of Chebyshev polynomials resulting in avoiding full matrices and allowing one to land with spares triangular of band matrices. A tremendous gain in computation is therefore achieved, see Bhrawy and Alofi [9], Gheorghiu [38], Trif [94, 95] and some more.

In this thesis, we propose some robust numerical methods for solving fractional

financial systems following this last approach mentioned previously and we extend it to large time scale problems by using multiple domain and also to higher dimension. In order to carry out our numerical experiments we used exclusively the software system MATLAB.

For our study methodology we begin with presenting first some terminologies together with some basic mathematical tools necessary for our study research. These include a quick review of fractional calculus, an introduction to Chebyshev polynomials and the design of the spectral methods based on Chebyshev polynomials. In the second part, we implement the methods to various types problems in finance. Here we mention the valuation of asset price under affine jump diffusion process, chaotic and hyperchaotic finance systems, and an extension to problems involving fractional derivatives in finance.

More precisely, the rest of thesis is organised as follows: In Chapter 2 we present fractional derivatives. Here some key basic functions related to theory are displayed together with the constructions of various fractional derivatives. The Grünwald-Letnikov construction is reviewed. The Riemann-Liouville fractional and the Caputo fractional derivatives and integrals are also presented. In addition to these approaches, a more recent approach that removes singularities is presented: The Atangana-Baleanu fractional derivative and integral. Important properties and convergence in all these approaches are discussed in this chapter.

In chapter 3 a brief introduction to spectral method using Chebyshev polynomials is presented. In this context, concepts of approximation, convergence, numerical differentiation and integration are reviewed. We also introduce a multiple step spectral method. Here the time domain is divided into subdomains and the spectral method is run over each subdomains. The convergence of this multiple spectral method is also studied.

Having laid the foundation, we can now go on part II where we implement the spectral method for various problems encountered in finance.

In chapter 4 we design and implement a time multidomain spectral method for

valuing affine stochastic volatility and jump diffusion models. The method is based on a matrix operatorial a approach using Chebyshev numerical differentiation in the frequency space. The method is also coupled with domain multiple steps to cater for large scale time domain. Convergence is investigated and a comparison with existing spectral method is performed. This work was published in *Communications in Nonlinear Science and Numerical Simulation* under the same title.

In chapter 5 we present a robust spectral integral method for solving chaotic finance system and synchronization. The method is based on Chebyshev numerical integration applied in the frequency domain. The multiple step is applied on the time domain, convergence is studied and we carry out extensive comparisons with other results obtained by using some existing methods found in literature. This work was published in *Alexandria Engineering Journal* under the same title.

In chapter 6 we provide a Comparative performance of time spectral methods for solving hyperchaotic finance system. Here, both spectral methods using differentiation matrix and integration matrix together with a multiple steps, are implemented on a higher dimensional case: the hyperchaotic finance system. Convergence and stability are investigated.

In chapter 7 we deal with more challenging problems involving cryptocurrency valuation in a fractional context. For such we propose a fractional spectral integral methods for valuing cryptocurrency asset flow fractional differential equations. The spectral integral method previously designed in chapter 5 is revisited and extended to the fractional case. Then we present numerical results to investigate the performance of our method together with other existing results from other methods.

Finally the last chapter 8 is devoted to concluding remarks and scope for future research.

Chapter 2

Literature review on fractional calculus

2.1 History of fractional calculus

Fractional calculus is a generalization of classical calculus, to a non-integer order. If this order is negative, the fractional derivative becomes a non-integer integration and if it is positive it is a non-integral differentiation. Fractional calculus provides several potentially useful tools for solving integral equations. It also comes naturally in the mechanical modeling of materials which preserve the memory of past transformations (see [55]). Hence the particular interest in calculus and fractional analysis have taken place in recent decades.

Although classical calculus provides powerful tools for the modeling of a good number of phenomena studied in applied sciences, these tools do not take into account of the abnormal dynamics that present certain complex systems encountered in real life or in the interactions of society. Experimental results show that several processes related to complex systems have a non-local dynamic that involves long-term effects. Fractional derivatives and integral operators have some similarities with some of these characteristics, which makes it a more suitable tool for modeling these phenomena.

The history of fractional order calculus goes back of the end of the 17th century [82]. specialists agree to trace its beginning to the last quarter of the year 1695 when LâĂŹHospital raised a question to Leibniz by asking the meaning of $\frac{d^n y}{dx^n}$ when $n = \frac{1}{2}$. Leibniz, in his response, wanted to initiate a reflection on a possible theory of non-integer derivative, and wrote to LâĂŹHospital: "... this would lead to a paradox from which, one day, we will have drawn useful conclusions." We had to wait for the years 1990 to see the first "useful consequences" appear.

A first acceptable attempt to that opened question was produced by Lacroix in 1819 [58, 60] who gave an answer claiming that $\frac{d^{\frac{1}{2}}x}{dx^{\frac{1}{2}}} = 2\sqrt{\frac{x}{\pi}}$ in his 700 pages long book on Calculus published in 1819. He developed a more generalized result from a case of integer order starting with

$$\frac{d^n y}{dx^n} = \frac{m!}{(m-n)!}x^{m-n}, \qquad m \geq n. \tag{2.1.1}$$

substituting the factorial by the Gamma function which we will defined later he gets

$$\frac{d^n y}{dx^n} = \frac{\Gamma(m+1)}{\Gamma(m-n+1)}x^{m-n}. \tag{2.1.2}$$

He gives the particular case of $y = x$ and $n = \frac{1}{2}$

$$\frac{d^{1/2}x}{dx^{1/2}} = \frac{\Gamma(2)}{\Gamma(3/2)}x^{1/2}2\sqrt{\frac{x}{\pi}} \tag{2.1.3}$$

Unfortunately up to that time, no possible application were given until Abel in 1823 that gave a first application of this non-integer order derivative in "tautochrome problem", [2]. Abel proposed that the solution of this problem could be obtained via an integral transform:

$$K = \int_0^x (x-t)^{-1/2} f(t)dt, \qquad K = cst. \tag{2.1.4}$$

The above integral is replaced by the fractional derivative of order $-1/2$ and becomes

$$K = \sqrt{\pi}\frac{d^{-1/2}}{dx^{-1/2}}\left[f(t)\right] \tag{2.1.5}$$

and by taking fractional derivative of order $1/2$ both side of the equation yields

$$\frac{d^{1/2}}{dx^{1/2}}K = \sqrt{\pi}f(x) \tag{2.1.6}$$

Remembering that fractional derivative of a constant is not always equal zero, unless if by chance the constant of integration is null.

It is few decades later that a first logical definition for the fractional derivative is given by Liouville who published nine documents on this subject between 1832 and 1837 on the monomial $x^{-a}, a > 0$.

$$D_L^q x^{-a} = (-1)^q \frac{\Gamma(q+a)}{\Gamma(a)} x^{-a-q}, a > 0. \tag{2.1.7}$$

Other interesting work was produced by Joseph Fourier but mostly Riemann proposed an approach which proved to be essentially that of Liouville, and it is since that she carries the no "Approach de Riemann-Liouville ". Later, other theories emerged like that of Grunwald-Leitnikov, Weyl and Caputo. AT that time there were hardly any practical applications of this theory, and it is for this reason that it was considered an abstract topic.

With the first conference organized B. Ross at the University of New Haven in June 1974 under the title "Fractional Calculus and Its Applications" and for the first study attributed to Oldham and Spanier [69] who published a book in 1974 after a joint collaboration, started in 1968 and devoted to the presentation of the methods and applications of calculus, fractional calculus started gaining momentum physics and engineering. Since then, fractional calculus has gained popularity and important consideration mainly due to the many applications in various fields of applied science and engineering where it has been noticed that the behavior of a large number of

physical systems can be described using the fractional order derivative which provides an excellent instrument for the description of several

Today various fractional operators along with significant properties have been studied by several mathematicians and scientists. Due to distinct kernel representations in distinct function spaces they generate diversity of definitions for fractional derivatives. These include Riemann-Liouville fractional derivative, Caputo fractional derivative, Caputo-Erdelyi-Kober fractional derivative, Caputo-Hadamard fractional derivative, and Caputo-Fabrizio fractional derivatives [18], to mention just a few. These derivatives actually reveal some few complications in applications; for instance, the Laplace transform of Riemann-Liouville derivative consists of terms without physical signification and its constant is not zero. These difficulties were eradicated by Caputo fractional derivative but they involve singular kernel. In order to avoid singularities, Caputo and Fabrizio have presented new fractional derivative, namely, Caputo-Fabrizio fractional derivatives based on exponential kernel [79]. Lately Atangana and Baleanu [5] proposed another operator that also removes any singularity by simply introducing the Mittag-Leffler function in the kernel.

Before we get into the fractional calculus world let us quickly recall some basic functions which are essential.

2.2 Basic functions

2.2.1 The Gamma function

In the integer-order calculus the factorial plays an important role because it is one of the most fundamental combinatorial tools. The Gamma function has the same importance in the fractional-order calculus.

Definition 1. *The function* $\Gamma : (0, +\infty) \to \mathbb{R}$ *defined by:*

$$\Gamma(x) := \int_0^{+\infty} t^{x-1} e^{-t} dt \tag{2.2.1}$$

is called the Euler's Gamma function (or Euler's integral of second kind).
In particular we have $\Gamma(n) = (n-1)!$ *for any positive integer* n

The exponential provides the convergence of this integral. The convergence at zero obviously occurs for all $x \in \mathbb{R}_+$, actually this definition extends to all complex number z from the right half of the complex plane ($Re(z) > 0$). Other generalizations for values in the left half of the complex plane can be obtained as follows: if in (2.2.1) we substitute e^{-t} by the well-known limit

$$e^{-t} = \lim_{n\to\infty} \left(1 - \frac{t}{n}\right)^n$$

and then use n-times integration by parts we obtain the following limit definition of the Gamma function:

$$\Gamma(x) = \lim_{n\to\infty} \frac{n! n^x}{x(x+1)...(x+n)}. \tag{2.2.2}$$

Even if this expression was derived for positive real part of x, it is possible to use it as well as a definition of the Gamma function at points with negative real part except negative integer numbers. So now the Gamma function is defined for all $z \in \mathbb{C} - \{0, 1, 2, ...\}$. Moreover in the sense of complex analysis the negative integers are simple poles of z. For a better understanding, the graph of $\Gamma(z)$ for real values of z is given in Figure 2.2.1a

In many formulas the reciprocal Gamma function occurs, so it is reasonable to define it simply by

$$\frac{1}{\Gamma(x)} = \lim_{n\to\infty} \frac{x(x+1)...(x+n)}{n! n^x}. \tag{2.2.3}$$

In this way we also avoided the problem in negative integers, i.e. the function $\frac{1}{\Gamma(x)}$ is defined for all complex x (especially for real values see Figure 2.2.1b bellow).

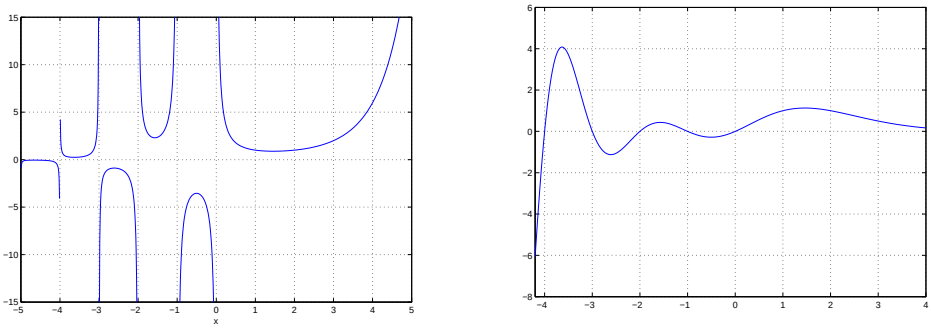

(a) $\Gamma(x)$) (b) $\frac{1}{\Gamma(x)}$

Figure 2.2.1: Plot of Gamma and inverse Gamma functions.

The main property of the factorial is $(n+1)n! = (n+1)!$. Of course an analogous rule holds for the Gamma function. In fact it can be proved from the definition (2.2.1) by integrating by parts that

$$\Gamma(x+1) = x\Gamma(x). \tag{2.2.4}$$

Despite the fact that we derived (2.2.4) only for points in the right half of the complex plane, it follows that this formula holds even for points z for which $-m < Re(x) \leq -m+1$, where $m \in \mathbb{N}$ since

$$\Gamma(x) = \frac{\Gamma(x+m)}{x(x+1)...(x+m-1)}.$$

It is natural to expect a connection between the Gamma and the factorial functions. This is provided by the formula (2.2.4) and by the fact that $\Gamma(1) = 1$:

$$\Gamma(n+1) = n! \quad \text{for } n \in \mathbb{N}. \tag{2.2.5}$$

2.2.2 The Beta function

The Beta function is very important for the computation of the fractional derivatives of the power function. It is defined by the two-parameter integral

$$B(z,w) = \int_0^1 t^{z-1}(1-t)^{w-1}dt, \qquad Re(z) > 0, \quad Re(w) > 0. \tag{2.2.6}$$

Applying a Laplace transform for convolution on Beta function shows that:

$$B(z,w) = B(w,z), \tag{2.2.7}$$

$$B(z,w) = \frac{\Gamma(z)\Gamma(w)}{\Gamma(z+w)}. \tag{2.2.8}$$

The Beta function allows to get some useful results about the Gamma function such as the following:

$$\Gamma(z)\Gamma(1-z) = \frac{\pi}{\sin \pi z}, \tag{2.2.9}$$

$$\Gamma(z)\Gamma\left(z+\frac{1}{2}\right) = \sqrt{\pi}2^{1-2z}\Gamma(2z), \tag{2.2.10}$$

$$\Gamma\left(n+\frac{1}{2}\right) = \frac{\sqrt{\pi}(2n)!}{2^{2n}n!}. \tag{2.2.11}$$

2.2.3 The Mittag-Leffler function

While the Gamma function is a generalization of the factorial function, the Mittag-Leffler function is a generalization of the exponential function, first introduced as a one-parameter function by the series (Podlubny [77], p.16). Later, the two-parameter generalization is introduced by Agarwal, which is of great importance for the fractional calculus. To see it clear let recall the definition of the exponential function:

$$e^z = \sum_{k=0}^{\infty} \frac{z^k}{\Gamma(k+1)}. \tag{2.2.12}$$

The generalization of (2.2.12) is:

$$E_\alpha(z) = \sum_{k=0}^{\infty} \frac{z^k}{\Gamma(\alpha k + 1)}, \quad \alpha > 0. \tag{2.2.13}$$

The two-parameter is

$$E_{\alpha,\beta}(z) = \sum_{k=0}^{\infty} \frac{z^k}{\Gamma(\alpha k + \beta)}, \qquad \alpha > 0, \quad \beta \in \mathbb{R}. \tag{2.2.14}$$

The following properties hold:

$$\begin{aligned}
E_{1,1}(z) &= e^z, \qquad & E_0(z) &= \frac{1}{1-z}, & (2.2.15)\\
E_{1,2}(z) &= \frac{e^z - 1}{z}, \qquad & E_1(z) &= e^z, & (2.2.16)\\
E_{2,1}(z^2) &= \cosh(z), \qquad & E_2(z^2) &= \cosh(z), & (2.2.17)\\
E_{2,2}(z^2) &= \frac{\sinh(z)}{z}, \qquad & E_2(-z^2) &= \cos(z), & (2.2.18)\\
E_{\frac{1}{2},1}(z) &= e^{z^2}\mathrm{erfc}(-z). & & & (2.2.19)
\end{aligned}$$

By differentiation term per term we get:

$$E^m_{\alpha,\beta}(z) = \sum_{k=0}^{\infty} \frac{(k+m)!}{k!} \frac{t^k}{\Gamma(\alpha k + \alpha m) + \beta}. \tag{2.2.20}$$

A more three-parameter generalization is given by:

$$E_{\alpha,m,l} = 1 + \sum_{k=1}^{\infty} \left(\prod_{j=0}^{k-1} \frac{\Gamma(\alpha(jm + l) + 1)}{\Gamma(\alpha(jm + l + 1) + 1)} \right) z^k. \tag{2.2.21}$$

2.3 Basic fractional Calculus

The main objects of classical calculus are derivatives and integrals of functions - these two operations are inverse to each other in some sense. If we start with a function $f(t)$ and put its derivatives on the left-hand side and on the right-hand side we continue

with integrals, we obtain a both-side infinite sequence.

$$..., \frac{d^2 f(t)}{dt^2}, \frac{df(t)}{dt}, f(t), \int_a^t f(\tau)d\tau, \int_a^t \int_a^{\tau_1} f(\tau)d\tau d\tau_1, ... \tag{2.3.1}$$

Fractional calculus tries to interpolate this sequence so that this operation unifies the classical derivatives and integrals and, generalises them for non-integer order. There are many ways to define the fractional derivative or integral and these approaches are called according to their authors. For example the Grunwald-Letnikov definition of fractional derivatives and integrals starts from classical definitions of derivatives and integrals based on infinitesimal division and limit. The disadvantages of this approach are the technical difficulty in the computations, the proofs and the large number of restrictions on functions. Fortunately there are other, more elegant approaches like the Riemann-Liouville definition and the Caputo definition. A more recent approach that removes singularities is the Atangana-Baleanu fractional derivative and integral which takes its roots from the Caputo-Fabrizio fractional derivative.
Let us now introduce some definitions and concepts behind the fractional derivatives and integrals.

2.3.1 The Grünwald-Letnikov construction

The construction takes its origin from the classical definition of the usual derivative of integer order, then generalises it to a fractional order. As such, let us then begin with the definition of the derivative of a continuous smooth function f at any point x in its domain [40].

$$\frac{d}{dx}f(x) = \lim_{h\to 0} \frac{f(x) - f(x-h)}{h}.$$

Repeated composition of this operation leads to

$$\frac{d^n}{dx^n}f(x) = \lim_{h\to 0} \frac{1}{h^n} \sum_{k=0}^{n} (-1)^n \binom{n}{k} f(x-kh), \forall n \in \mathbb{N}. \tag{2.3.2}$$

We illustrate this definition by obtaining a second order derivative of the function $f(x) = x^4$ as shown below

$$\begin{aligned}\frac{d^2}{dx^2}(x^4) &= \lim_{h\to 0}\frac{1}{h^2}\sum_{k=0}^{2}(-1)^j\binom{2}{k}(x-kh)^4 \\ &= \lim_{h\to 0}\frac{1}{h^2}\left[x^4 - 2(x-h)^4 + (x-2h)^4\right] \\ &= \lim_{h\to 0}\left[12x^2 - 24xh + 14h^2\right]\end{aligned}$$

We can generalise Equation (2.3.2) for non-integer order, but to do this we must not only generalize the binomial coefficients, we also need to determine the appropriate generalization of the upper limit in the summation, which we wrote as n in equation (2.3.2). So, let us go back and derive "from stratch" the operations of differentiation and integration. Consider an arbitrary smooth function $f(x)$. We define a shift operator σ_h such that: $\sigma_h f(x) = f(x-h)$. Let us consider a general operator D defined by

$$D^n[f(x)] = \lim_{h\to 0}\left(\frac{1-\sigma_h}{h}\right)^n f(x).$$

Recalling the geometric series expression $\frac{1}{1-z} = 1 + z + z^2 + z^3 + ...$, the effects of this operator with $n = +1$ or -1 are

$$\begin{aligned}D^1[f(x)] &= \left(\frac{1-\sigma_h}{h}\right)^1 f(x) = \frac{f(x) - f(x-h)}{h}, \\ D^{-1}[f(x)] &= \left(\frac{1-\sigma_h}{h}\right)^{-1} = h\left[f(x) + f(x-h) + f(x-2h) + ... + f(0)\right].\end{aligned}$$

Taking the limit as $h \to 0$, we see that D is simply the differentiation operator and its inverse, D^{-1}, is the integration operator. This reproduces the ordinary derivative. For example the second derivative of $f(x)$ is

$$D^2[f(x)] = \lim_{h\to 0}\left(\frac{1-\sigma_h}{h}\right)^2 f(x) = \lim_{h\to 0}\frac{f(x) - 2f(x-h) + f(x-2h)}{h^2},$$

which illustrates how we recover the binomial equation (2.3.2) for any ordinary differentiation. In this context, we should actually write the second derivative as

$$\left(\frac{1-\sigma_h}{h}\right)^2 f(x) = \frac{1f(x) - 2f(x-h) + 1f(x-2h) - 0f(x-3h) + ... + 0f(0)}{h^2}.$$

If n is a positive integer, all the binomial coefficients after the first $n+1$ are identically zero (i.e., we have $\binom{n}{k} = 0$ for all k greater than n), so we can truncate the series. But for any negative value of n or any positive fractional values of n, the binomial coefficients are non-terminating, so we must include the entire summation over the specified range. Consequently, the upper summation limit in (2.3.2) should actually be $\left[\frac{(x-x_0)}{h}\right]$, where x_0 is the lower bound on the range of evaluation. We often choose $x_0 = 0$ by convention, but it is actually arbitrary, and we will see below some circumstances in which the lower bound is not zero. In any case, we can re-write equation (2.3.2) in a more correct form that does not rely on n being a positive integer

$$f^{(n)}(x) = \lim_{h\to 0} \frac{1}{h^n} \sum_{k=0}^{\left[\frac{(x-x_0)}{h}\right]} (-1)^k \binom{n}{k} f(x-kh). \tag{2.3.3}$$

Introducing the Gamma function (2.2.1) in place of the factorial and rearranging terms allow to write an extension of the equation (2.3.3) to the real values of n:

$$f^{(q)}(x) = \lim_{h\to 0} \frac{1}{h^q} \sum_{k=0}^{\left[\frac{(x-x_0)}{h}\right]} (-1)^q \frac{\Gamma(q+1)}{\Gamma(q+1-k)k!} f(x-kh). \tag{2.3.4}$$

If n is an integer, the vanishing of the binomial coefficients for all k greater than n implies that we don't really need to carry the summation beyond $k = n$, and in the limit as h goes to 0 the n values of $f(x_k)$ with non-zero coefficients all converge near $f(x)$, so the derivative is local. However, in general, the binomial expansion has infinitely many non-zero coefficients, so the result depends on the values of x all the way down to x_0. We typically choose $x_0 = 0$. Thus, as mentioned previously, the generalized derivative is a non-local operation, just as is the integration. The general derivative depends on

the value of the function f over the whole range from x_0 to x. This can be seen from the factor $f(x - x_k)$ in the summation in equation (2.3.2), showing that as k ranges from 0 to $\frac{x-x_0}{h}$ the argument of f ranges from x down to 0. It just so happens that this non-locality disappears for positive ordinary derivatives.
Choosing $x_0 = 0$ as the low end of our differentiation interval, the formula (2.3.4) for the general derivative becomes

$$f^{(q)}(x) = \lim_{h\to 0} \frac{1}{h^q} \sum_{k=0}^{\left[\frac{x}{h}\right]} (-1)^k \frac{\Gamma(q+1)}{k!\Gamma(q+1-k)} f(x-kh). \tag{2.3.5}$$

We finally write an elegant definition of the Grünwald-Letnikov fractional derivative:

Definition 2. *Let q be a positive number, $f \in C^m[a,b], a \le x \le b$ and $m = [q] + 1$. Then*

$$f^{(q)}(x) = \lim_{h\to 0} \frac{1}{h_N^q} \sum_{k=0}^{N} (-1)^k \binom{q}{k} f(x - kh_N). \tag{2.3.6}$$

with $h_N = \frac{x-a}{N}$, is called the Grünwald-Letnikov fractional derivative of order q of the function f.

According to the previous definition of fractional derivative, we can propose the variable-order fractional operator now. Replacing the constant order with a given function, the fractional derivative is indeed extended to the variable-order fractional sense.

Definition 3. *Let $q(t)$ be a positive function of t, $f \in C^m[a,b], a \le t \le b$ and $m = [q] + 1$. Then*

$$f^{(q(t))}(t) = \lim_{h\to 0} \frac{1}{h_N^{q(t)}} \sum_{k=0}^{N} (-1)^k \binom{q(t)}{k} f(t - kh_N). \tag{2.3.7}$$

with $h_N = \frac{t-a}{N}$ is called the Grünwald-Letnikov variable fractional order of the function f.

2.3.2 The Classical fractional derivatives

By classical, we refer to Riemann-Liouville and Caputo derivatives. The construction is based on the Cauchy formula for integral. Assuming that a function $f(x)$ is well defined where $x > 0$, we can form the definite integral from 0 to x. Let call this

$$(J\,f)(x) = \int_0^x f(t)dt \tag{2.3.8}$$

Repeating the process twice gives

$$(J^2 f)(x) = \int_0^x (J\,f)(t)dt = \int_0^x \left(\int_0^t f(s)ds \right) dt, \tag{2.3.9}$$

and this can be extended to an arbitrary higher order integration..
The Cauchy formula for repeated integration, namely

$$(J^n f)(x) = \frac{1}{(n-1)!} \int_0^x (x-t)^{n-1} f(t)dt, \tag{2.3.10}$$

leads to a straightforward way to the generalisation for n being a real number. However the function defined in (2.3.10) is discrete. Let then remove the discrete nature of this integral operator for any n real by inserting the Gamma function defined in (2.2.1) which is a smooth extension of the factorial function. In this way, we get a natural candidate for the definition of fractional integral operator.

Definition 4. *Let α be a positive real number. The operator J^α defined on $L_1[a,b]$ by:*

$$(J^\alpha f)(x) = \frac{1}{\Gamma(\alpha)} \int_0^x (x-t)^{\alpha-1} f(t)dt. \tag{2.3.11}$$

is called the Riemann-Liouville fractional integral operator of order α. For $\alpha = 0$, $J^0 = \mathcal{I}$ is the Identity operator.

This is in fact a well-defined operator moreover the operator J^α is commutative.

Lemma 5. *[55, 77] Let f be an integrable function on $[a,b]$. For any positive real*

number α, β we have

$$J^{\beta}J^{\alpha}f = J^{\alpha}J^{\beta}f = J^{\alpha+\beta}f = \frac{1}{\Gamma(\alpha+\beta)}\int_0^x (x-t)^{\alpha+\beta-1}f(t)dt \tag{2.3.12}$$

and

$$(J^{\alpha})^n f(t) = J^{\alpha n}f(t), \qquad n = 1, 2, 3, ... \tag{2.3.13}$$

These results are already well known in the case of integer order integrals.

Proof. [77] Let first prove (2.3.12) then (2.3.13) will follow immediately as a consequence.

$$\begin{aligned} J^{\alpha}J^{\beta}f(t) &= \frac{1}{\Gamma(\alpha)\Gamma(\beta)}\int_a^t (t-s)^{\alpha-1}\int_a^s (s-u)^{\beta-1}f(u)du\,ds \\ &= \frac{1}{\Gamma(\alpha)\Gamma(\beta)}\int_a^t\int_a^s (t-s)^{\alpha-1}(s-u)^{\beta-1}f(u)du\,ds \\ &= \frac{1}{\Gamma(\alpha)\Gamma(\beta)}\int_a^t f(u)\int_a^s (t-s)^{\alpha-1}(s-u)^{\beta-1}du\,ds. \end{aligned}$$

Using the following change of variables: $v = \frac{s-u}{t-u}$, we get

$$\begin{aligned} J^{\alpha}J^{\beta}f(t) &= \frac{1}{\Gamma(\alpha)\Gamma(\beta)}\int_a^t f(u)(t-u)^{\alpha+\beta-1}\int_0^1 (1-v)^{\alpha-1}v^{\beta-1}dv\,du \\ &= \frac{1}{\Gamma(\alpha+\beta)}\int_a^t (t-s)^{\alpha+\beta-1}f(t-u)^{\alpha+\beta-1}f(u)du. \end{aligned}$$

□

Another important property regarding convergence is provided by the following lemma

Lemma 6. *[39] Let J^{α} be the Riemann-Liouville integral operator. Then*

$$J^{\alpha}f(t) \xrightarrow[uniformely]{} J^n f(t) \qquad n = 1, 2, ...$$

as $\alpha \to n$.

Proof. Consider $f \in L_1[a,b]$, then the following inequality holds:

$$\left|J^{\alpha}f(t) - J^{n}f(t)\right| \leq \int_a^t \left|\frac{(t-s)^{\alpha-1}}{\Gamma(\alpha)} - \frac{(t-s)^{n-1}}{\Gamma(n)}\right| |f(s)|ds.$$

But since $\frac{(t-s)^{\alpha-1}}{\Gamma(\alpha)} \to \frac{(t-s)^{n-1}}{\Gamma(n)}$ as $\alpha \to n$, $n = 1, 2...$
then $J^{\alpha}f(t) \to J^{n}f(t)$. □

Theorem 7. *[55] Let f be a continuous function on $[a,b]$, then*

$$\lim_{\alpha \to 0} J^{\alpha}f(t) = f(t).$$

Proof. Whenever f is differentiable in $[a,b]$ one just needs to apply integration by part. that is,

$$\begin{aligned} J^{\alpha}f(t) &= \int_a^t \frac{(t-s)^{\alpha-1}}{\Gamma(\alpha)} f(s)ds \\ &= \frac{(t-a)^{\alpha}}{\Gamma(\alpha+1)} f(a) + \int_a^t \frac{(t-s)^{\alpha}}{\Gamma(\alpha+1)} f'(s)ds, \end{aligned}$$

taking the limit we get

$$\begin{aligned} \lim_{\alpha \to 0} J^{\alpha}f(t) &= f(a) + \int_a^t f'(s)ds \\ &= f(a) + f(t) - f(a) \\ &= f(t). \end{aligned}$$

In the case f is not differentiable, then

$$\begin{aligned} J^{\alpha}f(t) &= \int_a^t \frac{(t-s)^{\alpha-1}}{\Gamma(\alpha)} f(s)ds \\ &= \int_a^t \frac{(t-s)^{\alpha-1}}{\Gamma(\alpha)} \left[f(s)-f(t)\right] ds + \frac{f(t)}{\Gamma(\alpha)} \int_a^t (t-s)^{\alpha-1} ds \\ J^{\alpha}f(t) &= \int_a^{t-\delta} \frac{(t-s)^{\alpha-1}}{\Gamma(\alpha)} \left[f(s)-f(t)\right] ds \\ &+ f(t)\frac{(t-s)^{\alpha}}{\Gamma(\alpha+1)} + \int_{t-\delta}^t \frac{(t-s)^{\alpha-1}}{\Gamma(\alpha)} \left[f(s)-f(t)\right] ds \end{aligned} \tag{2.3.14}$$

for some δ small enough.

Let us consider the second integral on the right hand side. For every $\delta > 0$ there exists $\epsilon > 0$ such that whenever $|f(s) - f(t)| < \delta$ then

$$\begin{aligned} \left| \int_{t-\delta}^t \frac{(t-s)^{\alpha-1}}{\Gamma(\alpha)} \left[f(s)-f(t)\right] ds \right| &< \frac{\epsilon}{\Gamma(\alpha)} \int_{t-\delta}^t (t-s)^{\alpha-1} ds \\ &< \frac{\epsilon \delta^{\alpha}}{\Gamma(\alpha+1)}. \end{aligned}$$

And taking into account that $\epsilon \to 0$ as $\delta \to 0$, we obtain that for all $\alpha > 0$

$$\lim_{\delta \to 0} \left| \int_{t-\delta}^t \frac{(t-s)^{\alpha-1}}{\Gamma(\alpha)} \left[f(s)-f(t)\right] ds \right| = 0,$$

considering an arbitrary $\epsilon > 0$ and choose δ such that

$$\left| \int_{t-\delta}^t \frac{(t-s)^{\alpha-1}}{\Gamma(\alpha)} \left[f(s)-f(t)\right] ds \right| \leq \epsilon, \qquad \forall \alpha \geq 0.$$

For fixed δ we obtain the following estimate of the first integral in the right hand side of the equation (2.3.14)

$$\begin{aligned} \left| \int_a^{t-\delta} \frac{(t-s)^{\alpha-1}}{\Gamma(\alpha)} \left[f(s)-f(t)\right] ds \right| &\leq \frac{\epsilon}{\Gamma(\alpha)} \int_a^{t-\delta} \left[(t-\alpha)^{\alpha-1}\right] ds \\ &\leq \frac{\epsilon}{\Gamma(\alpha+1)} \left[(t-a)^{\alpha} - \delta^{\alpha}\right]. \end{aligned}$$

Then it follows that for a fixed $\delta > 0$

$$\lim_{\alpha \to 0} \left| \int_a^{t-\delta} \frac{(t-s)^{\alpha-1}}{\Gamma(\alpha)} \left[f(s) - f(t) \right] ds \right| = 0.$$

Considering that

$$\begin{aligned} |J^\alpha f(t) - f(t)| &= \left| \int_a^t \frac{(t-s)^{\alpha-1}}{\Gamma(\alpha)} \left[f(s) - f(t) \right] ds \right| + \left| \int_a^t \frac{(t-s)^{\alpha-1}}{\Gamma(\alpha)} f(t) ds - f(t) \right| \\ &\leq \left| \int_a^{t-\delta} \frac{(t-s)^{\alpha-1}}{\Gamma(\alpha)} \left[f(s) - f(t) \right] ds \right| \\ &\quad + \left| \int_{t-\delta}^t \frac{(t-s)^{\alpha-1}}{\Gamma(\alpha)} \left[f(s) - f(t) \right] ds \right| + |f(t)| \left| \frac{(t-s)^\alpha}{\Gamma(\alpha+1)} - 1 \right|, \end{aligned}$$

and taking into account the limits and the estimates we obtain

$$\lim_{\alpha \to 0} \sup |J^\alpha f(t) - f(t)| \leq \epsilon,$$

where ϵ can be chosen as small as we wish, therefore

$$\lim_{\alpha \to 0} \sup |J^\alpha f(t) - f(t)| = 0,$$

and then

$$J^\alpha f(t) \to f(t), \qquad \text{as} \quad \alpha \to 0.$$

□

Example 8. *Let $t > 0$, then*

$$J^\alpha t^\gamma = \frac{\Gamma(1+\gamma)}{\Gamma(\gamma+\alpha+1)} t^{\gamma+\alpha}, \qquad \gamma > -1.$$

In particular for $\gamma = 0$, then the Riemann-Liouville fractional integral of a constant C of order α is

$$J^\alpha C = \frac{C}{\Gamma(\alpha+1)} t^\alpha.$$

Example 9. *Let $f(t) = (t-a)^\gamma$ for some $\gamma > -1$ and $\alpha > 0$. Then*

$$J^\alpha f(t) = \frac{\Gamma(\gamma+1)}{\Gamma(\gamma+\alpha+1)}(t-a)^{\alpha+\gamma}.$$

Example 10. *Let $f(t) = e^{at}$ where a is a constant. then*

$$\begin{aligned} J^\alpha e^{at} &= \frac{1}{\Gamma(\alpha)}\int_0^t (t-s)^{\alpha-1}e^{as}ds, \quad \alpha > 0 \\ &= \frac{e^{at}}{\Gamma}\int_0^t u^{\alpha-1}e^{-au}du, \qquad \text{where } u = t-s \\ &= t^\alpha e^{at}\Gamma^*(\alpha, \alpha t) \end{aligned}$$

where Γ^* stands for the incomplete Gamma function.

The Riemann-Liouville fractional order derivative of f is defined as the m^{th} derivative of the fractional integral of order $m-q$. That is:

Definition 11. *Let $f(t)$ be an integrable function on $[a,T]$. For all $a < t < T$ the Riemann-Liouville fractional derivative of order $q > 0$ of f is given by:*

$${}^{RL}_{a}D^q_t f(t) = \frac{d^m}{dt^m}\left[\frac{1}{\Gamma(m-q)}\int_a^t (t-\tau)^{m-q-1}f(\tau)d\tau\right], \qquad m = [q]+1. \tag{2.3.15}$$

And for the case $q = k \in \mathbb{N}$ then $m = k+1$, we recover the normal differentiation formula

$${}^{RL}_{a}D^k_t f(t) = \frac{1}{\Gamma(1)}\frac{d^{k+1}}{dt^{k+1}}\left[\int_a^t f(\tau)d\tau\right] = \frac{d^k}{dt^k}f(t).$$

The classical integer derivatives becomes like singularities among the Riemann-Liouville fractional derivatives. They turn out to be the only fractional derivatives that do not depend on the lower bound a. Remark that if f is a monomial i.e. $f(t) = t^r$ then,

$${}^{RL}_{a}D^\alpha_0 t^r = \frac{\Gamma(r+1)}{\Gamma(r+1-\alpha)}t^{r-\alpha}, \quad \alpha > 0, \quad r > -1, \quad t > 0. \tag{2.3.16}$$

Thus for a constant function f we have the remarkable fact that its fractional derivative will not be zero as with any normal integer differentiation. In fact from (2.3.16) and

taking $r = 0$ we have,

$$ {}^{RL}_{a}D^{\alpha}1 = \frac{t^{-\alpha}}{\Gamma(1-\alpha)}, \quad \alpha \geq 0, \quad t > 0. \tag{2.3.17} $$

Similarly to the Riemann-Liouville derivative, let introduce another fractional derivative: the Caputo derivative, which is defined as the fractional integral of the m^{th}-derivative. That is:

Definition 12. *Let q be a positive number, $f \in C^m[0,t]$ and $0 \leq \tau \leq t$. Then the Caputo fractional derivative of $f(t)$ is defined as*

$$ {}^{C}_{a}D^{q}_{t}f(t) = \frac{1}{\Gamma(m-q)} \int_a^t \frac{f^{(m)}(\tau)}{(t-\tau)^{q+1-m}} d\tau, \qquad m-1 \leq q < m \tag{2.3.18} $$

and for the case $k \in \mathbb{N}$ then $m = k+1$ thus we recover the usual derivative

$$ {}^{C}_{a}D^{k}_{t}f(t) = \frac{1}{\Gamma(1)} \int_a^t \frac{d^{k+1}}{dt^{k+1}} f(\tau) d\tau = \frac{d^k}{dt^k} f(t). $$

With the Caputo derivative we recover the fact that the derivative of a constant function is indeed zero, however we have to pay the price that f has to be m-differentiable. The following relations allows to see the equivalence between the Riemann-Liouville and the Caputo fractional derivatives:

$$ {}^{RL}_{a}D^{\alpha}f(t) = {}^{C}_{a}D^{\alpha}f(t) + \sum_{k=0}^{m-1} \frac{(t-a)^{k-\alpha}}{\Gamma(k-\alpha+1)} f^{(k)}(a), \qquad a > 0 \tag{2.3.19} $$

Consequently,

$$ {}^{RL}_{a}D^{\alpha}f(t) := D^m J^{m-\alpha} f(t) \neq J^{m-\alpha} D^m f(t) := {}^{C}_{a}D^{\alpha}f(t), \tag{2.3.20} $$

unless the function $f(t)$ along with its first $m-1$ derivatives vanishes at $t = a$.

2.3.3 Basic properties of classical fractional derivatives

Let f and g be two functions smooth enough and let λ, μ, q, a be constants real with $(a > 0)$ and $m = [q] + 1$. Then

$$
\begin{aligned}
{}_aD_t^q \left[\lambda f(t) + \mu g(t)\right] &= \lambda {}_aD_t^q f(t) + \mu {}_aD_t^q g(t), , && (2.3.21)\\
{}_aD_t^q \left[\sum_{k=0}^{\infty} f_k(t)\right] &= \sum_{k=0}^{\infty} {}_aD_t^q f_k(t), && (2.3.22)\\
{}_a^{RL}D^{\alpha} f(t) &= {}_a^{C}D^{\alpha} f(t) + \sum_{k=0}^{m-1} \frac{(t-a)^{k-\alpha}}{\Gamma(k-\alpha+1)} f^{(k)}(a), && (2.3.23)\\
{}_aD_t^q \left[{}_aD_t^r f(t)\right] &= {}_aD_t^{q+r} f(t), && (2.3.24)\\
\frac{d}{dt} J^q f(t) &= J^q \frac{d}{dt} f(t). && (2.3.25)
\end{aligned}
$$

Proof. [55, 77] For Equation (2.3.22) we will illustrate the proof using the Riemann-Liouville integral. The case of the Caputo derivative is similar.

$$
\begin{aligned}
{}_a^{RL}D_t^q \left[\sum_{k=0}^{\infty} f_k(t)\right] &= \frac{1}{\Gamma(n-q)} \frac{d^n}{dt^n} \int_a^t (t-\tau)^{n-q-1} \sum_{k=0}^{\infty} f_k(t) d\tau\\
&= \frac{1}{\Gamma(n-q)} \frac{d^n}{dt^n} \int_a^t \sum_{k=0}^{\infty} (t-\tau)^{n-q-1} f_k(t) d\tau\\
&= \frac{1}{\Gamma(n-q)} \frac{d^n}{dt^n} \sum_{k=0}^{\infty} \int_a^t (t-\tau)^{n-q-1} f_k(t) d\tau\\
&= \frac{1}{\Gamma(n-q)} \sum_{k=0}^{\infty} \frac{d^n}{dt^n} \int_a^t (t-\tau)^{n-q-1} f_k(t) d\tau\\
&= \sum_{k=0}^{\infty} {}_a^{RL}D_t^q f_k(t).
\end{aligned}
$$

As for Equation (2.3.23) we have

$$\begin{aligned}
{}_a^{RL}D_t^q f(t) &= \frac{1}{\Gamma(n-q)}\frac{d^n}{dt^n}\int_a^t (t-\tau)^{n-q-1} f(\tau)d\tau \\
&= \frac{1}{\Gamma(n-q)}\frac{d^n}{dt^n}\left[\frac{(t-a)^{n-q}f(a)}{n-q} + \int_a^t \frac{(t-\tau)^{n-q}}{n-q} f'(\tau)d\tau\right] \\
&= \frac{d^n}{dt^n}\left[\sum_{k=0}^{n-1}\frac{(t-a)^{n+k-q}f^{(k)}(a)}{\Gamma(n+k-q+1)} + \frac{1}{\Gamma(2n-q)}\int_a^t (t-\tau)^{2n-q-1} f^{(n)}(\tau)d\tau\right] \\
&= \sum_{k=0}^{n-1}\frac{(t-a)^{k-q}f^{(k)}(a)}{\Gamma(k-q+1)} + \frac{1}{\Gamma(n-q)}\int_a^t (t-\tau)^{n-q-1} f^{(n)}(\tau)d\tau \\
&= \sum_{k=0}^{n-1}\frac{(t-a)^{k-q}f^{(k)}(a)}{\Gamma(k-q+1)} + {}_a^C D_t^q f(t).
\end{aligned}$$

□

2.3.4 Convergence

We will start our analysis by first introducing the following preliminary result:

Lemma 13. *[40, 55] Let $n-1 < q < n$, $n \in \mathbb{N}$, $q \in \mathbb{R}$ and $f(t)$ be such that ${}_0^C D^q f(t)$ exists. Then the following properties for Caputo fractional derivative operator holds*

$$\begin{aligned}
\lim_{q\to n} {}_0^C D_t^q f(t) &= f^{(n)}(t), \\
\lim_{q\to n-1} {}_0^C D_t^q f(t) &= f^{(n-1)}(t) - f^{(n-1)}(0).
\end{aligned}$$

Proof. [40, 55] The proof uses integration by parts.

$$\begin{aligned}
{}_0^C D_t^q f(t) &= \frac{1}{\Gamma(n-q)}\int_0^t \frac{f^{(n)}(s)}{(t-s)^{q-n+1}}ds \\
&= \frac{1}{\Gamma(n-q)}\left[-f^{(n)}(s)\frac{(t-s)^{n-q}}{n-q}\bigg|_0^t + \int_0^t f^{(n+1)}(s)\frac{(t-s)^{n-q}}{n-q}ds\right] \\
&= \frac{1}{\Gamma(n-q+1)}\left[f^{(n)}(0)t^{n-q} + \int_0^t f^{(n+1)}(s)(t-s)^{n-q}ds\right].
\end{aligned}$$

Now by taking limit for $q \to n$ and $q \to n-1$, respectively, we get

$$\lim_{q\to n} {}_0^C D_t^q f(t) = \left[f^{(n)}(0) + f^{(n)}(s)(t-s)\right]_{s=0}^{s=t} = f^{(n)}(t),$$

and

$$\begin{aligned}\lim_{q\to n-1} {}_0^C D_t^q f(t) &= \left[f^{(n)}(0)t + f^{(n)}(s)(t-s)\right]_{s=0}^{s=t} + \int_0^t f^{(n)}(s)ds \\ &= \left[f^{(n-1)}(s)\right]_{s=0}^{s=t} \\ &= f^{(n)}(t) - f^{(n)}(0).\end{aligned}$$

For the Riemann-Liouville fractional derivative the corresponding property reads

$$\begin{aligned}\lim_{q\to n} {}_0^{RL} D_t^q f(t) &= f^{(n)}(t), \\ \lim_{q\to n-1} {}_0^{RL} D_t^q f(t) &= f^{(n-1)}(t).\end{aligned}$$

□

Example 14. *Let $q \in (0,1]$ and consider $\gamma > -1$, then*

$${}_a^C D_t^q (t-a)^\gamma = \frac{\Gamma(\gamma+1)}{\Gamma(1+\gamma-q)}(t-a)^{\gamma-q},$$

and also,

$$\begin{aligned}\lim_{q\to 1} {}_a^C D_t^q (t-a)^\gamma &= \gamma(t-a)^{\gamma-1}, \\ \lim_{q\to 0} {}_a^C D_t^q (t-a)^\gamma &= \gamma(t-a)^\gamma.\end{aligned}$$

Example 15.

$$\begin{aligned} {}_a^C D_t^q(1+t^\gamma) &= J^{1-q}(\gamma t^{\gamma-1}) \\ &= \gamma J^{1-q} t^{\gamma-1} \\ &= \gamma \frac{\Gamma(\gamma)}{\Gamma(\gamma-q+1)t^{\gamma-q}} \\ &= \frac{\Gamma(\gamma+1)}{\Gamma(\gamma-q+1)} t^{\gamma-q}, \end{aligned}$$

and

$$\begin{aligned} {}_a^{RL} D_t^q(1+t^\gamma) &= {}_a^{RL} D J^{1-q}(1+t^\gamma) \\ &= {}_a^{RL} D_t^q \left[\frac{t^{1-q}}{\Gamma(2-q)} + \frac{\Gamma(\gamma+1)}{\Gamma(\gamma-q+2)} t^{\gamma-q+1} \right] \\ &= \frac{(1-q)t^{-q}}{\Gamma(2-q)} + \frac{(\gamma-q+1)\Gamma(\gamma+1)}{\Gamma(\gamma-q+2)} t^{\gamma-q} \\ &= \frac{t^{-q}}{\Gamma(1-q)} + \frac{\Gamma(\gamma+1)}{\Gamma(\gamma-q+1)} t^{\gamma-q}. \end{aligned}$$

The fractional derivatives presented above have all one common issue: They contain singularities due to their kernel. Let us now provide a new fractional derivative that removes singularities.

2.4 Atangana-Baleanu fractional derivative

We recall that the Mittag-Leffler function is the solution of the following fractional ordinary differential equation:

$$\frac{d^\alpha y}{dx^\alpha} = ay, \quad 0 < \alpha < 1. \tag{2.4.1}$$

The Mittag-Leffler function and its generalized versions are therefore considered as nonlocal functions. Let us recall the generalized Mittag-Leffler function (2.2.13) at

$z = -t$:

$$E_\alpha(-t^\alpha) = \sum_{k=0}^{\infty} \frac{(-t)^{\alpha k}}{\Gamma(\alpha k + 1)}. \tag{2.4.2}$$

The Taylor series of $e^{-a(t-y)}$ at the point t is given by:

$$e^{-a(t-y)} = \sum_{k=0}^{\infty} \frac{(-a(t-y))^k}{k!}. \tag{2.4.3}$$

By changing the kernel $\frac{1}{(t-\tau)}$ with the function $e^{-\frac{\alpha t}{1-\alpha}}$ and $\frac{1}{\Gamma(1-\alpha)}$ with $\frac{M(\alpha)}{1-\alpha}$ we get the new Caputo-Fabrizio fractional derivative

$${}^{CF}_{a}D^q_t f(t) = \frac{M(\alpha)}{1-\alpha} \int_a^t f'(\tau) e^{-\frac{\alpha(t-\tau)}{1-\alpha}} d\tau. \tag{2.4.4}$$

The function $M(\alpha)$ is termed as the normalizing function. If we choose $a = \frac{\alpha}{1-\alpha}$ and replace the above expression into Caputo-Fabrizio derivative we conclude that

$${}^{CF}_{a}D^\alpha_t f(t) = \frac{M(\alpha)}{1-\alpha} \sum_{k=0}^{\infty} \frac{(-a)^k}{k!} \int_b^t \frac{df(y)}{dy} (t-y)^k dy. \tag{2.4.5}$$

To solve the problem of non-locality, we derive the following expression. In equation(2.4.5), we replace $k!$ by $\Gamma(\alpha k + 1)$ also $(t-y)^k$ is replaced by $(t-y)^{ak}$ to obtain:

$$D^\alpha_t f(t) = \frac{M(\alpha)}{1-\alpha} \sum_{k=0}^{\infty} \frac{(-a)^k}{\Gamma(\alpha k + 1)} \int_b^t \frac{df(y)}{dy} (t-y)^{ak} dy. \tag{2.4.6}$$

Definition 16. *Let $f \in H^1(a,b)$, $b > a$, $\alpha \in [0,1]$, then the definition of the new fractional derivative is given as:*

$${}^{ABC}_{b}D^\alpha_t f(t) = \frac{B(\alpha)}{1-\alpha} \int_b^t f'(x) E_\alpha \left[-\alpha \frac{(t-x)^\alpha}{1-\alpha} \right] dx. \tag{2.4.7}$$

Of course $B(\alpha)$ has the same properties as in Caputo-Fabrizio case. The above definition will be helpful to discuss real world problems and it also will have great advantage when using the Laplace transform to solve some physical problem with

initial condition. However, when $\alpha = 0$ we do not recover the original function except when the function vanishes at the origin. To avoid this issue, we propose the following definition.

Definition 17. *Let $f \in H^1(a,b), b > a, \alpha \in [0,1]$ then, the definition of the new fractional derivative is given as:*

$$ {}^{ABR}{}_{b}D_t^{\alpha} f(t) = \frac{B(\alpha)}{1-\alpha}\frac{d}{dt}\int_b^t f(x)E_{\alpha}\left[-\alpha\frac{(t-x)^{\alpha}}{1-\alpha}\right]dx. \tag{2.4.8} $$

Equation (2.4.7) and (2.4.8) have a non-local kernel. Also in equation (2.4.7) when the function is constant we get zero.

2.4.1 Properties of the new derivatives

In this section, we start by presenting the relation between both derivatives with Laplace transform. By simple calculation we conclude that

$$ \mathcal{L}\left[{}^{ABR}{}_{0}D_t^{\alpha} f(t)\right](p) = \frac{B(\alpha)}{1-\alpha}\frac{p^{\alpha}\mathcal{L}[f(t)](p)}{p^{\alpha} + \frac{\alpha}{1-\alpha}}, \tag{2.4.9} $$

and

$$ \mathcal{L}\left[{}^{ABC}{}_{0}D_t^{\alpha} f(t)\right](p) = \frac{B(\alpha)}{1-\alpha}\frac{p^{\alpha}\mathcal{L}[f(t)](p) - p^{\alpha-1}f(0)}{p^{\alpha} + \frac{\alpha}{1-\alpha}}, \tag{2.4.10} $$

respectively. The following theorem can therefore be established

Theorem 18. *[5] Let $f \in H^1(a,b), b > a, \alpha \in [0,1]$ then, there exists a function H such that the following relation holds*

$$ {}^{ABC}{}_{0}D_t^{\alpha} f(t) = {}^{ABR}{}_{0}D_t^{\alpha} f(t) + H(t). \tag{2.4.11} $$

Proof. [5] By using the definition (2.4.11) and Laplace transform applied on both sides we obtain easily the following result:

$$\mathcal{L}\left[{}^{ABC}{}_0D_t^{\alpha}f(t)\right](p) = \frac{B(\alpha)}{1-\alpha}\frac{p^{\alpha}\mathcal{L}[f(t)](p)}{p^{\alpha}+\frac{\alpha}{1-\alpha}} - \frac{p^{\alpha-1}f(0)}{p^{\alpha}+\frac{\alpha}{1-\alpha}}\frac{B(\alpha)}{1-\alpha}. \tag{2.4.12}$$

Following equation (2.4.9) we have

$$\mathcal{L}\left[{}^{ABC}{}_0D_t^{\alpha}f(t)\right](p) = \mathcal{L}\left[{}^{ABC}{}_0D_t^{\alpha}f(t)\right](p) - \frac{p^{\alpha-1}f(0)}{p^{\alpha}+\frac{\alpha}{1-\alpha}}\frac{B(\alpha)}{1-\alpha}. \tag{2.4.13}$$

Applying the inverse Laplace on both sides of the equation (2.4.13) we obtain:

$${}^{ABC}{}_0D_t^{\alpha}f(t) = {}^{ABR}{}_0D_t^{\alpha}f(t) - \frac{B(\alpha)}{1-\alpha}f(0)E_{\alpha}\left[-\frac{\alpha}{1-\alpha}t^{\alpha}\right]. \tag{2.4.14}$$

This completes the proof. □

Theorem 19. *[5] Let f be a continuous function on a closed interval $[a,b]$. Then the there exists a constant K such that the following inequality is obtained on $[a,b]$.*

$$\left\|{}^{ABR}{}_0D_t^{\alpha}f(t)\right\| < \frac{B(\alpha)}{1-\alpha}K, \tag{2.4.15}$$

where the norm here and throughout the rest of this chapter, is defined by: $\|f(t)\| = \max_{a\leq t\leq b}|f(t)|$.

Proof.

$$\begin{aligned}
\left\|{}^{ABC}{}_0D_t^\alpha f(t)\right\| &= \left\|\frac{B(\alpha)}{1-\alpha}\int_0^t \frac{d}{dx}f(x)E_\alpha\left[-\alpha\frac{(t-x)^\alpha}{1-\alpha}\right]dx\right\| \\
&< \frac{B(\alpha)}{1-\alpha}\int_0^t \left|\frac{d}{dx}f(x)\right| E_\alpha\left[-\alpha\frac{(t-x)^\alpha}{1-\alpha}\right]dx \\
&< \frac{B(\alpha)}{1-\alpha}\int_0^t \sup_{0\le x\le t}\left|\frac{d}{dx}f(x)\right| E_\alpha\left[-\alpha\frac{(t-x)^\alpha}{1-\alpha}\right]dx \\
&\le \frac{B(\alpha)}{1-\alpha}\left\|\frac{d}{dx}f(x)\right\|\int_0^t E_\alpha\left[-\alpha\frac{(t-x)^\alpha}{1-\alpha}\right]dx \\
&\le \frac{B(\alpha)}{1-\alpha}\left\|\frac{d}{dx}f(x)\right\|\sup_{0\le x\le t}\int_0^t E_\alpha\left[-\alpha\frac{(t-x)^\alpha}{1-\alpha}\right]dx \\
&\le \frac{B(\alpha)}{1-\alpha}\left\|\frac{d}{dx}f(x)\right\| M \\
&\le \frac{B(\alpha)}{1-\alpha}K.
\end{aligned}$$

where M is a constant large enough and K is taken to be $\left\|\frac{d}{dt}f(x)\right\| M$. Now given

$$\begin{aligned}
\left\|{}^{ABR}{}_0D_t^\alpha f(t)\right\| &= \left\|{}^{ABC}{}_0D_t^\alpha f(t) + \frac{B(\alpha)}{1-\alpha}f(0)E_\alpha\left[-\frac{\alpha}{1-\alpha}t^\alpha\right]\right\| \\
&\le \frac{B(\alpha)}{1-\alpha}K + \frac{B(\alpha)}{1-\alpha}\left|f(0)E_\alpha\left[-\frac{\alpha}{1-\alpha}t^\alpha\right]\right| \\
&\le \frac{B(\alpha)}{1-\alpha}\left[K + \left|f(0)E_\alpha\left[-\frac{\alpha}{1-\alpha}t^\alpha\right]\right|\right] \\
&\le \frac{B(\alpha)}{1-\alpha}L.
\end{aligned}$$

This completes the proof. □

Theorem 20. *[5] The AB derivative in Riemann and Caputo sense possess the Lipschitz condition, that is to say, for a given couple function f and g, there exists a function $H(t)$ such that the following inequalities can be established:*

$$\left\|{}^{ABR}{}_0D_t^\alpha f(t) - {}^{ABR}{}_0D_t^\alpha g(t)\right\| \le H(t)\|f(t)-g(t)\| \tag{2.4.16}$$

and also

$$\left\|{}^{ABC}{}_0D_t^\alpha f(t) - {}^{ABC}{}_0D_t^\alpha g(t)\right\| \leq H(t)\|f(t) - g(t)\|. \tag{2.4.17}$$

We present the proof of (2.4.16) as the proof of (2.4.17) can be obtained similarly.

Proof. [5, 7]

$$\begin{aligned}
\left\|{}^{ABC}{}_0D_t^\alpha f(t) - {}^{ABC}{}_0D_t^\alpha g(t)\right\| &= \left\|\frac{B(\alpha)}{1-\alpha}\int_0^t \frac{d}{dx}[f(x)-g(x)]E_\alpha\left[-\alpha\frac{(t-x)^\alpha}{1-\alpha}\right]\right\| dx \\
&\leq \frac{B(\alpha)}{1-\alpha}\int_0^t \left|\frac{d}{dx}[f(x)-g(x)]\right| E_\alpha\left[-\alpha\frac{(t-x)^\alpha}{1-\alpha}\right] dx \\
&\leq \frac{B(\alpha)}{1-\alpha}\left\|\frac{d}{dt}[f(t)-g(t)]\right\| \int_0^t E_\alpha\left[-\alpha\frac{(t-x)^\alpha}{1-\alpha}\right] dx
\end{aligned}$$

Using the Lipschitz condition of the first order derivative, we can find positive constant M such that

$$\begin{aligned}
\left\|\frac{d}{dt}[f(t)-g(t)]\right\| &< \theta \\
&< \frac{M}{\|f-g\|}\|f-g\| = \theta\|f-g\|
\end{aligned}$$

for $\theta = \frac{M}{\|f-g\|}$. This implies

$$\left\|{}^{ABC}{}_0D_t^\alpha f(t) - {}^{ABC}{}_0D_t^\alpha g(t)\right\| < K\|f-g\|,$$

taking $K = \frac{B(\alpha)\theta}{1-\alpha}\left|\int_0^t E_\alpha\left[-\alpha\frac{(t-x)^\alpha}{1-\alpha}\right| dx\right|$ completes the proof. □

2.4.2 AB Derivative and the Related Fractional Integral

From the properties of the fractional derivative, we can easily prove by taking the inverse Laplace transform and using the convolution theorem that the following time fractional ordinary differential equation:

$${}^{ABC}{}_0D_t^\alpha f(t) = u(t) \tag{2.4.18}$$

has a unique solution, namely

$$f(t) = \frac{1-\alpha}{B(\alpha)}u(t) + \frac{\alpha}{B(\alpha)\Gamma(\alpha)}\int_0^t u(y)(t-y)^{\alpha-1}dy. \tag{2.4.19}$$

Definition 21. *The fractional integral associated to the new fractional derivative with non-local kernel is defined as:*

$${}^{AB}{}_aI_t^\alpha[f(t)] = \frac{1-\alpha}{B(\alpha)}f(t) + \frac{\alpha}{B(\alpha)\Gamma(\alpha)}\int_a^t f(y)(t-y)^{\alpha-1}dy. \tag{2.4.20}$$

When α is zero, we recover the initial function and also for α is 1, we obtain the ordinary integral.

The ABR fractional derivative can be expressed as

$${}^{ABR}{}_0D_t^\alpha f(t) = \frac{B(\alpha)}{1-\alpha}\frac{d}{dt}\sum_{k=0}^{\infty}\left(\frac{-\alpha}{1-\alpha}\right)^k \frac{d}{dt}\left[J_t^{\alpha k+1}f(t)\right]. \tag{2.4.21}$$

where J_t^α stands for the Riemann-Liouvile fractional integral defined in (2.3.11). The AB fractional integral operator ${}^{AB}I_t^\alpha$ follows directly from the solution (2.4.19) and be precisely defined as:

$${}^{AB}I_t^\alpha f(t) = \frac{1-\alpha}{B(\alpha)}f(t) + \frac{\alpha}{B(\alpha)}J_t^\alpha f(t). \tag{2.4.22}$$

The relation (2.4.22) can be easily developed by applying the Laplace transform to equation (2.4.18) as it was demonstrated by Baleanu and Fernandez [7]. Further, we have the following left and right inverse properties:

$${}^{AB}I_t^\alpha\left[{}^{ABR}{}_0D_t^\alpha f(t)\right] = f(t), \tag{2.4.23}$$

$${}^{ABR}{}_0D_t^\alpha\left[{}^{AB}I_t^\alpha f(t)\right] = f(t) \tag{2.4.24}$$

and the commutative properties for $\beta \in (0,1)$

$$ {}^{ABR}D_t^{\alpha}\left[{}^{ABR}D_t^{\beta}f(t)\right] = {}^{ABR}D_t^{\beta}\left[{}^{ABR}D_t^{\alpha}f(t)\right], \tag{2.4.25} $$

All proves regarding the above relations can be found in details in Baleanu and Fernandez [7].

Having discussed fractional derivatives and fractional integral together with their basic properties, let us now explore the numerical tool that will unable us to solve differential equations in a most efficient way. Here we mention spectral method.

Chapter 3

Spectral Method

One of the most well known spectral method is the Fourier spectral method. However it is only appropriate for problems with periodic boundary conditions. If a Fourier method is applied to a non-periodic problem, it inevitably induces the so-called Gibbs phenomenon, and reduces the global convergence rate to $O(N-1)$ (cf. Gottlieb and Orszag [41]). Consequently, one should not apply a Fourier method to problems with non-periodic boundary conditions. Instead, one should use orthogonal polynomials which are eigenfunctions of some singular Sturm-Liouville problems. The commonly used orthogonal polynomials include the Legendre, Chebyshev, Hermite and Laguerre polynomials. In this part we present spectral method based on Chebyshev polynomials.

3.1 Heuristic and construction of smooth periodic version of a function

The idea in this approach is that given a function f we approximate the function by a series of trigonometric functions. In the case where f is already periodic with period T, then we know it has a Fourier series representation of the form

$$f(t) = \sum_{n=-\infty}^{\infty} c_n e^{i(n\omega_0 t)}. \tag{3.1.1}$$

If f is smooth enough, then the Fourier series coefficients c_n decay rapidly with n. This means we can get a very high accurate approximation of f from just a few of its Fourier coefficients. More precisely if we consider N points then the error in our approximation would be of the order of $e^{-\alpha N}$ for a large α. Finally, it is also known that we can get the Fourier coefficients in a very simple way at some suitable N sample points.
With such a powerful tool how can such approach be extended to the case of non-periodic function? This is answered in a simple way as follows: We transform the non-periodic function into a periodic function then apply the fourier transform in (3.1.1).

To construct a periodic function out of the non-periodic function f we restrict ourself to the interval $[-1, 1]$ and define:

$$g(\theta) = f(\cos\theta).$$

This a smooth periodic function. As θ varies from 0 to π, $g(\theta)$ describes f over the interval $[-1, 1]$, but in a "backward" way. Next, from π to 2π, $g(\theta)$ describes f over $[-1, 1]$ this time in the correct orientation, ie from $f(-1)$ to $f(1)$, see Figure 3.1.1. Notice also that g admits turning points at $\theta = 0$ and $\theta = \pi$ corresponding to $x = 1$ and $x = -1$ respectively, which are just end points and not necessary turning points in f.

Since g is now periodic hence Equation (3.1.1) applies so it can be expressed in terms of its fourier cosine series as:

$$g(\theta) = \frac{a_0}{2} + \sum_{k=1}^{\infty} a_k \cos k\theta, \tag{3.1.2}$$

with coefficients

$$a_k = \frac{2}{\pi} \int_0^{\pi} g(\theta) \cos k\theta \, d\theta. \tag{3.1.3}$$

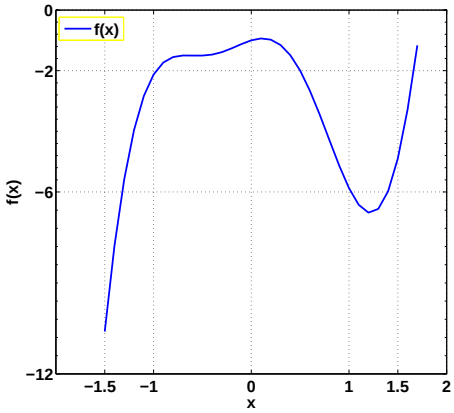

(a) Initial non periodic function $f(x)$ on $[-1.5, 1.7]$

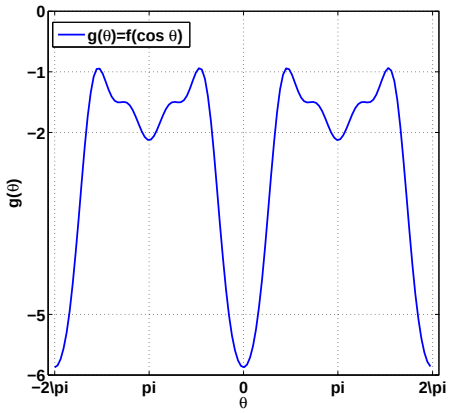

(b) Periodic function $g(\theta)$

Figure 3.1.1: Construction of a periodic function $g(\theta)$ out of initial non-periodic function $f(x)$

We can then write f as:

$$f(t) = g(\arccos t) \tag{3.1.4}$$

$$f(t) = \frac{a_0}{2} + \sum_{k=1}^{N/2} a_k \cos(k \arccos t). \tag{3.1.5}$$

The last equation (3.1.5) is looking a priori ugly, but it was actually well redesigned by the Russian mathematician Pafnuty Lvovich Chebyshev in a form of chebyshev polynomials. Let us enter this new space of chebyshev polynomials...

3.2 Chebyshev polynomials

The Chebyshev polynomial $T_n(x)$ of 1st kind is a polynomial in $x \in [-1, 1]$ of degree $n > 0$ defined by the relation:

$$T_n(x) = \cos n\theta, \text{ for } x = \cos\theta \tag{3.2.1}$$

$$ie. \quad T_n(x) = \cos(n \arccos(x))$$

Note that the definition of the Chebyshev polynomials can easily be extended to any interval by just considering the shift mapping $s : x \to s(x) = \frac{2}{b-a}x - \frac{b+a}{b-a}$. We can therefore work on the interval $[-1, 1]$ then apply the inverse the shift mapping to allow the catering of any interval $[a, b]$.

As such the first few Chebyshev polynomials are plotted is Figure 3.2.1 and there respective algebraic expressions are as follows:

$$\begin{aligned} T_0(x) &= 1, \\ T_1(x) &= x, \\ T_2(x) &= 2x^2 - 1, \\ T_3(x) &= 4x^3 - 3x, \\ T_4(x) &= 8x^4 - 8x^2 + 1, \\ T_5(x) &= 16x^5 - 20x^3 + 5x. \end{aligned}$$

From the trigonometric relation

$$\cos(n\theta) + \cos(n-2)\theta = 2\cos\theta\cos(n-1)\theta \tag{3.2.2}$$

we derive the three-term recurrence formula:

$$T_{k+1}(x) = 2xT_k(x) - T_{k-1}(x), \qquad k = 1, 2, 3.... \tag{3.2.3}$$

with $T_0(x) = 1$ and $T_1(x) = x$.

The Chebyshev polynomials are eigenfunctions of the Sturm-Liouville problem:

$$\sqrt{1-x^2}(\sqrt{1-x^2}T_n'(x))' + n^2T_n(x) = 0, \tag{3.2.4}$$

or equivalently,

$$(1-x^2)T_n''(x) - xT_n'(x) + n^2T_n(x) = 0. \tag{3.2.5}$$

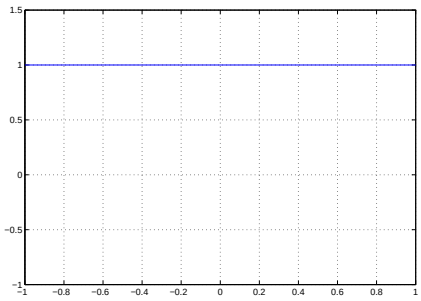

(a) $T_0(x) = 1$

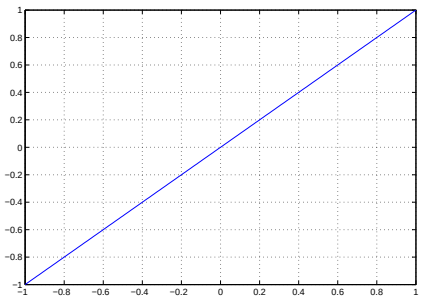

(b) $T_1(x) = x$

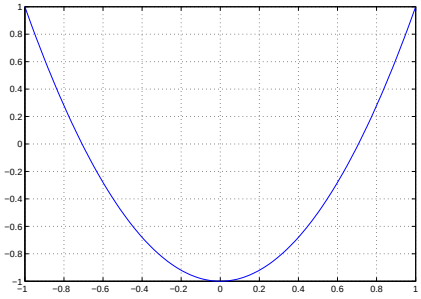

(c) $T_2(x) = 2x^2 - 1$

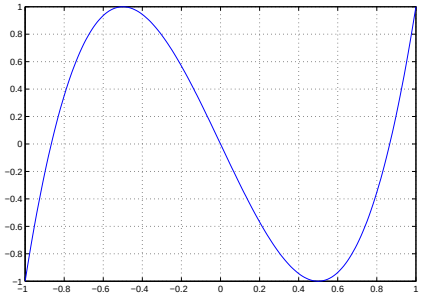

(d) $T_3(x) = 4x^3 - 3x$

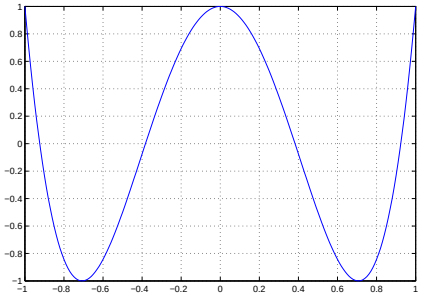

(e) $T_4(x) = 8x^4 - 8x^2 + 1$

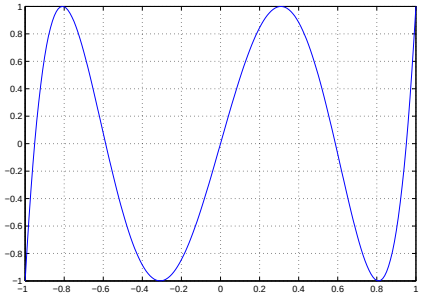

(f) $T_5(x) = 16x^5 - 20x^3 + 5x$

Figure 3.2.1: Plot of the first six Chebyshev polynomials

Chebyshev polynomials (of 1st kind) are a special case of Jacobi polynomials $\{J_n^{\alpha,\beta}\}$ for $(\alpha, \beta) = (-1/2, -1/2)$. Hence one can also derive its properties from those a Jacobi polynomals.

An immediate consequence is the recurrence relation

$$2T_n(x) = \frac{1}{n+1}T'_{n+1}(x) - \frac{1}{n-1}T'_{n-1}(x), \qquad n \geq 2. \tag{3.2.6}$$

One can derive from (3.2.1) that

$$T_n(-x) = (-1)^n T_n(x), \quad T_n(\pm 1) = (\pm 1)^n, \tag{3.2.7}$$

$$|T_n(x)| \le 1, \quad |T_n'(x)| \le n^2, \tag{3.2.8}$$

$$(1-x^2)T_n'(x) = \frac{n}{2}T_{n-1}(x) - \frac{n}{2}T_{n+1}(x), \tag{3.2.9}$$

$$2T_m(x)T_n(x) = T_{m+n}(x) + T_{m-n}(x), \quad m \ge n \ge 0. \tag{3.2.10}$$

and

$$T_n'(\pm 1) = (\pm 1)^{n-1} n^2, \tag{3.2.11}$$

$$T"_n(\pm 1) = \frac{1}{3}(\pm 1)^n n^2(n^2-1). \tag{3.2.12}$$

It is also easy to show that

$$\int_{-1}^{1} T_n(x)T_m(x)\frac{1}{\sqrt{1-x^2}} = \frac{c_n\pi}{2}\delta_{mn}, \tag{3.2.13}$$

where $c_0 = 2$ and $c_n = 1$ for $n \ge 1$. Hence, we find from (3.2.4) that

$$\int_{-1}^{1} T_n'(x)T_m'(x)\frac{1}{\sqrt{1-x^2}} = \frac{n^2 c_n\pi}{2}\delta_{mn}, \tag{3.2.14}$$

i.e., $\{T_n'(x)\}$ are mutually orthogonal with respect to the weight function $\sqrt{1-x^2}$. We can obtain from (3.2.6) that

$$T_n'(x) = 2n \sum_{k=0,k+n \text{ odd}}^{n-1} \frac{1}{c_k} T_k(x), \tag{3.2.15}$$

$$T"_n(x) = \sum_{k=0,k+n \text{ even}}^{n-2} \frac{1}{c_k} n(n^2-k^2)T_k(x). \tag{3.2.16}$$

Another remarkable consequence of (3.2.1) is that the Gauss-type quadrature nodes and weights can be derived explicitly.

Theorem 22. *[64, 87] Let $\{x_j, w_j\}_{j=0}^N$ be a set of Chebyshev-Gauss-type quadrature nodes and weights.*
For Chebyshev-Gauss (CG) quadrature,

$$x_j = -\cos\frac{(2j+1)\pi}{2N+2}, \qquad w_j = \frac{\pi}{N+1}, \quad 0 \le j \le N.$$

For Chebyshev-Gauss-Radau (CGR) quadrature,

$$x_j = -\cos\frac{2\pi j}{2N+1}, \quad 0 \le j \le N$$
$$w_0 = \frac{\pi}{N+1}, \qquad w_j = \frac{2\pi}{2N+1}, \quad 1 \le j \le N.$$

For Chebyshev-Gauss-Lobatto (CGL) quadrature,

$$x_j = -\cos\frac{\pi j}{N}, \qquad w_j = \frac{\pi}{\tilde{c}_j N}, \quad 0 \le j \le N.$$

where $\tilde{c}_0 = \tilde{c}_N = 2$ and $\tilde{c}_j = 1$ for $j = 1, 2, ..., N-1$.
With the above choices, there holds

$$\int_{-1}^{1} p(x)\frac{1}{\sqrt{1-x^2}}dx = \sum_{j=0}^{N} p(x_j)w_j, \quad \forall p \in P_{2N+\delta}, \tag{3.2.17}$$

where $\delta = 1, 0, -1$ for the CG, CGR and CGL respectively.

In the Chebyshev case, the nodes $\{\theta_j = \arccos(x_j)\}$ are equally distributed on $[0, \pi]$, whereas $\{x_j\}$ are clustered in the neighbourhood of $x = \pm 1$ with density $O(N^2)$, for instance, for the CGL points

$$1 - x_1 = 1 - \cos\frac{\pi}{N} = 2\sin^2\frac{\pi}{2N} \simeq \frac{\pi^2}{2N^2} \quad \text{for } N \gg 1.$$

For more properties on Chebyshev polynomials, we refer to Rivlin [81].

3.2.1 Chebyshev approximation

Given that the set of Chebyshev polynomials is complete and that polynomials are dense in $C([-1,1])$ it is thus natural to approximate any function by a unique series of Chebyshev polynomials. Therefore we have the following theorem, see theorem 3.1 of [87], more details also in Mason and Handscomb [64]

Theorem 23. *[14, 64] Let f be a Lipschitz continuous function on the interval [-1,1]. Then f admits a unique representation as a series of the form:*

$$u(x) = \frac{c_0}{2} + \sum_{k=1}^{\infty} c_k T_k(x). \tag{3.2.18}$$

where $T_k(x)$ are Chebyshev polynomials,

$$c_k = \frac{2}{\pi} \int_{-1}^{1} \frac{u(x)T_k(x)}{\sqrt{1-x^2}} dx, \qquad k = 0, 1, 2, 3, ... \tag{3.2.19}$$

This series converges uniformly and absolutely.

Thus, any continous function u on the interval $[-1,1]$ can be approximated by the following Chebyshev expansion:

$$\begin{aligned} u_n(x) &= \sum_{k=0}^{n} c_k T_k(x) && (3.2.20) \\ &= \underline{c} \cdot T(x) && (3.2.21) \end{aligned}$$

for some coefficients c_k and $\underline{c} = (c_0, c_1, \ldots, c_n)$ is the vector of coefficients associated with the approximation u_n.

Since this representation is unique and from Equation (3.1.3), a naive way to calculate the coefficients c_k is to view them as coefficients in the Fourier cosine series of the even 2π-periodic function $g(\theta) = f(\cos\theta)$. That is,

$$c_k = \frac{2}{\pi} \int_0^{\pi} f(\cos\theta)\cos(k\theta) d\theta \tag{3.2.22}$$

This integral can be computed in a simple manner by $(n+1)-$trapezoidal rule

$$c_k = \frac{2}{n}\left[\frac{1}{2}f_0 + f_1\cos\left(\frac{k\pi}{n}\right) + f_1\cos\left(\frac{k\pi}{n}\right) + ... \right. \tag{3.2.23}$$

$$... \quad \left. + f_{n-1}\cos\left(\frac{(n-1)k\pi}{n}\right) + \frac{1}{2}f_n\cos n\pi\right] \tag{3.2.24}$$

where $f_k = f(\cos\frac{k\pi}{n})$. Writing this equation at each node generates the following

$$\begin{bmatrix} c_0 \\ c_1 \\ c_2 \\ c_3 \\ c_4 \\ \vdots \\ c_{n-1} \\ c_n \end{bmatrix} = \frac{2}{n}\begin{bmatrix} \frac{1}{2} & 1 & 1 & 1 & \dots & 1 & \frac{1}{2} \\ \frac{1}{2} & \cos\frac{\pi}{n} & \cos\frac{2\pi}{n} & \cos\frac{3\pi}{n} & \dots & \cos\frac{\pi}{n} & \frac{1}{2}\cos\pi \\ \frac{1}{2} & \cos\frac{2\pi}{n} & \cos\frac{4\pi}{n} & \cos\frac{6\pi}{n} & \dots & \cos\frac{\pi}{n} & \frac{1}{2}\cos 2\pi \\ \frac{1}{2} & \cos\frac{3\pi}{n} & \cos\frac{6\pi}{n} & \cos\frac{9\pi}{n} & \dots & \cos\frac{\pi}{n} & \frac{1}{2}\cos 3\pi \\ \frac{1}{2} & \cos\frac{4\pi}{n} & \cos\frac{8\pi}{n} & \cos\frac{12\pi}{n} & \dots & \cos\frac{\pi}{n} & \frac{1}{2}\cos 4\pi \\ \vdots & \vdots & \vdots & \vdots & \ddots & \vdots & \vdots \\ \frac{1}{2} & \cos\frac{\pi}{n} & \cos\frac{4\pi}{n} & \cos\frac{6\pi}{n} & \dots & \cos\frac{\pi}{n} & \frac{1}{2}\cos\pi \\ \frac{1}{2} & \cos\frac{2\pi}{n} & \cos\frac{4\pi}{n} & \cos\frac{6\pi}{n} & \dots & \cos\frac{\pi}{n} & \frac{1}{2}\cos\pi \end{bmatrix}\begin{bmatrix} f_0 \\ f_1 \\ f_2 \\ f_3 \\ f_4 \\ \vdots \\ f_{n-1} \\ f_n \end{bmatrix} \tag{3.2.25}$$

This writes in matrix notation as:

$$\mathbf{c} = \mathbf{\Lambda f} \tag{3.2.26}$$

where $\mathbf{c}, \mathbf{f}$ are Chebyshev coefficients and function values of f at the quadrature points respectively, and the matrix Λ is defined by:

$$\Lambda_{jk} = \begin{cases} \frac{1}{n} & k = 0, \\ \frac{2}{n}\cos\frac{jk\pi}{n} & k = 1, ..., n-1, \\ \frac{1}{n}\cos j\pi & k = n. \end{cases}$$

3.2.2 Convergence

Let $M_n \geq 1$ be an integer, $\mathcal{P}_{M_n}$ be the set of polynomials of degree at most M_n and $\{x_{n,j}, \omega_{n,j}\}_{j=0}^{M_n}$ be the standard Chebyshev-Gauss-Lobatto quadrature, nodes and

weights with

$$x_{n,j} = -\cos\left(\frac{\pi j}{M_n}\right), \qquad 0 \le j \le M_n,$$
$$\omega_{n,0} = \omega_{n,M_n} = \frac{\pi}{2M_n}, \quad \omega_{n,j} = \frac{\pi}{M_n}, \quad 1 \le j \le M_n - 1.$$

It is clear that

$$T_{M_n+1}(x_{n,j}) - T_{M_n-1}(x_{n,j}) = 0. \tag{3.2.27}$$

Next, denote by $\mathcal{I}_{M_n} : C(\Lambda) \to \mathcal{P}_{M_n}$ the Chebyshev-Gauss-Lobatto interpolant, such that

$$\mathcal{I}_{M_n} u(_{n,j}) = u(x_{n,j}), \qquad 0 \le j \le M_n.$$

According to the property of standard Chebyshev-Gauss-Lobatto quadrature, it follows that for any $\phi \in \mathcal{P}_{2M_n-1}(\Lambda)$,

$$\int_\Lambda \phi(x)\omega(x)dx = \sum_{j=0}^{M_n} \phi(x_{n,j})\omega_{n,j} \tag{3.2.28}$$

Moreover, a direct computation shows that

$$\sum_{j=0}^{M_n} T^2_{M_n}(x_{n,j})\omega_{n,j} = \pi. \tag{3.2.29}$$

In particular, the following equivalence holds (cf.Guo [43]),

$$\int_\Lambda \phi^2(x)\omega(x)dx \le \sum_{j=0}^{M_n} \phi^2(x_{n,j})\omega_{n,j} \le 2\int_\Lambda \phi^2(x)\omega(x)dx, \qquad \forall \phi \in \mathcal{P}_{M_n}. \tag{3.2.30}$$

Let $H^r(\Lambda)$ be the usual Sobolev space associated with the semi-norm $|\cdot|_{H^r(\Lambda)}$ and norm $\|\cdot\|_{H^r(\Lambda)}$. Denote by c a generic positive constant independent of M_n, h_n and any functions. Then the following holds

Lemma 24. *[100] For any $u \in H^r(\Lambda)$ with integer $1 \le r \le M_n + 1$,*

$$\|u - \mathcal{I}_{M_n} u\|_{H^k(\Lambda)} \le c M_n^{k-r} \|(1-x^2)^{\frac{r-1}{2}} \partial_x^r u\|_{L^2(\Lambda)}, \qquad k = 0, 1. \tag{3.2.31}$$

Proof. (cf [100]) Thanks to results from Ma [62], we have

$$\|\partial_x \mathcal{I}_{M_n} u\|_{L^2(\Lambda)} + M_n \|\mathcal{I}_{M_n} u - u\|_{L^2} \le c \|\partial_x u\|_{L^2(\Lambda)}, \qquad \forall u \in H^1(\Lambda). \tag{3.2.32}$$

Next, let $\mathcal{I}^L_{M_n}$ be the standard Legendre-Gauss-Lobatto interpolant. Due to (2.16) of [42], we have that for any integer $r \ge 1$,

$$\|\partial(u - \mathcal{I}^L_{M_n} u)\|_{L^2(\Lambda)} \le c M_n^{1-r} \|(1-x^2)^{\frac{r-1}{2}} \partial_x^r u\|_{L^2(\Lambda)}. \tag{3.2.33}$$

Applying (3.2.32) to the function $u - \mathcal{I}^L_{M_n} u$ and using (3.2.33), we get

$$\begin{aligned} \|\partial(\mathcal{I}_{M_n} u - \mathcal{I}^L_{M_n} u)\|_{L^2(\Lambda)} + M_n \|\mathcal{I}_{M_n} u - u\|_{L^2(\Lambda)} &\le c \|\partial(u - \mathcal{I}^L_{M_n} u)\|_{L^2(\Lambda)} \\ &\le c M_n^{1-r} \|(1-x^2)^{\frac{r-1}{2}} \partial_x^r u\|_{L^2(\Lambda)}. \end{aligned} \tag{3.2.34}$$

Then the desired result follows from the triangle inequality and the approximation result (3.2.33). □

3.3 Differentiation and Integration

3.3.1 Differentiation in the Physical Space

We recall the Chebyshev approximation of any function (3.2.20)

$$u(x) = \sum_{k=0}^{n} c_k T_k(x). \tag{3.3.1}$$

By differentiation, its derivative is

$$u'(x) = \sum_{k=0}^{n} c_k T_k'(x). \tag{3.3.2}$$

On the collocation points, the equation becomes

$$\begin{aligned} u'(x_0) &= \sum_{k=0}^{n} c_k T_k'(x_0), \\ u'(x_1) &= \sum_{k=0}^{n} c_k T_k'(x_1), \\ &\vdots \\ u'(x_n) &= \sum_{k=0}^{n} c_k T_k'(x_n), \end{aligned}$$

which translates in matrix from as follows

$$\begin{bmatrix} u_0' \\ u_1' \\ \vdots \\ u_n' \end{bmatrix} = \begin{bmatrix} T_0'(x_0) & T_1'(x_0) & \dots & T_n'(x_0) \\ T_0'(x_1) & T_1'(x_1) & \dots & T_n'(x_1) \\ \vdots & & \ddots & \vdots \\ T_0'(x_n) & T_1'(x_n) & \dots & T_n'(x_n) \end{bmatrix} \begin{bmatrix} c_0 \\ c_1 \\ \vdots \\ c_n \end{bmatrix}$$

or simply

$$\mathbf{u}' = \mathbf{T}'\mathbf{c}.$$

Using (3.2.26) we get

$$\mathbf{u}' = \mathbf{T}'\mathbf{\Lambda}\mathbf{u}.$$

Therefore the matrix of the derivative operator is

$$\mathbf{D}' = \mathbf{T}'\mathbf{\Lambda}. \tag{3.3.3}$$

Which actually can be simply determined as follows:

$$d_{kj} = \begin{cases} -\frac{2n^2+1}{6}, & k = j = 0, \\ \frac{c_k}{c_j}\frac{(-1)^{k+j}}{x_k - x_j}, & k \neq j, 0 \leq k, j \leq n, \\ -\frac{x_k}{2(1-x_k^2)}, & 1 \leq k = j \leq n-1, \\ \frac{2n^2+1}{6}, & k = j = n, \end{cases} \tag{3.3.4}$$

3.3.2 Differentiation in the frequency space

Recall again equation (3.2.20) and differentiate it

$$u'(x) = \sum_{k=0}^{n} c_k T_k'(x). \tag{3.3.5}$$

The differentiation of relation (3.2.3)gives

$$T_0 = T_1', \tag{3.3.6}$$

$$T_1 = \frac{T_2'}{2}, \tag{3.3.7}$$

$$T_{n+1}(x) = nT_{n-1}'(x) - 2(1-x^2)T_n'(x), \tag{3.3.8}$$

$$\text{ie.} \quad T_n = \frac{T_{n+1}'}{2(n+1)} - \frac{T_{n-1}'}{2(n-1)}, \quad n = 2, 3, ... \tag{3.3.9}$$

Also remembering $u'(x)$ can be written directly using Equation (3.2.20) as:

$$u'(x) = \sum_{k=0}^{n} c_k' T_k(x) \tag{3.3.10}$$

where $\{c_k\}$ are coefficients of $u'(x)$. That implies that

$$\sum_{k=0}^{n} c_k' T_k(x) = c_0' + c_1' T_1 + \sum_{k=2}^{n-1} c_k' \left[\frac{T_{k+1}'}{2(k+1)} - \frac{T_{k-1}'}{2(k-1)}\right] \tag{3.3.11}$$

$$= \frac{c_{n-1}'}{2n} T_n' + \sum_{k=1}^{n-1} \frac{1}{2k}(\delta_k c_{k-1}' - c_{k+1}') T_k' \tag{3.3.12}$$

where $\delta_0 = 2$ and $\delta_k = 1$ for $k \geq 1$. Since $\{T'_k\}$ are mutually orthogonal, we compare the expansion coefficients in terms of $\{T'_k\}$ and find that $\{c'_k\}$ can be computed from $\{c_k\}$ via the backward recurrence relation:

$$\begin{aligned} c'_n = 0, c'_{n-1} = nc_n, \\ c'_{k-1} = \frac{2kc_k + c'_{k+1}}{c_{k-1}}, \quad k = n-1, ..., 1. \end{aligned} \tag{3.3.13}$$

Another way of computing the coefficients of the derivative is by means of induction. From the equation (3.3.5) and combining it with the recurrence formula in (3.3.9) yields an expression of u in terms of T_k's which writes as follows

$$\sum_{k=0}^{n} c'_k T_k(x) = \sum_{k=0}^{n}\sum_{l=0}^{n} d_{kl} c_l T_k(x), \tag{3.3.14}$$

$$ie. \quad \underline{c}' = D\underline{c} \tag{3.3.15}$$

For a certain matrix $D = (d_{kl})_{0<k,l<n}$. defined as follows:

$$\begin{cases} d_{kl} = 0, & \text{for } k \leq l, \\ d_{kl} = 0, & \text{if } l-k \text{ is even}, \\ d_{kl} = 2k, & \text{if } l-k \text{ is odd}. \end{cases} \tag{3.3.16}$$

As such D is a sparse upper triangular matrix. The later computation shall be used for differentiation in the frequency domain. So for higher derivatives we apply the above result recursively to get the spectral representation $c^{(p)}$ of the derivative at order p of u:

$$\underline{c}^{(p)} = D^p \underline{c}. \tag{3.3.17}$$

Having covered differentiation let us now have a look at numerical integration in the frequency space.

3.3.3 Integration

For the case of integration, recall again relation (3.3.9)

$$\begin{aligned} T_{n+1}(x) &= nT_{n-1}(x) - 2(1-x^2)T_n(x), && (3.3.18)\\ \int T_n(x)dx &= \frac{1}{2}\Big[\frac{T_{n+1}(x)}{n+1} - \frac{T_{n-1}(x)}{n-1}\Big], n = 2, 3..., && (3.3.19)\\ \int T_1(x)dx &= \frac{1}{4}T_2(x), && (3.3.20)\\ \int T_0(x)dx &= \frac{1}{2}T_1(x). && (3.3.21) \end{aligned}$$

As a linear operator, the integral of u will also be a continuous Lipschitz function in $[-1, 1]$, which will in turn have a unique expansion series of the form

$$\int u(x)dx = \sum_{k=0}^{n} I_k T_k(x), \qquad x \in [a, b],$$

where I_k's are coefficients of the integral of u, and similarly as with differentiation there exists a $n \times n$-matrix J such that

$$I_k = \sum_{l=0}^{n} J_{kl} c_l, \tag{3.3.22}$$

or simply

$$\underline{I} = J \cdot \underline{c} \tag{3.3.23}$$

where $\underline{I}$ is the spectral representation of the integral of u. In fact,

$$\begin{aligned} \int u(x)dx &= \int \sum_{k=0}^{n-1} c_k T_k(x), \\ i.e \qquad \sum_{k=0}^{n-1} I_k T_k(x) &= \int \sum_{k=0}^{n-1} c_k T_k(x)\ dx \\ &= \sum_{k=0}^{n-1} c_k \int T_k(x)\, dx \\ \sum_{k=0}^{n-1}\sum_{j=2}^{n-1} J_{kj} c_j T_k(x) &= \sum_{k=2}^{n} c_k \frac{1}{2}\Big[\frac{T_{k+1}}{k+1} - \frac{T_{k-1}}{k-1}\Big]. \end{aligned}$$

Performing a smart multiplication and rearranging terms we get the coefficients of J recursively as follows:

$$J_{kk} = 0, \quad J_{01} = \frac{1}{2}, \quad J_{k,k-1} = -J_{kk+1} = \frac{1}{k}.$$

So then, the spectral representation of the integral of u is the vector $\underline{d} = J.\underline{c}$. In other words, J is the spectral representation of the integral operator.

3.4 The multi-step spectral method

Consider a function u defined on an interval $[0, T]$ and let I_h be a mesh on the interval $[0, T]$:

$$I_h := \{t_n : 0 = t_0 < t_1 < \cdots < t_n = T\}$$

We denote by $\Lambda_n[t_{n-1}, t_n], h_n = t_n - t_{n-1}$ and $u^n(t)$ the projection of $u(t)$ on the n-th element Λ_n, namely,

$$u^n(t) = u(t), \qquad \forall t \in \Lambda_n, \qquad 1 \le n \le N.$$

Let $\omega_n(t) = \frac{1}{\sqrt{(t-t_{n-1})(t_n-t)}}$. We define the shifted Chebyshev polynomials by

$$T_{n,j}(t) := T_j\left(\frac{2t - t_{n-1} - t_n}{h_n}\right), \qquad t \in \Lambda_n.$$

Clearly, $T_{n,0}(t) = 1, T_{n,1}(t) = (2t - t_{n-1} - 2t_n)/h_n$, and

$$T_{n,j+1}(t) = \frac{4t - 2t_{n-1} - 2t_n}{h_n} T_{n,j}(t) - T_{n,j-1}(t), \qquad j \geq 1.$$

The set of $T_{n,j}(t)$ is a complete $L^2_{\omega_n}(\Lambda_n)$-orthogonal system, namely,

$$\int_{\Lambda_n} T_{n,j}(t) T_{n,k}(t) \omega_n(t) dt = \frac{\pi}{2} c_j \delta_{j,k}. \tag{3.4.1}$$

Thus, for any $v(t) \in L^2_{\omega_n}(\Lambda_n)$, we can write

$$v(t) = \sum_{j=0}^{\infty} v_j T_{n,j}(t), \qquad v_j = \frac{2}{\pi c_j} \int_{\Lambda_n} v(t) T_{n,j}(t) \omega_n(t) dt.$$

Moreover, we have

$$T_{n,j}(t) = \frac{h_n}{4(j+1)} T'_{n,j+1}(t) - \frac{h_n}{4(j-1)} T'_{n,j-1}(t), \tag{3.4.2}$$

$$T_{n,j}(t_{n-1}) = (-1)^j, \quad T_{n,j}(t_n) = 1. \tag{3.4.3}$$

Set

$$t_{n,j} = \frac{1}{2}\left(h_n x_{n,j} + t_{n-1} + t_n\right).$$

According to (3.2.27),

$$T_{n,M_n+1}(t_{n,j}) - T_{n,M_n-1}(t_{n,j}) = 0. \tag{3.4.4}$$

Further, it follows from (3.2.28) that for any $\psi \in \mathcal{P}_{2M_n-1}(\Lambda_n)$,

$$\int_{\Lambda_n} \psi(t) \omega_n(t) dt = \sum_{j=0}^{M_n} \psi(t_{n,j}) \omega_{n,j}. \tag{3.4.5}$$

Next, let $(u,v)_{\omega_n}$ and $\|v\|_{\omega_n}$ be the inner product and the norm of space $L^2_{\omega_n}(\Lambda)$ with

$$(u,v)_{\omega_n}=\int_{\Lambda_n} u(t)v(t)\omega_n(t)dt, \qquad \|v\|_{\omega_n}=(v,v)^{1/2}_{\omega_n}.$$

We also introduce the following discrete inner product and norm in the interval Λ_n,

$$< u,v >_{M_n}=\sum_{j=0}^{M_n} u(t_{n,j})v(t_{n,j})\omega_{n,j}, \qquad \|v\|_{M_n}=< v,v >^{1/2}_{M_n}. \tag{3.4.6}$$

Thanks to (3.4.5), for any $\phi\psi\in\mathcal{P}_{2M_n-1}(\Lambda_n)$ and $\varphi\in\mathcal{P}_{M_n-1}(\Lambda_n)$,

$$(\phi,\psi)_{\omega_n}=< \phi,\psi >_{M_n}, \qquad \|\varphi\|_{\omega_n}=\|\varphi\|_{M_n}. \tag{3.4.7}$$

According to (3.2.30) we deduce readily that for any $\phi(t)\in\mathcal{P}_{M_n}$,

$$\|\varphi\|_{\omega_n}\le\|\varphi\|_{M_n}\sqrt{2}\|\varphi\|_{\omega_n}. \tag{3.4.8}$$

Furthermore, by (3.2.29) we get

$$< T_{n,M_n},T_{n,M_n} >_{M_n}=\pi. \tag{3.4.9}$$

Let $H^r(\Lambda_n)$ be the usual Sobolev space associated with the semi-norm $|\cdot|_{H^r(\Lambda_n)}$ and the norm $\|\cdot\|_{H^r(\Lambda_n)}$. Particularly, $\|\cdot\|_{L^2(\Lambda_n)}=\|\cdot\|_{H^0(\Lambda_n)}$. Denote by $\pi_{M_n}:C(\Lambda_n)\to\mathcal{P}_{M_n}$ the shifted Chebyshev-Gauss-Lobatto interpolant such that

$$\pi_{M_n}v(t_{n,j})=v(t_{n,j}), \qquad 0\le j\le M_n.$$

Theorem 25. *[100] For any $v\in H^r(\Lambda_n)$ with integer $1\le r\le M_n+1$,*

$$\|v-\pi_{M_n}v\|_{L^2(\Lambda_n)} \le ch_n^r M_n^{-r}|v|_{H^r(\Lambda_n)}, \tag{3.4.10}$$

$$|v-\pi_{M_n}v|_{H^1(\Lambda_n)} \le ch_n^{r-1}M_n^{1-r}|v|_{H^r(\Lambda_n)} \tag{3.4.11}$$

This proof and the next theorem are taken from Wang and Mu [100]

Proof. Let $u(x) = v(t)|_{t=\frac{h_n x + t_{n-1} + t_n}{2}}$. Then we have

$$\pi_{M_n} v(t_{n,j}) = v(t_{n,j}) = u(x_{n,j}) = \mathcal{I}_{M_n} u(x_{n,j}), \qquad 0 \le j \le M_n.$$

Moreover, $\pi_{M_n} v(t)|_{t=\frac{h_n x + t_{n-1} + t_n}{2}}$ and $\mathcal{I}_{M_n} u(x)$ belong to $\mathcal{P}_{M_n}$ in the variable x. Hence

$$\pi_{M_n} v(t)|_{t=\frac{h_n x + t_{n-1} + t_n}{2}} = \mathcal{I}_{M_n} u(x). \tag{3.4.12}$$

This with (3.2.31) leads to

$$\begin{aligned} \|v - \pi_{M_n} v\|_{L^2(\Lambda_n)^2} &= \frac{h_n}{2} \int_{\Lambda_n} [u(x) - \mathcal{I}_{M_n} u(x)]^2 \, dx \\ &\le c h_n M_n^{-2r} \int_{\Lambda_n} [\partial_t^r u(x)]^2 (1 - x^2)^{r-1} dx \\ &\le c h_n^2 M_n^{-2r} \int_{t_{n-1}}^{t_n} [\partial_t^r v(t)]^2 (t - t_{n-1})^{r-1} (t_n - t)^{r-1} dt \\ &\le c h_n^2 M_n^{-2r} |v|^2_{H^r(\Lambda_n)}. \end{aligned} \tag{3.4.13}$$

similarly,

$$\begin{aligned} |v - \pi_{M_n} v|_{H^1(\Lambda_n)^2} &\le c M_n^{2-2r} \int_{\Lambda_n} (\partial_t^r v(t))^2 (t - t_{n-1})^{r-1} (t_n - t)^{r-1} dt \\ &\le c h_n^{2r-2} M_n^{2-r} |v|^2_{H^r(\Lambda_n)}. \end{aligned} \tag{3.4.14}$$

This ends the proof. □

As for the global error on the entire interval Λ let denote

$$h_{\max} = \max_{1 \le n \le N} h_n \qquad \text{and} \qquad M_{\min} = \min_{1 \le n \le N} M_n.$$

For our convergence analysis, we need the following discrete Gronwall lemma

Lemma 26. *Let $\{a_n\}_{n=1}^N$ be two sequences of nonnegative real numbers with $b_1 \le b_2 \le \cdots \le b_N$. Assume tha for $c \ge 0$ and $k_i > 0, i = 1, \cdots, N-1$, the following inequalities hold*

$$a_1 \le b_1, a_n \le b_n + c\sum_{i=1}^{n-1} k_i a_i, \quad n = 2, \cdots, N. \tag{3.4.15}$$

Then, we have

$$a_n \le b_n e^{c\sum_{i=1}^{n-1} k_i}, \text{ for } n = 1, \cdots, N. \tag{3.4.16}$$

Next let $U_M(t)$ be the global approximation of u, which is given by

$$U_M(t) = U_{M_n}(t), \quad t \in \Lambda_n, \quad 1 \le n \le N.$$

Theorem 27. *[64, 100] Assume that u belongs to the broken Sobolev space: $u \in H^1(0,T)$ and $u|_{\Lambda_n} \in H^{r_n}(\Lambda_n)$, $1 \le n \le N$ with integers $2 \le r_n \le M_n + 1$, and there exists a constant $L \ge 0$ such that for any z_1 and z_2,*

$$|f(z_1, t) - f(z_2, t)| \le L|z_1 - z_2|. \tag{3.4.17}$$

Then for

$$2\sqrt{2\pi}h_{\max}L \le \beta < 1, \tag{3.4.18}$$

we have

$$\|u - U_M\|^2_{H^1(0,T)} \le c_\beta T e^{c_\beta T} \sum_{i=1}^{N} h_i^{2r_i-2} M_i^{2-2r_i} |u|^2_{H^{r_i}(\Lambda)}, \tag{3.4.19}$$

where c_β is a positive constant depending only on β.

For full proof the reader can refer to Wang and Mu [100].

The next part of this dissertation is devoted to applications of the designed spectral methods to financial problems. Let us begin with pricing under general affine jump diffusion models which is a very large class of pricing problems in finance.

Part II

Application to Finance

Chapter 4

A time multidomain spectral method for valuing affine stochastic volatility and jump diffusion models

This chapter is a slightly modified version of the article published in *Communications in Nonlinear Science and Numerical Simulation*, and has been reproduced here with the permission of Elsevier, the copyright holder. The paper is available at the following link: `https://www.sciencedirect.com/science/article/abs/pii/S1007570419304782`.

4.1 Introduction

A quest for efficient solutions for option pricing problems in the financial market has been an on going topic of research among academics and practitioners. In the early 70's, Fisher Black and Myron Scholes published an influential paper where they presented the Black-Scholes model which soon became a major source for most financial traders for pricing and hedging options. The model represents a parabolic partial differential equations (PDE) with constant coefficients to be solved, see [11, 21]. In this context closed form solutions could still be found in case of one dimension with few parameters.

However empirical studies show that volatility of financial assets follows a stochas-

tic process and also that underlying stock prices experience jumps. In this case, option pricing problems result into solving a multi-dimensional partial integro-differential equation (PIDE) which gets more complicated to solve as the dimension increases. Various numerical solutions have been proposed for solving these problems.

In one dimension, classical numerical methods such as Finite Difference Methods (FDM) or Finite Element Method (FEM) [31, 45] were used to solve these PIDEs, numerically. Pindza et al. [73, 74, 75] proposed a robust spectral method to obtain accurate solutions to these PIDEs. Ngounda et al. [68] provided a combined spectral domain decomposition method and an inverse Laplace transform with Bromwich contour integral to obtained spectral convergence for pricing of European options.

In two dimensions, in't Hout et. al [90] proposed new ADI schemes to solve the pricing of the European option under the Bates model numerically, Zhu et. al [109] developed a Legendre quadrilateral spectral element approximation for the Black-Scholes equation to price European options with two underlying assets. Their methodology displayed an exponential convergence. Clift et. al [84] derived a modified finite differential method by combining a fixed point iteration scheme with an FFT to avoid dense linear system solutions and improve the efficiency of the existing methods.

In three dimensions, computational intensive works were conducted by Taruvinga et. al [91], they used an accurate and efficient method of line to compute a three-asset American options with jumps. The above methods are without doubt very effective in the sense they provide accurate solutions of Black-Sholes PIDE directly in a reasonable time. However as the dimension gets higher, these numerical methods begin to suffer the curse of dimensionality. A tremendous amount of computation can be reduced if one could avoid the PIDE by taking advantage of the dynamics of the underlying asset and considering volatility models without departing so much from reality, unlike the original Black-Scholes model that considered volatility to be constant.

So, in order to maintain a balance between effectiveness of solution and solvability of option pricing problems, Heston [47] presents a model with stochastic volatility

that includes correlation and capable to provide semi-closed form solution for option prices in terms of the characteristic function of the Log-stock price. The solution is more realistic, consistent with the smile and the skewness observed from empirical data. The model is later on generalised by Duffie et al. [28] to cater for an entire class of affine jump diffusion processes. The main advantage with such processes lies in applying some transform analysis to arrive at a system of stiff Riccati equations that can still be solved analytically although costly, but also numerically.

Many approaches have been used to obtain numerical solution of the stiff Riccati equations, these approaches include finite difference methods, homotopy perturbation methods [66]. Unfortunately these methods tend to require many points to achieve good results and also turn out to lose their accuracy for larger time scale. This is due to the fact that some component in the solution decays more rapidly than others, forcing thus any numerical method with a finite region of stability, to excessively use more stepsizes in order to get smoothness of solution. This inevitably leads to decrease of the efficiency and accumulates more machine roundoff error [50]. Dahlquist and Bjorck [22], Huang [51] recommend the use of implicit methods when comes to stiff problems. For these reasons we introduce a time spectral domain decomposition method for solving Riccati system of equations, numerically.

The literature around spectral methods is rich. These methods have been used in several areas such as computational fluid dynamics Canuto et al. [16], Hussaini and Zang [52], modeling different types of wave motion Komatitsch and Tromp [57], weather forecasting Bourke et al. [13] and finance Pindza et al. [73, 74]. Spectral methods have the particularity of handling technical boundary value problems in the sense that the solution is approximated by a series of polynomials, the particularity of the polynomials reside on the way coefficients are calculated. In the case of Chebyshev spectral method, the solution is given as a Chebyshev series and the differential equation is shifted to the interval $[-1, 1]$. Chebyshev spectral methods could be implemented as Galerkin and Tau methods, where the work takes place in the frequency space or as pseudospectral methods where the work takes place in the physical space [14]. Since most softwares

are matrix orientated, an effective way to apply the above methods computationally would be in an operatorial way. That is the solution is presented as $U = A^{-1}F$ where U is the solution vector at some given points, A is a matrix, and F is some vector.

Bhrawy and Alofi [9] introduces operational matrix to the shifted Chebyshev method to generate already a fast algorithm for fractional integration in the sense that only a small number of shifted Chebyshev polynomials is needed to obtain a satisfactory result. More on this approach can be found in Weideman and Reddy [101], Trefethen [93] with some variants but still based on the pseudospectral methods. Although accurate, one main disadvantage with pseudospectral is that the differention matrix is full making the computation of A^{-1} a heavy task. However significant computational savings can be realized via representation in frequency domain. Trif [94] proposed a solution based on Tau method allowing to avoid full matrices. We shall follow these footsteps.

In this chapter, we develop a time-spectral domain decomposition method based the Tau-matrix operational approach using a differentiation matrix method on a time interval divided into disjoint domains. The obtained matrices have the advantage of being sparse upper triangular instead of full as most operational matrix methods produce. The methodology is applied to solve systems of stiff Riccati equations that are encountered in pricing under stochastic volatility model even in presence of jumps. Numerical results show that our method is fast, accurate and robust as compared to the existing Chebfun method [76], which is to my knowledge one the most well-known and leading package of Matlab using spectral methods.

This work is organised as follows. Section 4.2 gives a quick layout of the mathematical model and results under affine settings. Section 4.3 introduces the numerical method, and Section 4.4 is applications on case studies. In the last Section 8, we draw a conclusion.

4.2 The mathematical model setup

Consider the financial market model $\mathcal{M} = \left(\Omega, \mathcal{F}, \mathbb{P}, (\mathcal{F}_t)_{t\geq 0}, (S_t)_{t\geq 0}\right)$ where Ω is the set of all possible outcomes of an experiment known as the sample space, $\mathcal{F}$ is the set of all events, i.e. permissible combinations of outcomes, $\mathbb{P}$ is a map $\mathcal{F} \longrightarrow [0,1]$ which assigns a probability to each event, $(\mathcal{F}_t)_{t\geq 0}$ is a natural filtration and S_t a risky underlying asset price process. The triplet $(\Omega, \mathcal{F}, \mathbb{P})$ is defined as a probability space. Let $(W_t)_{t\geq 0}$ be a $\mathbb{P}$-Wiener process, $(Z_t)_{t\geq 0}$ is a pure jump process (a poisson process with parameter λ_t), $\sigma(t, X_t) > 0$ the volatility of the underlying asset, $\mu(t, X_t)$ the drift parameter. We consider a state (underlying) process X_t satisfying the following stochastic differential equation

$$dX_t = \mu(t, X_t)dt + \sigma(t, X_t)dW_t + dZ_t. \tag{4.2.1}$$

In order to avoid arbitrage, the price $\Psi(t, X_t)$ at time t of a contingent claim that pays off Φ_T at maturity time $T \geq t$, under an equivalent martingale measure $\mathbb{Q}$, is given by

$$\Psi(t, X_t) = E^{\mathbb{Q}}\left(e^{-\int_0^T r(s,X_s)ds}\Phi_T|\mathcal{F}_t\right), \tag{4.2.2}$$

where the expectation is taken with respect to the risk-neutral measure $\mathbb{Q}$. The application of Ito differentiation on equation (4.2.2) (see [66]) yields the partial integro differential equation (PIDE) of the form

$$\frac{\partial \Psi_t}{\partial t} + \mu_t \frac{\partial \Psi_t}{\partial X_t} + \frac{1}{2}\sigma_t \sigma_t^{\top} \frac{\partial^2 \Psi_t}{\partial X_t^2} - \lambda_t \Psi_t + \lambda_t \int_{\mathbb{R}\setminus 0} \Psi(x_s + z)d\nu_0(z) = 0. \tag{4.2.3}$$

In affine framework (see also [21]), the drift vector μ_t, the instantaneous covariance matrix $\sigma_t\sigma_t^{\top}$, the jump intensity λ_t and the risk free rate r_t have an affine dependence

on X_t:

$$\begin{aligned}
\mu_t &= K_0 + K_1 \cdot X_t, && (K_0, K_1) \in \mathbb{R}^d \times \mathbb{R}^{d\times d} \\
\sigma_t \sigma_t^\top &= H_0 + H_1 \cdot X_t, && (H_0, H_1) \in \mathbb{R}^{d\times d} \times \mathbb{R}^{d\times d\times d} \\
\lambda_t &= l_0 + l_1 \cdot X_t, && (l_0, l_1) \in \mathbb{R}^d \times \mathbb{R}^{d\times d} \\
r_t &= \rho_0 + \rho_1 \cdot X_t, && (\rho_0, \rho_1) \in \mathbb{R}^d \times \mathbb{R}^{d\times d}.
\end{aligned}$$

Duffie et al. [28] show that under some conditions the solution of the PIDE (4.2.3) can be computed via the complex-valued Riccati ordinary differential equations (ODEs) defined as follows:

Theorem 28. *[28] Under technical conditions, if the pay-off function Φ_T, at maturity time T, is chosen such that*

$$\Phi_T = e^{uX_T}, \text{ for some } u \in \mathbb{R}^d$$

then Ψ is of the form

$$\Psi(t, X_t) = e^{\alpha(t)+\beta(t)X_t} \tag{4.2.4}$$

with α and β verifying the following Riccati equation

$$\begin{cases}
\frac{\partial \alpha}{\partial t}(t) = \rho_0 - K_0 \cdot \beta(t) - \frac{1}{2}\beta(t)^\top H_0 \beta(t) - l_0 \left[\Lambda(\beta(t)) - 1\right], \\
\\
\frac{\partial \beta}{\partial t}(t) = \rho_1 - K_1^\top \beta(t) - \frac{1}{2}\beta(t)^\top H_1 \beta(t) - l_1 \left[\Lambda(\beta(t)) - 1\right],
\end{cases} \tag{4.2.5}$$

with terminal conditions $\alpha(T) = 0$ and $\beta(T) = u$.

It is without doubt that equation (4.2.5) is analytically difficult to solve and in general they present stiffness. We require numerical methods to come to the rescue. In the next section, we introduce the time multidomain spectral method based on operational matrix.

4.3 Multidomain Spectral method

Recall the spectral representation of any function u given by Equation (3.2.20) and its derivative:

$$u'(x) = \sum_{k=0}^{n} c_k T_k'(x). \tag{4.3.1}$$

Section 3.3.2 tells us of the existence of a matrix $D = (d_{kl})_{0<k,l<n}$ such that

$$\begin{aligned} \sum_{k=0}^{n} \underline{c}_k' T_k(x) &= \sum_{k=0}^{n}\sum_{l=0}^{n} d_{kl} c_l T_k(x), & (4.3.2)\\ ie. \quad \underline{c}' &= D\underline{c} & (4.3.3) \end{aligned}$$

where $\underline{c}'$ stands for the spectral representation of the derivative function u'. Moreover, D is a sparse upper triangular matrix, with the following properties

$$\begin{cases} d_{kl} = 0, & \text{for } k \leq l, \\ d_{kl} = 0, & \text{if } l-k \text{ is even}, \\ d_{kl} = 2k, & \text{if } l-k \text{ is odd}. \end{cases} \tag{4.3.4}$$

Applying the above result recursively we get the spectral representation $c^{(p)}$ of the derivative at order p of u as:

$$\underline{c}^{(p)} = D^p \underline{c}. \tag{4.3.5}$$

Consequently, if we consider a general differential equation $\mathcal{A}u = f$ of order m with constant coefficients for which the differential operator can be written as $\mathcal{A} = L + \mathcal{N}$ where L and $\mathcal{N}$ are respectively the linear part and the nonlinear part, then the equation can be written as

$$\begin{aligned} Lu(t) + \mathcal{N}u(t) &= f(t) & (4.3.6)\\ \sum_{k=0}^{m} u^{(k)}(t) &= -\mathcal{N}u(t) + f(t) & (4.3.7) \end{aligned}$$

The above equation can be represented in the frequency space as:

$$\begin{aligned} \sum_{k=0}^{m} D^k \underline{c} &= -\mathbf{n} + \tilde{\mathbf{f}}, \\ A\,\underline{c} &= \mathbf{f}, \\ \text{implying} \qquad \underline{c} &= A^{-1}(\mathbf{f}) \end{aligned} \tag{4.3.8}$$

for some $A = \sum_{k=0}^{m} D^k$; where $\mathbf{n}, \tilde{\mathbf{f}}$ are the spectral representation of $\mathcal{N}u$ and f respectively, and $\mathbf{f} = -\mathbf{n} + \tilde{\mathbf{f}}$. we use the following algorithm 1:

Algorithm 1 Pseudo code

```
u_0 ← initial solution
INITIALIZE A
Evaluate N, and f at u_0
u := A^{-1} * (N + f)
while ||u − u_0|| > ε do
    u_0 ← u
    Evaluate N, and f at u_0
    u = A^{-1} * (N + f)
end while
RETURN u
```

The above method has proven to struggle when T gets larger. For this reason, we suggest a domain decomposition of the interval $[0, T]$.

Recall the partition I_h to be a mesh on the interval $[0, T]$ and N be the number of subintervals, as defined in section 3.4

$$I_h := \{t_n : 0 = t_0 < t_1 < \cdots < t_N = T\}.$$

We denote by $\Lambda_n = [t_{n-1}, t_n]$, $h_n = t_n - t_{n-1}$ and $u^n(t)$ the solution of (4.3.6) on the n-th element of the partition I_h, namely,

$$u^n(t) = u(t), \qquad \forall t \in \Lambda_n, \qquad 1 \le n \le N.$$

Let $M_n > 0$ be an integer and consider $\mathcal{P}_{M_n}$ to be the space of polynomials of order

at most M_n built on Λ_n. We apply the spectral method as described is algorithm 1 to obtain a numerical solution $U_{M_n} \in \mathcal{P}_{M_n}$ on Λ_n. The Time Multidomain Spectral Method on the interval $[0, T]$ consists of a successive application of the spectral method on each Λ_n to obtain a global numerical solution $U_M(t)$ of (4.3.6) defined such that:

$$U_M(t) = U_{M_n}(t), \quad t \in \Lambda_n, \quad 1 \leq n \leq N.$$

where M is taken to be the smallest of the M_n's: that is, $M = \inf_{0<n\leq N} M_n$.

For each subinterval $[t_i, t_{i+1}]$ equation (4.3.8) is applied.

$$A^{(i)}\mathbf{c}^{(i)} = \mathbf{f}^{(i)}, \qquad i = 0, ..., m-1. \tag{4.3.9}$$

The overall matrix A of the entire problem is then a diagonal of block matrices $A^{(i)}$.

$$\begin{pmatrix} A^{(1)} & 0 & & \\ 0 & A^{(2)} & 0 & \\ & \ddots & \ddots & \\ & & 0 & A^{(m)} \end{pmatrix} \begin{pmatrix} \mathbf{c}^{(1)} \\ \mathbf{c}^{(2)} \\ \vdots \\ \mathbf{c}^{(m)} \end{pmatrix} = \begin{pmatrix} \mathbf{f}^{(1)} \\ \mathbf{f}^{(2)} \\ \vdots \\ \mathbf{f}^{(m)} \end{pmatrix} \tag{4.3.10}$$

By inversion of the matrix $A^{(i)}$ on each domain Λ_i, we obtain $c^{(i)}$ and therefore u_{M_i} which is U_M on Λ_i.

In this case a global error can arise and jeopardise the convergence. But thanks be to the theorem 27 that still guaranties an exponential convergence even after discretization.

4.4 Applications and numerical results

In this section, we apply our method to different problems found in finance and test the convergence and the efficiency of the proposed method again the existing Chebfun method [76]. In all numerical experiments, when analytical solutions are not available,

we choose the solution from ODE15s with relative and absolute tolerances to be 10^{-14} as the benchmark solution as one of the appropiate Matlab package for stiff problems [70]. The error E is the maximal error given by:

$$||E|| = ||Sol_{Benchmark} - Sol_{Numerical}||_{\infty}. \tag{4.4.1}$$

4.4.1 Oil price model

The model for oil pricing is derived as follows. Let S_t be the spot price of the crud oil and V_t the stochastic variance. We allow the log-stock price to be driven by

$$d\ln S_t = \mu_t dt + \sqrt{V_t} dW_t^s + dZ_t^s. \tag{4.4.2}$$

The stochastic variance is considered to be square root process. In absence of jump, the mean reverting toward the parameter v is the long run mean of V. The process reverts at a speed controlled by the parameter κ and σ_v is the volatility of the volatility. It measures the responsiveness to diffuse volatility shocks. The volatility is driven by the following dynamics:

$$dV_t = \kappa(v - V_t)dt + \sigma_v \sqrt{V_t} d\tilde{W}_t^v \tag{4.4.3}$$

with $corr[dW_t^s, dW_t^v] = \rho$ and that the jump process Z_t^s of S_t arrive exponentially with rate λ_t and with size normally distributed $N(\bar{\mu}_s, \sigma_s)$. Therefore the model is expressed as:

$$d\begin{bmatrix} Y_t \\ V_t \end{bmatrix} = \begin{bmatrix} r - \lambda_t m_s - \frac{1}{2}V_t \\ \kappa(v - V_t) \end{bmatrix} dt + \sqrt{V_t} \begin{bmatrix} 1 & 0 \\ \rho\sigma_v & \sqrt{1-\rho^2}\sigma_v \end{bmatrix} dW_t + dZ_t. \tag{4.4.4}$$

Considering the state process $X_t = \begin{bmatrix} Y_t \\ V_t \end{bmatrix}$, equation (4.4.4) can then be written

as:

$$dX_t = \mu_t dt + \sigma_t dW_t + dZ_t$$

where

$$\mu_t = \begin{bmatrix} r - \lambda_t m_s \\ \kappa v \end{bmatrix} + \begin{bmatrix} 0 & -\frac{1}{2} \\ 0 & -\kappa \end{bmatrix} X_t \quad \text{and} \quad \sigma_t \sigma_t^\top = \begin{bmatrix} 1 & \rho\sigma_v \\ \rho\sigma_v & \sigma_v^2 \end{bmatrix} V_t$$

Referring to affine settings in (4.2.5), we see that:

$$\rho_0 = r,\ \rho_1 = (0,0),\ l_0 = \lambda_t,\ l_1 = (0,0),$$

$$K_0 = \begin{bmatrix} r - \lambda m_s \\ \kappa v \end{bmatrix},\ K_1 = \begin{bmatrix} 0 & -\frac{1}{2} \\ 0 & -\kappa \end{bmatrix},\ H_0 = \begin{bmatrix} 0 & 0 \\ 0 & 0 \end{bmatrix} \text{ and } H_1 = \left[\begin{array}{cc:cc} 0 & 0 & 1 & \rho\sigma_v \\ 0 & 0 & \rho\sigma_v & \sigma_v^2 \end{array}\right].$$

The oil price is given by:

$$\begin{aligned} \phi_t &= e^{\alpha(t)+\beta(t)\,x} \\ &= e^{\alpha(t)+\beta_1(t)y_t+\beta_2(t)V_t} \\ &= S_t^{\beta_1(t)}\, e^{\alpha(t)+\beta_2(t)V_t} \end{aligned}$$

where α and $\beta = (\beta_1, \beta_2)$ are real valued functions that satisfy the Riccati equation

$$\begin{cases} \dot{\alpha}(t) = r - (r - \lambda m_s)\beta_1(t) + \kappa v \beta_2(t) - \lambda(\Lambda(\beta(t)) - 1), \\ \dot{\beta}_1(t) = 0, \\ \dot{\beta}_2(t) = \frac{1}{2}\beta_1(t) + \kappa\beta_2(t) - \frac{1}{2}\beta_1^2(t) - \beta_1(t)\beta_2(t)\rho\sigma_v - \frac{1}{2}\beta_2^2(t)\sigma_v^2, \end{cases} \tag{4.4.5}$$

together with terminal conditions

$$\alpha(T) = 0 \text{ and } \beta(T) = (u, 0).$$

and Λ is defined as $\Lambda(c) = \int_{\mathbb{R}^2} \exp(c\,z) d\nu(z)$. In other words, $\Lambda(c)$ is the moment generating function of the random vector Z taken at c. The risk neutral condition

imposes $m_s = \Lambda(1,0) - 1$, that is $m_s = e^{\mu_s + \frac{\sigma_s^2}{2}}$ (see Duffie et al. [28]).

Considering the jump distribution to be of Gaussian type, that is $Z_t^s = N(\bar{\mu}_s, \sigma_s)$, we get

$$\Lambda(\beta(s)) = \Lambda(u, \beta_2(s)) = e^{u\bar{\mu}_s + \frac{u^2}{2}\sigma_s^2} \quad \text{and} \quad m_s = \Lambda(1,0) - 1 = e^{\mu^s + \frac{1}{2}\sigma_s^2}$$

Operating the change in time $\tau = T - t$ the system of equations reduces to

$$\begin{cases} \dot{\alpha}(\tau) = -r + (r - \lambda m_s)\beta_1(\tau) - \kappa v \beta_2(\tau) + \lambda(g(\tau) - 1) \\ \dot{\beta}_2(\tau) = -\frac{1}{2}\beta_1(\tau) - \kappa\beta_2(\tau) + \frac{1}{2}\beta_1^2(\tau) + \rho\sigma_v\beta_1(\tau)\beta_2(\tau) + \frac{1}{2}\sigma_v^2\beta_2^2(\tau) \end{cases}, \tag{4.4.6}$$

with

$$\alpha(0) = 0 \qquad \beta_2(0) = 0 \qquad \beta_1(\tau) = u$$

The exact solution of the above equation is:

$$\beta_2(\tau) = \frac{-a\,(1 - e^{-\gamma\tau})}{2\gamma - (\gamma + b)\,(1 - e^{-\gamma\tau})}, \tag{4.4.7}$$

$$\begin{aligned} \alpha(\tau) &= -r\tau + r\,u\tau - \kappa v \left[\frac{\gamma + b}{\sigma_v^2}\tau + \frac{2}{\sigma_v^2}\ln\left(1 - \frac{\gamma + b}{2\gamma}(1 - e^{-\gamma\tau})\right)\right] \\ &- \lambda(1 + m_s u)\tau + \lambda g(\tau), \end{aligned} \tag{4.4.8}$$

where $\gamma = b^2 - a\sigma_v^2$, and $g(\tau) = \tau\, e^{\mu^s + \frac{1}{2}\sigma_s^2}$.

For numerical illustration, we choose the parameters to have the following values, as illustrated in [59] :

$\mu_s = -1.8521, \quad \sigma_s = 1.9578, \quad \lambda = 0.0294, \quad \kappa = 0.0118, \quad v = 4.6978, \quad \sigma_v = 0.1655294,$
$\rho = -0.0083, \quad r = 0, \quad m_s = 0.0642.$

We compare our numerical solution with the exact solution and evaluate the error

as the L_∞ distance between the exact and the numerical solution. The plots in Figure 4.4.1a and 4.4.1b show that the exact and numerical solutions for variable α and β are in a good agreement.

We also run a comparison with another appropriate well known numerical method, here we mention Chebfun, which is based on spectral chebyshev polynomials too. As we vary the number of collocation points for both methods, we record in Figure 4.4.2a the error on variable α. It shows that as the number of collocation points gets larger ($n > 8$) TMDSM achieves better accuracy quicker than Chebfun. The same remark holds also for variable β.

In figure 4.4.2b a plot of the efficiency of the TMDSM and of Chebfun is provided. It is interesting to see that we achieve accuracy of order 10^{-15} within 0.005s, whereas Chebfun would take close to 0.02s to achieve the same order of accuracy on the same problem with the same processor Core I5-8th Gen. This is mostly due to the structure of the matrices inherited from the differentiation in the frequency space rather than in the physical space, which was mentioned to be sparse upper triangular whereas chebfun matrices differentiation matrices are full, see Figure 4.4.3. More elaborately, Figure 4.4.3a exhibits two upper triangles together with lines, it represents the plot of matrix operator A. The first triangle cares for the first variable x together with its boundary condition, and the second triangle is for the second variable y also with its boundary condition too. In reality these triangles contains trips of zeros, due to the relation (4.3.4). For a case of 100 collocation points for instance, the operator A is a (200×200)-matrix which has normally $40,000$ elements but in our case the total number of nonzero elements is 5398 and the rest are zeros. The sparsity coefficient is hence about 86.5% reducing considerably the amount of calculation of A^{-1}. As for the structure of the Chebfun matrix in 4.4.3b we have a totally dense matrix.

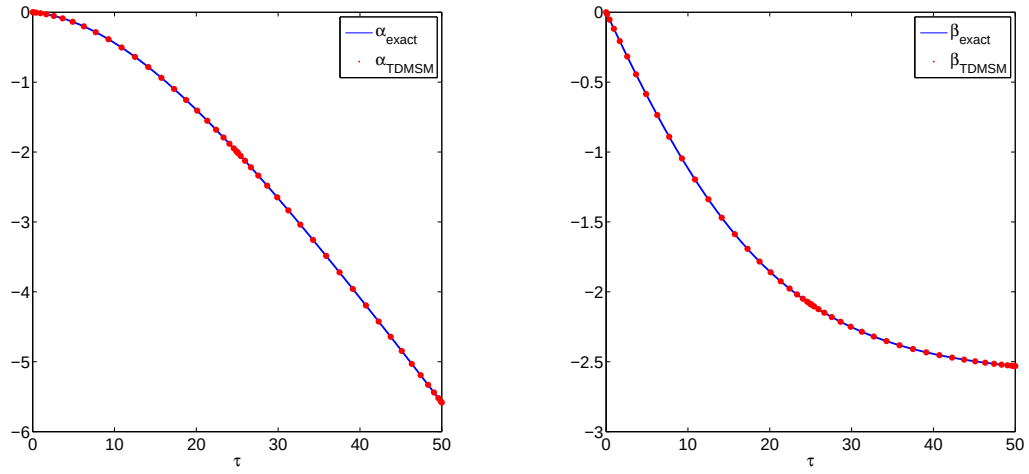

(a) α (b) β

Figure 4.4.1: Exact and numerical solutions plot for $T = 50$ with 2 domains

4.4.2 Interest rate model

Short rate models are helpful in pricing of assets such as bonds. It has been shown that most short rate time series experience mean reverting phenomenon that varies with time. It also appears that interest rates r_t converge rather quickly towards a time varying mean level μ_t which itself reverts more slowly toward an unconditional mean θ. One reason for this mean reversion is due to inflation factor that manifest itself in the required nominal interest rate, as mentioned by Andersen et al. [4]. Another key feature is that theory predicts that an unexpected information arrival should induce a discontinuity in the return process. An announced shift in monetary policy for instance, can induce the appearance of jumps in the interest rate process. Plus having jumps as part of the modeling can improve model description, calibration as jumps can also accommodate outliers in the short rate distribution. For this example we will restrict to jumps which are normally distributed and uncorrelated.

Thus, we consider the interest rate r to be driven by the following process:

$$dr_t = (\kappa_1 \bar{\mu}_t - \lambda \bar{\mu}_J - \kappa_1 r)\, dt + \sqrt{V_t} dW_t^r + dZ_t^r \tag{4.4.9}$$

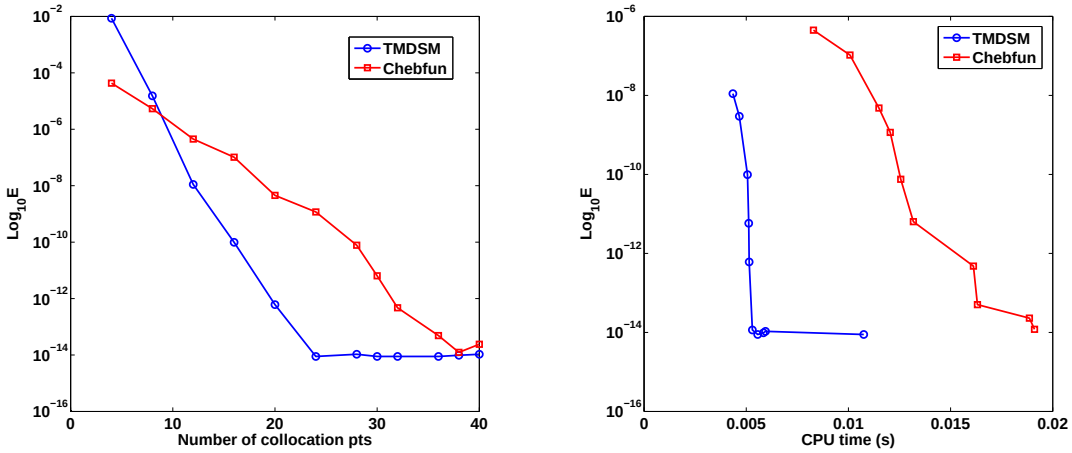

(a) Convergence (b) Efficiency

Figure 4.4.2: Convergence and efficiency of TMDSM vs Chebun on α.

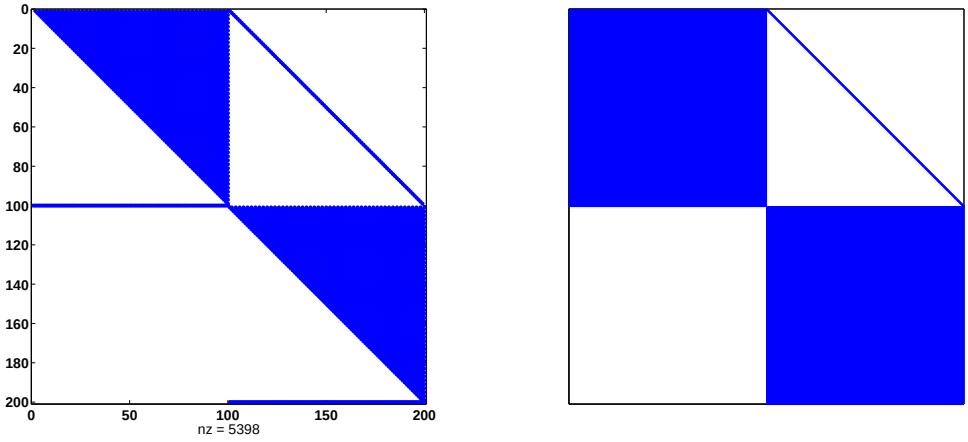

(a) 1-Domain TMDSM matrix (b) Chebfun matrix

Figure 4.4.3: Plots of the structure of the underlying matrix A for 1-Domain TMDSM vs Chebfun

where W_t^r, Z_t^r are respectively a Brownian process and a pure jump process (with constant intensity λ) associated with the stock price process. The stock price volatility $\sqrt{V_t}$ is stochastic with the following dynamics,

$$dV_t = \kappa_2(v - V_t)dt + \sigma_v\sqrt{V_t}dW_t^v$$

where W_t^r, W_t^v are independent Brownian motions.
Note in this model that the volatility is mean reverting, with mean v and κ_2 as mean reversion coefficient, σ_v is the volatility of the volatility. Also we consider the mean value $\bar{\mu}_t$ of the drift to be stochastic. This is due to some unsual change by governments in their monetary policies. Let write the dynamics of $\bar{\mu}_t$ be driven by the following equation:

$$d\bar{\mu}_t = \kappa_3(\bar{v} - \bar{\mu}_t)dt + \sigma_m\sqrt{\bar{\mu}_t}dW_t^m. \tag{4.4.10}$$

As it stands, a good candidate to consider as a state process is $X_t = (r_t, V_t, \bar{\mu}_t)$ where r_t is the short rate process.

$$d\begin{bmatrix} r_t \\ V_t \\ \bar{\mu}_t \end{bmatrix} = \begin{bmatrix} \kappa_1\bar{\mu}_t - \lambda\bar{\mu}_J - \kappa_1 r_t \\ \kappa_2 v - \kappa_2 V_t \\ \kappa_3\bar{v} - \kappa_3\bar{\mu}_t \end{bmatrix} dt + \sqrt{V_t}\begin{bmatrix} 1 & 0 & 0 \\ 0 & \sigma_v & 0 \\ 0 & 0 & \sigma_m \end{bmatrix} dW_t + dZ_t,$$

where $W_t = (W_t^r, W_t^v, 0)$ is a three-dimensional Brownian motion and $Z_t = (Z_t^r, 0, 0)$ is a three-dimensional Poisson process in t with mean arrival rate λ_t. As such the entire process X_t jumps only when r_t jumps. Hence the intensity arrival $\lambda_t = \lambda$ and the multivariate distribution of the jump size of Z_t is identical to the distribution of Z_t^r.

Referring to affine settings from section 4.2 and if we consider a financial claim that pays off $\Psi_T = e^{\bar{u}\cdot X_T}$ at time T for some constant $\bar{u} = (u_1, u_2, u_3) \in \mathbb{R}^3$ then theorem 28 ensures that its price ϕ_t at time $0 < t < T$ is of the form

$$\phi_t = e^{\alpha(t) + \beta(t)\,x} \tag{4.4.11}$$

where α and $\beta = (\beta_1, \beta_2, \beta_3)$ are deterministic functions of t that satisfy the Riccati equation (4.4.5), which yields the following:

$$\begin{cases} \dot{\alpha}(t) = 0 - (-\lambda^r \mu_J)\beta_1(t) - \kappa_2 v(\beta_2(t)) - \kappa_3 \eta \beta_3(t) - \lambda^r(\Lambda(\beta(t)) - 1), \\ \dot{\beta}_1(t) = 1 + \kappa_1 \beta_1, \\ \dot{\beta}_2(t) = \kappa_2 \beta_2(t) - \frac{1}{2}\beta_1^2(t) - \frac{1}{2}\sigma_v^2 \beta_2^2(t), \\ \dot{\beta}_3(t) = -\kappa_1 \beta_1(t) + \kappa_3 \beta_3(t) - \frac{1}{2}\sigma_m^2 \beta_3^2(t), \end{cases} \tag{4.4.12}$$

together with terminal conditions

$$\alpha(T) = 0 \text{ and } \beta(T) = (0, 0, 1).$$

Operate the rescaling time $\tau = T - t$. Also it is not difficult to see that the solution of β_1 is:

$$\beta_1(\tau) = \frac{1}{\kappa_1}[e^{-\kappa_1 \tau} - 1] \text{ i.e. } \beta_1(t) = \frac{1}{\kappa_1}[e^{\kappa_1 (t-T)} - 1]. \tag{4.4.13}$$

The simultaneous equations (4.4.12) then results to the following initial value problem

$$\begin{cases} \dot{\alpha}(\tau) = -\lambda^r \mu_J \beta_1(\tau) + \kappa_2 v \beta_2(\tau) + \kappa_3 \eta \beta_3(\tau) + \lambda^r(\Lambda(\beta(\tau)) - 1), \\ \dot{\beta}_2(\tau) = -\kappa_2 \beta_2(\tau) + \frac{1}{2}\beta_1^2(\tau) + \frac{1}{2}\sigma_v^2 \beta_2^2(\tau), \\ \dot{\beta}_3(\tau) = \kappa_1 \beta_1(\tau) - \kappa_3 \beta_3(\tau) + \frac{1}{2}\sigma_m^2 \beta_3^2(\tau) \end{cases}, \tag{4.4.14}$$

with initial conditions

$$\alpha(0) = 0, \quad \text{and} \quad \beta(0) = (0, 0, 1).$$

Once again for the case of a jump distribution of Z_t^s being of Gaussian type, that is $Z_t^s = N(\mu_s, \sigma_s)$ then,

$$\Lambda(\beta(s)) = \Lambda(\beta_1, \beta_2(s)) = e^{\mu_s \beta_1(s) + \frac{\sigma_s^2 \beta_1^2(s)}{2}}.$$

For numerical implementation let consider the same set of parameters (see 4.4.15) used

by Andersen et al. [4]. As such the problem present a moderate stiffness factor. A similar problem with a severe stiffness factor is encountered in bond pricing [50].

$$\kappa_1 = 1.7887, \quad \kappa_2 = 1.7895, \quad \kappa_3 = 0.2792, \quad \sigma_m = 0.0459, \quad \mu_J = 0, \tag{4.4.15}$$

$$v = 0.000052, \quad \sigma_v = 0.0110, \quad \eta = 0.0525, \quad \sigma_J = 0.0016, \quad \lambda^r = 3.2688. \tag{4.4.16}$$

Equation (4.4.14) is a system of nonlinear ordinary differential equation of order 3. It can be written as:

$$Au + Nu = f. \tag{4.4.17}$$

Using our Time MultiDomain Spectral Method described in section 3..., we transport the equation in the frequency space and it becomes

$$A\underline{c} = \mathbf{f} \tag{4.4.18}$$

where c and $\mathbf{f}$ are spectral representations of the unknown solution vector $u = (\alpha, \beta_2, \beta_3)$ and the nonlinear part $f - Nu$, respectively. In addition, the matrix A is of the form:

$$A = \begin{bmatrix} D & \kappa_2 v I_n & \kappa_3 \eta I_n \\ 0 & D - \kappa_2 I_n & 0 \\ 0 & 0 & D - \kappa_3 I_n \end{bmatrix}$$

where I_n is the identity matrix of order n and D is the differentiation matrix as defined in (4.3.3). The nonlinear part will write as:

$$N = \begin{bmatrix} -\lambda \mu_J \beta_1(\tau) - l_r[\Lambda(\beta(\tau)) - 1] \\ \frac{1}{2}\beta_1(\tau)^2 - \frac{1}{2}\sigma_v^2 \beta_2^2(\tau) \\ \kappa_1 \beta_1(\tau) \frac{1}{2}\sigma_m^2 \beta_3^2(\tau) \end{bmatrix}.$$

A plot of the benchmark solution generated from ODE15s (with absolute tolerence

10^{-14}) and TMDSM is provided in Figure 4.4.4 for each variable α, β_2 and β_3.

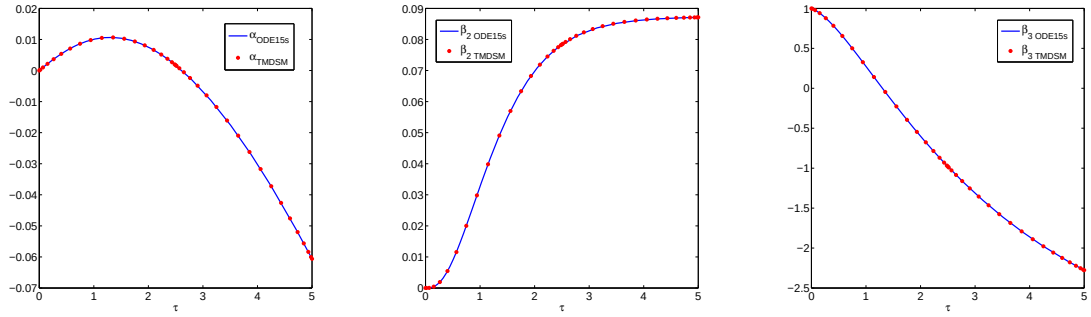

(a) α (b) β_2 (c) $\beta_3(\tau)$

Figure 4.4.4: Plot of the 3 variables for $T = 5$

As we vary the number of collocation points from $n = 4, 8, 16, 32, 64, 128, 256$ and 512, we record in table 4.4.1 the error on each variable α, β_2 and β_3. The results show again that it only requires few points to reach to the solution with high precision. The table shows that we achieve an error of about 10^{-8} within 16 points. The same holds also for the other two variables. This is in line with Figure 4.4.2a observed earlier. In other words, the spectral convergence still holds even in a higher dimension case.

	$n = 4$	$n = 8$	$n = 16$	$n = 32$	$n = 64$	$n = 128$	$n = 256$	$n = 512$
α	2.223E-5	1.526E-7	7.591E-9	4.070E-10	2.383E-11	1.398E-12	8.40E-14	5.551E-15
β_2	6.058E-4	8.195E-6	3.367E-7	1.768E-8	1.024E-9	6.183E-11	3.839E-13	2.703E-14
β_3	2.890E-3	1.972E-5	9.704E-7	5.204E-8	3.042E-9	1.781E-10	1.078E-12	6.90E-14

Table 4.4.1: Convergence of the error of α, β_2 and β_3

Given that chebfun returns the solution in 1.31 seconds, we also record in figure 4.4.5 the accuracy achieved as the running time increases. The graph shows that for the very same problem, the TMDSM achieves an accuracy of order 10^{-13} within 0.06 seconds. Again this is mostly due to the structure of the matrices produced from our differentiation for the system, compared to those from Chebfun which are full, see figure 4.4.6.

Let increase T to 100 and introduce different partition in 1,2 and 4 subintervals for a total number of Chebyshev collocation points varying from 256, 512, 1024, 2048 and

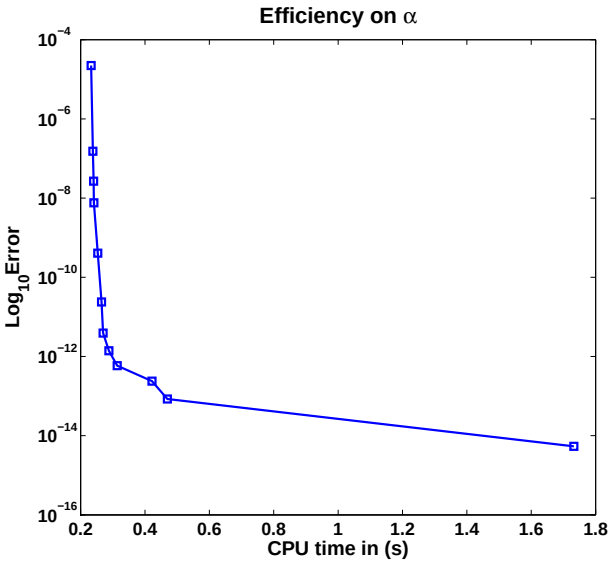

Figure 4.4.5: Efficiency of 2-Domain TMDSM for α

4096. Let record the error as well as the CPU running time in the table 4.4.2. Clearly the discretization of our interval $[0, T]$ is uniform, that is $h_n = h = \frac{T}{N}$ where N is the number of subintervals. We also consider $M_n = M$ to be constant since we generate the same number of Chebyshev points in each subinterval. Moreover it is not difficult to see that our function f here abides to the Lipschitz conditions. Therefore we should expect an exponential decay of the error.

		$n = 256$	$n = 512$	$n = 1024$	$n = 2048$	$n = 4096$
$N = 1$	CPU	0.450	1.653	8.875	66.589	607
	Error	6.136E-9	3.802E-10	2.368E-11	1.485E-12	5.337E-13
$N = 2$	CPU	0.397	0.765	2.883	16.870	156
	Error	2.158E-8	1.327E-9	7.960E-11	5.117E-12	4.993E-13
$N = 4$	CPU	0.394	0.501	1.160	5.18	45
	Error	7.572E-8	4.538E-9	2.779E-10	1.672E-11	1.068E-12

Table 4.4.2: Convergence and efficiency of TMDSM with 1, 2 and 4 domains at $T = 100$.

The table 4.4.2 shows that as the number of collocation points gets larger (here $n > 1000$) on the interval $[0, T]$, the TMDSM tends to suffer. Indeed the matrix A gets very large, making inversion a complicated task. But if the structure of A gets more porous (lower sparsity factor) then the spectral method would still be capable of

handling such even larger problem without losing much in accuracy. For instance, when the total number of points is 4092 it takes 607 seconds (nearly 10min) for TMDSM to deliver the solution whereas it will take the same TMDSM only 45 seconds when the interval $[0, 100]$ is splitted into 4 subintervals $[0, 25] \cup [25, 50] \cup [50, 75] \cup [75, 100]$. This is a tremendous gain in computational time. Indeed the structure of the linear operator A plays an important role. We plot the structure of the matrix A in figure 4.4.6 using 200 collocation points. The matrix is 600×600 and for the case of one domain the total number of nonzero elements is 31396 (see Figure 4.4.6a) implying a sparsity of 91.2% whereas when splitting the domain into 4 subdomains the number of nonzero terms reduces to 8884 (see Figure 4.4.6c) resulting to a sparsity of 97.5%. It is also remarkable to notice that the overall error did not suffer, it remained in the order of 10^{-12}. The method is stable. The accuracy depends not on the number of subinterval but on the total number of Chebyshev collocation points.

4.4.3 Electricity pricing under affine process

Energy commodity prices are important to model as their cost of storage is usually very high. Modeling their dynamics with affine jump diffusion looks reasonable in order to capture salient features of energy commodity prices, [23]. For instance electricity cannot be stored or inventoried economically once generated. Electricity demand and supply in bulk electricity power network has to be balanced continuously so as to prevent network from collapsing.

The most noticeable behaviour of energy commodities is the mean-reverting aspect. That is, when price of the commodity is high, its supply tends to increase, thus putting a downward pressure on the price. When the spot price is low, the supply of commodity tends to decrease thus providing an upward lift to the price. Another feature is the presence of jumps and spikes. These happen when a massive storage of commodity is not economically available and demand exhibits low elasticity. Also a forced outage of a major power plant or sudden uprise of demand would either cause the supply

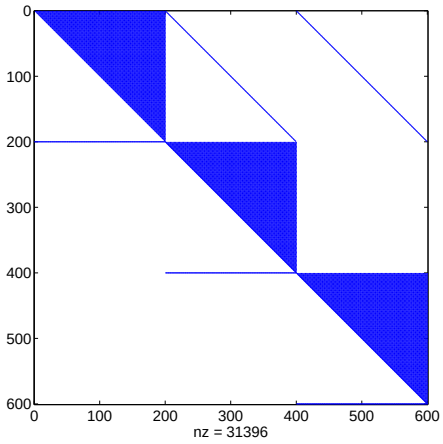

(a) 1-Domain TMDSM matrix

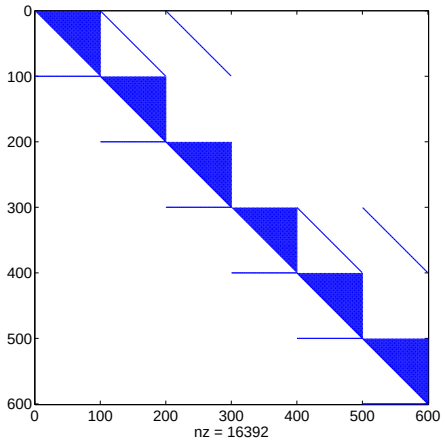

(b) 2-Domain TMDSM matrix

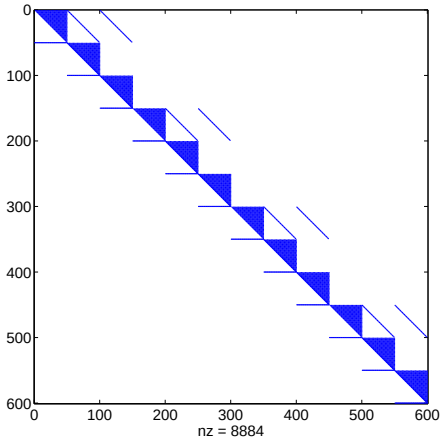

(c) 4-Domain TMDSM matrix

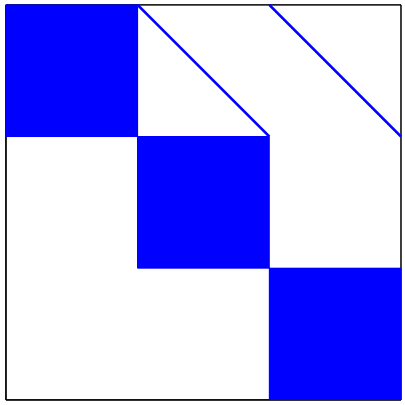

(d) Chebfun matrix

Figure 4.4.6: Plots of the underlying matrix A for 1, 2, 4-Domain TMDSM vs Chebfun

curve to shift to the left or lift up the demand curve, therefore causing a price jump. For electricity, spikes can be observed when an unexpected breakdown of some power plant occurs, the spot price can experience an abrupt upward increase, but as the lost generator gets restored, the price falls back quickly to their normal range [23].
A suitable equation that can capture the above mentioned features is:

$$d\begin{bmatrix} X_t \\ V_t \\ Y_t \end{bmatrix} = \begin{bmatrix} \kappa_1\theta_1 - \kappa_1 X_t \\ \kappa_2\theta_2 - \kappa_2 V_t \\ \kappa_3\theta_3 - \kappa_3 Y_t \end{bmatrix} dt + \begin{bmatrix} \sqrt{V_t} & 0 & 0 \\ \rho_1\sigma_2\sqrt{V_t} & \sqrt{1-\rho_1^2}\sigma_2\sqrt{V_t} & 0 \\ \rho_2\sigma_3\sqrt{V_t} & 0 & \sigma_3 \end{bmatrix} dW_t + dZ_t \tag{4.4.19}$$

where X_t is the log stock price, V_t is the volatility and Y_t is the product supply of raw material, $W_t = (W_t^x, W_t^v, W_t^y)$ is a three-dimensional Brownian motion and $Z_t = (Z_t^x, Z_t^v, 0)$ is a three-dimensional Poisson process in t with mean arrival rate $\lambda = \lambda^x + \lambda^v + \lambda^c$. The process can then be written as:

$$dX_t = \mu_t dt + \sigma_t dW_t + dZ_t \tag{4.4.20}$$

and the electricity price is of the form:

$$\phi_t = e^{\alpha(t)+\beta(t)\,x} \tag{4.4.21}$$

where α and $\beta = (\beta_1, \beta_2, \beta_3)$ are real valued functions that satisfy the Riccati equation

$$\dot{\alpha} = r - \sum_{i=1}^{3} \kappa_i\theta_i\beta_i - \frac{1}{2}\sigma_3^2\beta_3^2 - \lambda^x\left[\Lambda(\beta)\right], \tag{4.4.22}$$

$$\dot{\beta}_1 = \kappa_1\beta_1 - \frac{1}{2}\sigma_3^2\beta_3^2, \tag{4.4.23}$$

$$\dot{\beta}_2 = \kappa_2\beta_2 - \frac{1}{2}[\beta_1^2 + \sigma_2^2\beta_2^2 + \rho_2^2\sigma_3^2\beta_3^2] - \lambda_2[\Lambda(\beta) - 1], \\ -\rho_1\sigma_2\beta_1\beta_2 - \rho_2\sigma_3\beta_1\beta_3 - \rho_1\rho_2\sigma_2\sigma_3\beta_2\beta_3, \tag{4.4.24}$$

$$\dot{\beta}_3 = \kappa_3\beta_3 \tag{4.4.25}$$

together with terminal conditions

$$\alpha(T) = 0 \text{ and } \beta(T) = (0, 0, 1).$$

This problem can only be solved by numerical method. Operating again the rescaling $\tau = T - t$ the system becomes

$$\begin{aligned}
\dot{\alpha} &= -r + \sum_{i=1}^{3} \kappa_i \theta_i \beta_i + \frac{1}{2}\sigma_3^2 \beta_3^2 + \lambda^x \left[\Lambda(\beta) - 1\right], && (4.4.26)\\
\dot{\beta}_1 &= -\kappa_1 \beta_1 + \frac{1}{2}\sigma_3^2 \beta_3^2, && (4.4.27)\\
\dot{\beta}_2 &= -\kappa_2 \beta_2 + \frac{1}{2}[\beta_1^2 + \sigma_2^2 \beta_2^2 + \rho_2^2 \sigma_3^2 \beta_3^2] + \lambda_2[\Lambda(\beta) - 1] \\
&\quad + \rho_1 \sigma_2 \beta_1 \beta_2 + \rho_2 \sigma_3 \beta_1 \beta_3 + \rho_1 \rho_2 \sigma_2 \sigma_3 \beta_2 \beta_3, && (4.4.28)\\
\dot{\beta}_3 &= -\kappa_3 \beta_3, && (4.4.29)
\end{aligned}$$

with initial condition:

$$\alpha(0) = 0 \text{ and } \beta(0) = (0, 0, 1).$$

As in the previous problem we will compute the numerical solution using the set of parameters considered in [23]:

$$\begin{aligned}
&\kappa_1 = 2.17, \quad \kappa_2 = 3.5, \quad \kappa_3 = 1.8, \quad \theta_1 = 3.2, \quad \theta_2 = 0.85, \quad \theta_3 = 0.87,\\
&\sigma_2 = 0.8 \quad , \sigma_3 = 0.54, \quad \rho_1 = 0.25, \quad \rho_2 = 0.2\\
&,\lambda_1 = 6.43, \quad \lambda_2 = 5, \quad \mu_{11} = 0.23, \quad \mu_{12} = 0.22, \quad \mu_{21} = -0.14.
\end{aligned}$$

The associated differentiation matrix is:

$$A = \begin{bmatrix} D & -k_1\theta_1 & -k_2\theta_2 & -k_3\theta_3 \\ 0 & D + k_1 & 0 & 0 \\ 0 & 0 & D + k_2 & 0 \\ 0 & 0 & 0 & D + k_3 \end{bmatrix},$$

the corresponding nonlinear part of the equation is:

$$N = \begin{bmatrix} -r + l_r[\Lambda(\beta) - 1] \\ \frac{1}{2}\sigma_3^2\beta_3^2 \\ \lambda_2[\Lambda(\beta) - 1] + N_3 \\ 0 \end{bmatrix}$$

where $N_3 = \frac{1}{2}[\beta_1^2 + \sigma_2^2\beta_2^2 + \rho_2^2\sigma_3^2\beta_3^2] + \rho_1\sigma_2\beta_1\beta_2 + \rho_2\sigma_3\beta_1\beta_3 + \rho_1\rho_2\sigma_2\sigma_3\beta_2\beta_3$. Once again we run the spectral method and compare the solution against ODE15s solution. The resulting error is captured in Figure 4.4.7a It can be seen that with a number of Chebyshev collocation points $n = 16$ the accuracy is relatively good.

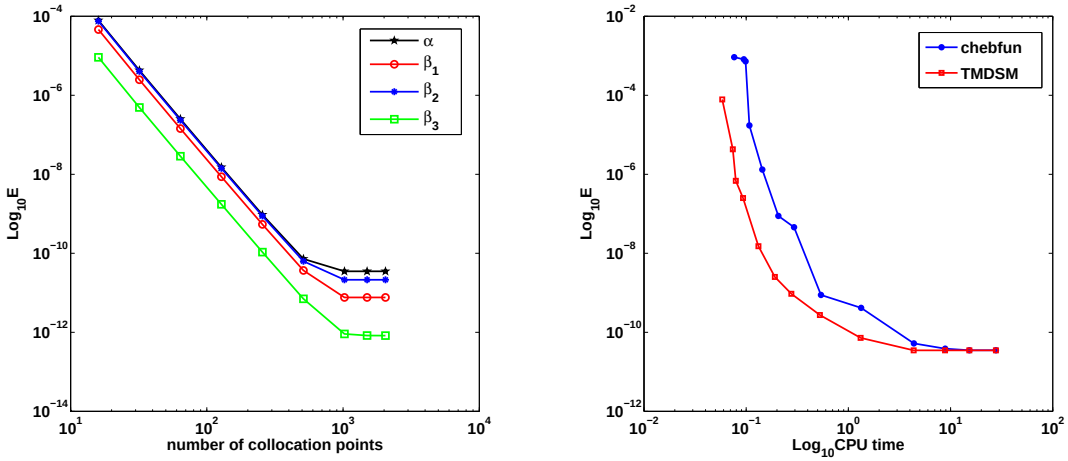

(a) Convergence of TMDSM vs Chebfun (b) Efficiency of TMDSM vs Chebfun

Figure 4.4.7: Comparison of the convergence and efficiency of TMDSM against Chebfun

A log-log plot of the efficiency of the two methods (TMDSM and Chebfun) is provided in figure 4.4.7b. As in the previous example, the TMDSM achieves better accuracy in quicker time Chebfun. Once again the sparsity of the matrix A, (see figure 4.4.8) inherited from the sparsity of the differentiation matrix D obtained in each subinterval, is the main cause of such difference in efficiency. Here we considered 200 collocation points generating therefore 800×800 matrix. Using a single domain, the number of nonzero terms is 41994 resulting a sparsity factor of 93.4%. With a 2

domain, Figure 4.4.8b shows 21988 nonzero terms in A that is a sparsity of 96.5%. For the case of 4 domains, the sparsity increases to 98.1%.

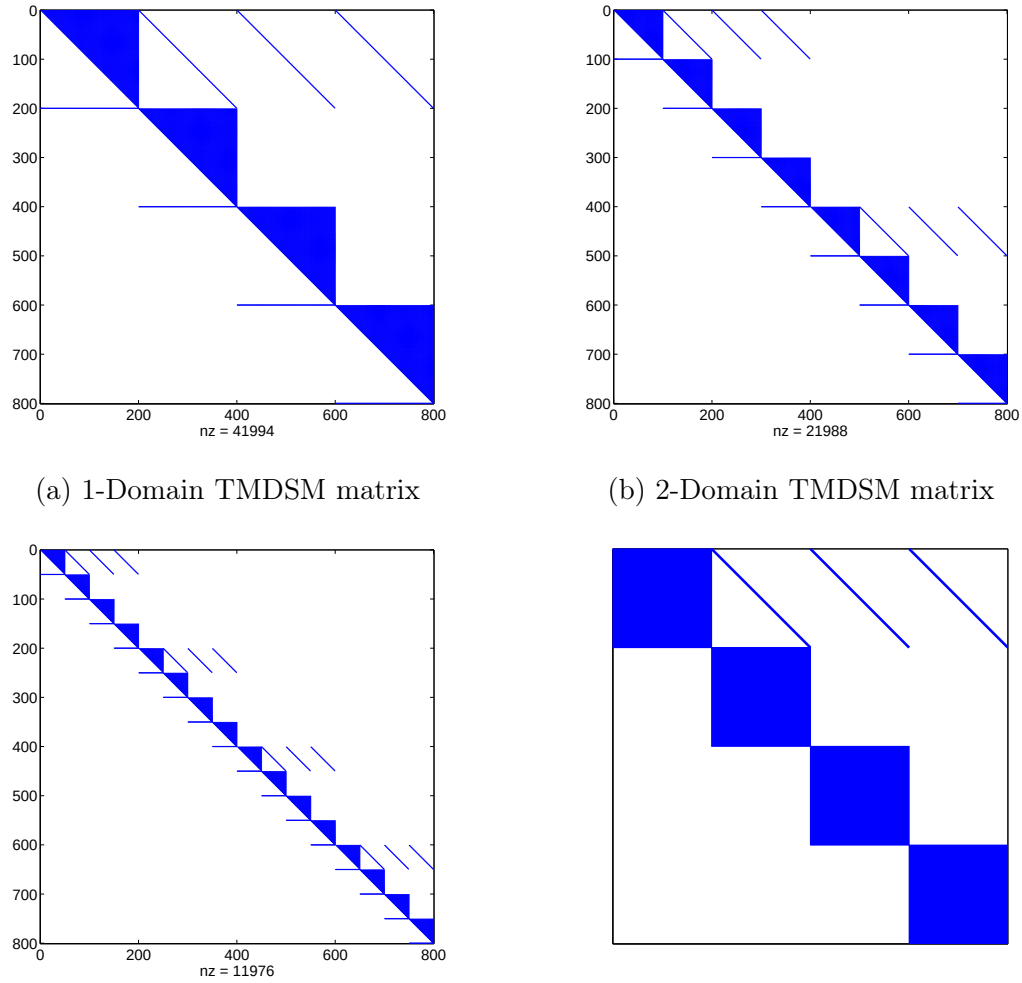

(a) 1-Domain TMDSM matrix

(b) 2-Domain TMDSM matrix

(c) 4-Domain TMDSM matrix

(d) Chebfun matrix

Figure 4.4.8: Plots of the underlying matrix A for 1, 2, 4-Domain TMDSM vs Chebfun

4.5 Conclusion

We have designed a spectral method that accommodates differential equations arising from financial models of affine type. The affine structure of these financial models is used to avoid solving the PIDE but rather to solving a system of Riccati equations. The

proposed numerical method to solve theses Riccati equations presents an operational matrix based on Chebyshev polynomials and the solution is obtained in the frequency domain. In doing so, the original problem is transformed into an iterative system of algebraic equations making it easier to solve. In addition the time domain is discretized into small domains allowing for spectral convergence to still hold. Three numerical examples are implemented and solutions are compared to numerical solutions from Chebfun, a leading package available for solving differential equation using spectral method. The result from error calculation shows that our method still maintains its spectral convergence even as we increase the time space interval. In addition, the method shows robustness and competitiveness compared to other numerical methods on the field, here ODE15s and Chebfun. The method can be applied in the entire class of affine models with jumps. Consequently it can be applied for the pricing of many other financial derivatives such as swaptions, coupon-bearing bonds, captions, currency options etc, just to mention a few. For further possible applications it would be interesting to see how TMDSM would perform when affine structure is not taken into account, that is, directly on the PIDE. Also, it worths to investigate how does the method apply to chaotic problems. In this coming chapter, we shall approach the spectral method from an integration angle in order to solve the chaotic finance system, with the hope of achieving quicker solution.

Chapter 5

A robust spectral integral method for solving chaotic finance system and synchronization

This chapter is a slightly modified version of the article published in *Alexandria Engineering Journal*and has been reproduced here with the permission of Elsevier, the copyright holder. This article is available here `https://www.sciencedirect.com/science/article/pii/S111001682030017X`.

5.1 Introduction

Nonlinear chaotic systems have attracted many research works in the sense that they can describe the evolution of more complex systems in a reasonable manner. The presence of parameters is typical for many models of economic processes. For example, in economic growth models, they may represent tools for influencing the economy, while the aim of the analysis is to find such quantities that would lead to the optimal path of growth. However, if the analyzed model has chaotic dynamics, the matter is essentially complicated. The high sensitivity of chaotic system to a change in the initial conditions makes it impossible to predict the effects of economic decisions in a long time scale.

Considering that government are usually interested in stimulating investment in order to cope with unemployment rate, exports, etc..., this may cause a total new trajectory for the system. Therefore, an effective and rapid control method is very much needed when chaos appears in order to avoid undesired trajectory and make suitable economic adaptation and prediction possible, specially from government and investors side. Ma and Chen [53, 54] provided a practical way to analyse and predict the chaotic economic systems from a bifurcation approach.

By control, we refer to redesigning the system in which parameters are added and controlled in order to eradicate the chaotic behaviour of the system and reach a desired goal. Lots of research has been conducted on the nonlinear chaotic finance problem, mostly with the aim of achieving control and synchronization. Several techniques are used for control of the chaotic system including sliding mode, feedback control [1], integral sliding mode control [99], inverse optimal control [19], passive control [83], adaptive control [98], backstepping control [97] to name these only.

In the synchronization process, we are given two identical systems with different starting points. One initial system, also called driving, and a second system called response, or slave, similar to the driving system. The aim is that by adding some parameters on the slave system we should match the driving system after some time. In the world of finance, this means from one chaotic finance system generated from a certain economy we can add some parameters to it in order to match another desired chaotic system generated by another economy. Various synchronization methods have been introduced so far and some with extension to fractional cases, namely, the projective synchronisation [104, 108], sliding mode [56, 96], and the nonlinear control [71, 107]. In this paper, a two sliding controller mode synchronisation is used as it regulates synchronisation of chaotic finance system more effectively than passive control, while keeping also the system internally stable [56].

Analytical solutions for nonlinear chaotic systems are almost nonexistent. Therefore, we rely on numerical methods to study these systems. In the field of numerical methods for solving differential equations, two main classes can be distinguished, clas-

sical methods and spectral methods. By classical methods we refer to the class of finite difference, finite element methods. These methods are very accurate, but computationally costly.

However, spectral methods have the advantage of being fast converging methods. Their truncation error decays as fast as the global smoothness of the underlying solution permits. Their definite integrals are calculated once by the quadrature rule [33], see also [35, 86] for more on spectral methods. For ordinary differential equations in which some coefficient functions or solutions are not analytic, Babolian [6] introduced a modified spectral method that is more efficient than the existing spectral methods. Various quadrature and modified quadrature rules can be found in the literature of spectral methods, including quadrature based on Chebyshev polynomials. Shifted Chebyshev polynomials for instance are used to solve the Klein-Gordon equation, [44]. The method is referred to as shifted Chebyshev-Tau method. An extension of this method is applied in the case of fractional differential equations [25]. Two years later, Bhrawy [9] introduced an operational matrix to the shifted Chebyshev method to generate a faster algorithm for fractional integration in the sense that only a small number of shifted Chebyshev polynomials is needed to obtain a satisfactory result. Liu [61] applies a quasi-inverse technique to solve differential equations directly. The method performs very well and shows obvious advantage especially when it comes to multi-dimensional cases.

Driscoll [27] presents a fast algorithm based on operational matrices in which the matrices have a lower density. In integral form, large condition numbers associated with differentiation matrices in high-order problems are avoided. The Chebfun package of Matlab [93] is used in the algorithm, as it exploits results from approximation theory, spectral methods, and object-oriented software design to reduce the distance between analytical expressions and numerical solutions for one-dimensional problems. Like the Matlab Differentiation Matrix Suite (DMS) package [101], Chebfun also suffers from the fact that the differentiation matrix gets full (while it is sparse for the finite difference or the finite element method) and, more importantly, it is very sensitive to rounding

errors. Reason being that these two packages are based on the spectral collocation method where the approach focuses more on the physical space generated from the quadrature.

Following the same matrix based operational approach, an improvement of these packages is brought by Trif [94] in introducing the chebpack package that is based on the Chebyshev-Tau method where the focus is more on the spectral space of coefficients rather than the physical space. This approach takes advantage of the spectral properties of Chebyshev polynomials resulting in avoiding full matrices. Actually the obtained matrices are sparse upper triangular and for the particular case of constant coefficient in the system, the matrices become diagonal almost everywhere. Hence a tremendous gain in computation is achieved.

In this chapter we intend to solve the chaotic finance system by means of the robust spectral integral method (RSIM), to compute the solution of three dimensional and four dimensional problems. In addition, a splitting method is used in order to achieve fast convergence without compromising on the accuracy over a long time period.

This chapter is organised as follows, Section 5.2 presents the chaotic finance system with a brief analysis on the stability. In Section 5.3 we introduce the robust spectral integral method In Section 5.4, we present numerical results and conduct an error analysis as well as a synchronisation via sliding mode. The last section is devoted to the conclusion.

5.2 Chaotic finance systems

The chaotic finance system, under study, is driven by the interaction of three main variables influencing the market economy. This interaction is modeled in the form of three nonlinear simultaneous ordinary differencial equations (ODEs) as follows (see

[54])

$$\begin{cases} \dot{x} = z + (y - a)\, x, \\ \dot{y} = 1 - by - x^2, \\ \dot{z} = -x - cz. \end{cases} \tag{5.2.1}$$

where x component stands for the interest rate dynamics which is defined as the percentage amount of the principal a borrower promises to pay the lender, y is the investment demand which is the desired capital and inventories by firms, and z represents the price index of a stock. The positive constant parameters a, b, c are the saving, the per-investment cost and the elasticity of the demand, respectively.

By applying some appropriate change of coordinate system and settings, different views of the chaotic finance system can be presented [24]. In this paper we shall stick to the presentation given in (5.2.1). The system admits three equilibrium points $X_0 = (0, \frac{1}{b}, 0)$, $X_1 = \left(\sqrt{1 - ba - \frac{b}{c}}, a + \frac{1}{c}, -\frac{1}{c}\sqrt{1 - ba - \frac{b}{c}}\right)$ and $X_2 = \left(-\sqrt{1 - ba - \frac{b}{c}}, a + \frac{1}{c}, \frac{1}{c}\sqrt{1 - ba - \frac{b}{c}}\right)$. The Jacobian matrix is

$$J_{\mathrm{x}} = \begin{bmatrix} y - a & x & 1 \\ -2x & -b & 0 \\ -1 & 0 & -c \end{bmatrix}, \tag{5.2.2}$$

and at the equilibrium point X_0,

$$J_{\mathrm{x}_0} = \begin{bmatrix} \frac{1}{b} - a & 0 & 1 \\ 0 & -b & 0 \\ -1 & 0 & -c \end{bmatrix}.$$

The characteristic polynomial is

$$P(\lambda) = \lambda^3 - \left(\frac{1}{b} - a - b - c\right)\lambda^2 - \left(\frac{c}{b} - ab - ac - bc\right)\lambda - (c - b - abc). \tag{5.2.3}$$

According to the Routh-Hurwitz criterion for polynomial of order 3, the real parts of

the three eigenvalues are all negative if the following simultaneous inequalities hold:

$$\begin{aligned} -\left(\frac{1}{b} - a - b - c\right) &> 0, && (5.2.4)\\ -(c - b - abc) &> 0, && (5.2.5)\\ \left(\frac{1}{b} - a - b - c\right)\left(\frac{c}{b} - ab - ac - bc\right) + (c - b - abc) &> 0. && (5.2.6) \end{aligned}$$

In addition, we also see that the root $\lambda = -b$ of the characteristic polynomial (5.2.3) has a negative real part if $b > 0$. Now, if we arbitrarily consider $b = 0.1$, $c = 1$ and if we take a to be our control parameter, then the above set of conditions is written as:

$$\begin{aligned} a &> \frac{89}{10},\\ a &> 9,\\ \left(a - \frac{89}{10}\right)\left(\frac{11a - 99}{10}\right) - \frac{a - 9}{10} &> 0. \end{aligned}$$

This means for $a > 9$ all the eigenvalues will have a negative real part. As a result, X_0 is asymptotically stable.

At the equilibrium point $X_1 = \left(\sqrt{1 - ba - \frac{b}{c}}, a + \frac{1}{c}, -\frac{1}{c}\sqrt{1 - ba - \frac{b}{c}}\right)$, the Jacobian is given by

$$J_{x_1} = \begin{bmatrix} \frac{1}{c} & \sqrt{1 - ba - \frac{b}{c}} & 1 \\ -2\sqrt{1 - ba - \frac{b}{c}} & -b & 0 \\ -1 & 0 & -c \end{bmatrix}.$$

Therefore, the corresponding characteristic polynomial is obtained in Equation (5.2.7)

$$P(\lambda) = \lambda^3 + \left(b + c - \frac{1}{c}\right)\lambda^2 + \left(2 + bc - 2ab - \frac{3b}{c}\right)\lambda + (2c - 2b - 2abc). \quad (5.2.7)$$

Accordingly, the real parts of all the eigenvalues are all negative if

$$b + c - \frac{1}{c} > 0, \tag{5.2.8}$$

$$2c - 2b - 2abc > 0, \tag{5.2.9}$$

$$\left(b + c - \frac{1}{c}\right)\left(2 + bc - 2ab - \frac{3b}{c}\right) - (2c - 2b - 2abc) > 0. \tag{5.2.10}$$

Choosing the constants $b = 0.1$, $c = 1$, the above set of conditions result to

$$\begin{aligned} a &< 9, \\ a &> 9 \end{aligned}$$

implying X_1 cannot be stable no matter the value of a. The same analysis can also be conducted for the equilibrium point $X_2 = \left(-\sqrt{1 - ba - \frac{b}{c}}, a + \frac{1}{c}, \frac{1}{c}\sqrt{1 - ba - \frac{b}{c}}\right)$. Abd-Elouahab et al. [1] proved the existence of a chaotic behaviour of problem (5.2.1) for the constants $b = 0.1$, $c = 1$ and $0 < a < 7$ from the Lyapunov theory.

In the next section, we present a pseudo-spectral method used to solve the system of ODEs (5.2.1). The main advantage of this method is that it can handle large time values while preserving high accuracy.

5.3 The Robust Spectral Integral Method

We recall section 3.3 and consider two functions a and u of a variable x, with spectral representation $\underline{a}$ and $\underline{u}$ respectively. Then the product $a(x) \cdot u(x)$ admits also a spectral representation, denoted as $\underline{\phi}$ which is defined by

$$\underline{\phi} = \mathbf{a}.\underline{c} \tag{5.3.1}$$

where $\mathbf{a}$ is termed as the matrix representation of the function $a(x)$ and $\underline{c}$ is the spectral representation of function u, see [27]

An efficient way of getting matrix **a** is to write the product in its discrete form.

$$\text{Since} \qquad a(x)u(x) = \left[\sum_{k=0}^{n} a_k T_k(x)\right]\left[\sum_{k=0}^{n} c_k T_k(x)\right], \tag{5.3.2}$$

$$\text{then} \qquad \sum_{k=0}^{n} \phi_k T_k(x) = \sum_{k=0}^{n}\sum_{l=0}^{n} \alpha_{kl} a_k c_l T_k T_l \tag{5.3.3}$$

for some coefficients α_{kl}, $0 \le k, l \le n$. In addition, given the following relation

$$T_k(x)T_l(x) = \frac{1}{2}\left[T_{k+l}(x) + T_{|k-l|}(x)\right], \qquad \text{for all } k, l = 0, 1, ...n \tag{5.3.4}$$

and in rearranging terms properly, it brings to existence a matrix **a** such that

$$\sum_{k=0}^{n} \phi_k T_k(x) = \sum_{k=0}^{n}\left[\sum_{l=0}^{n} \mathbf{a}_{kl} c_l\right] T_k(x).$$

In the frequency space, this will written in the form

$$\underline{\phi} = \mathbf{a}\underline{c}. \tag{5.3.5}$$

As a linear operator, the integral of u is a continuous Lipschitz function in $[-1, 1]$, which has a unique expansion series of the form

$$\int u(x)dx = \sum_{k=0}^{n} I_k T_k(x), \qquad x \in [a, b],$$

where I_k's are coefficients of the integral of u. Section 3.3.3 shows the existence of a $n \times n$-matrix J such that

$$I_k = \sum_{l=0}^{n} J_{kl} c_l, \tag{5.3.6}$$

or simply

$$\underline{I} = J \cdot \underline{c}, \tag{5.3.7}$$

where $\underline{I}$ is the spectral representation of the integral of $u.$ and J defined in 5.3.6

$$J_{kk} = 0, \quad J_{01} = \frac{1}{2}, \quad J_{k,k-1} = -J_{kk+1} = \frac{1}{k}. \tag{5.3.8}$$

So then, the spectral representation of the integral of u is the vector $\underline{d} = J.\underline{c}$, and for any continuous function $a(x)$, the corresponding spectral representation for the integral of the product $a(x)\,u(x)$ is $J\,\mathbf{a}\,\underline{c}$ where $\mathbf{a}$ is the matrix representation of the function a. We shall write

$$\int a(x)u(x)dx \to J\,\mathbf{a}\,\underline{c}. \tag{5.3.9}$$

Consequently it can be seen with the help of elementary technique of integration by parts that

$$\begin{aligned}
\int a_1(x)u'(x)dx &\to (\mathcal{I} - JD)\mathbf{a}_1\,\underline{c} \\
\int\int a_2(x)u''(x)dx &\to (\mathcal{I} - JD)^2\mathbf{a}_2\,\underline{c} \\
\int a_3(x)\frac{d^3u}{dx^3}(x)dx &\to (\mathcal{I} - JD)^3\mathbf{a}_3\,\underline{c} \\
&\vdots \\
\int ...\int a_m(x)\frac{d^mu}{dx^m}(x)dx...dx &\to (\mathcal{I} - JD)^m\mathbf{a}_m\,\underline{c}
\end{aligned}$$

where $\mathcal{I}$ stands for the identity matrix and D is differentiation matrix as defined by (3.3.16). Thus, for a general linear differential operator L

$$L\,u(x) = \sum_{i=0}^{m} a_i(x)\frac{d^iu}{dx^i}(x), \tag{5.3.10}$$

$$\text{we have } \int ...\int L\,u(x)dx^m \to \sum_{i=0}^{m} J^{m-i}(\mathcal{I} - JD)^i\mathbf{a}_i\,\underline{c}. \tag{5.3.11}$$

The matrix

$$A = \sum_{i=0}^{m} J^{m-i}(\mathcal{I} - JD)^i \mathbf{a}_i \tag{5.3.12}$$

is the spectral representation of the integral operator of L.

If we consider a general differential equation $\mathcal{A}u = f$ of order m for which the differential operator can be written as $\mathcal{A} = L + \mathcal{N}$ where L and $\mathcal{N}$ are respectively the linear part and the nonlinear part, then
the differential equation then writes as

$$\begin{aligned} Lu(t) + \mathcal{N}u(t) &= f(t) && (5.3.13)\\ Lu(t) &= -\mathcal{N}u(t) + f(t) && (5.3.14)\\ \int \dots \int Lu(t) \to A\underline{c} &= -\mathbf{n} + J^m \underline{f} && (5.3.15)\\ A\underline{c} &= \mathbf{f} && (5.3.16)\\ \text{implying} \qquad \underline{c} &= A^{-1}\mathbf{f} && (5.3.17) \end{aligned}$$

where $\mathbf{n}$ is the spectral representation of the integral of $\mathcal{N}u$ at order m, and $\mathbf{f} = -\mathbf{n} + J^m \underline{f}$ is the spectral representation of $-\mathcal{N}u + f(t)$. We make use the algorithm 1 to generate the numerical solution:

As in section 4.3 we apply the domain decomposition by considering I_h to be a mesh on the interval $[0, T]$ and N to be the number of subintervals and

$$I_h := \{t_n : 0 = t_0 < t_1 < \cdots < t_N = T\}.$$

Denote by $\Lambda_n = [t_{n-1}, t_n]$, $h_n = t_n - t_{n-1}$ and $u^n(t)$ the solution of (5.3.13) on the n-th element, namely

$$u^n(t) = u(t), \qquad \forall t \in \Lambda_n, \qquad 1 \le n \le N.$$

Let $M_n > 0$ be an integer and consider $\mathcal{P}_{M_n}$ to be the space of polynomials of order at most M_n built on Λ_n. We apply the spectral method as described in the algorithm 1 to

obtain a numerical solution $U_{M_n} \in \mathcal{P}_{M_n}$ on Λ_n. The Robust Spectral Integral Method on the interval $[0, T]$ consists of a successive application of the obtained spectral method on each Λ_n to obtain a global numerical solution $U_M(t)$ of (5.3.13) defined in such way that

$$U_M(t) = U_{M_n}(t), \quad t \in \Lambda_n, \quad 1 \leq n \leq N.$$

where M is taken to be the smallest of the M_n's. That is,

$$M = \inf_{0<n\leq N} M_n$$

,

For each subinterval $[t_i, t_{i+1}]$, equation (5.3.16) is applied.

$$A^{(i)}\mathbf{c}^{(i)} = \mathbf{f}^{(i)}, \qquad i = 0, ..., m-1. \tag{5.3.18}$$

The overall matrix A of the entire problem is then a diagonal of the block of matrices $A^{(i)}$.

$$\begin{pmatrix} A^{(1)} & 0 & & \\ 0 & A^{(2)} & 0 & \\ & \ddots & \ddots & \\ & & 0 & A^{(m)} \end{pmatrix} \begin{pmatrix} \mathbf{c}^{(1)} \\ \mathbf{c}^{(2)} \\ \vdots \\ \mathbf{c}^{(m)} \end{pmatrix} = \begin{pmatrix} \mathbf{f}^{(1)} \\ \mathbf{f}^{(2)} \\ \vdots \\ \mathbf{f}^{(m)} \end{pmatrix}. \tag{5.3.19}$$

By inversion of the matrix $A^{(i)}$ on each domain Λ_i, we obtain $c^{(i)}$ and therefore u_{M_i} which is U_M on Λ_i.

Exponential convergence in this case is still guaranteed by theorem 27.

5.4 Applications and numerical results

In this section, we apply our method to different problems found in financial economics and test the convergence, and efficiency of the proposed method against the existing Chebfun method [76]. In addition we provide an application of our method for syn-

chronization. Since the exact solution is not available we choose the ODE15s with relative and absolute tolerance 10^{-14} to serve as the benchmark solution. The error E is the maximal error given by:

$$||E|| = ||Sol_{Benchmark} - Sol_{Numerical}||_{\infty}. \tag{5.4.1}$$

Let us apply the above technique described in Section 5.3 to the nonlinear chaotic problems stated in Section 5.2. First lets recall the problem (5.2.1) in its initial form

$$\begin{cases} \dot{x} + ax - z &= xy, \\ \dot{y} + by &= 1 - x^2, \\ \dot{z} + x + cz &= 0, \end{cases} \tag{5.4.2}$$

which can also be written as:

$$\underline{a}\, u'(t) + B\, u(t) = f(t), \quad t \in [0, T] \tag{5.4.3}$$

where $\underline{a} = (1, 1, 1),\ u(t) = [x(t), y(t), z(t)]\,,\ B = \begin{bmatrix} a & 0 & -1 \\ 0 & b & 0 \\ 1 & 0 & c \end{bmatrix}$ and $f(t) = (x(t)y(t), 1 - x^2(t), 0)$. Integrating (5.4.3) yields

$$\underline{a}\, u(t) + B \int_0^T u(t)\ dt = \int_0^T f(t)\ dt. \tag{5.4.4}$$

The Chebyshev approximation of problem (5.4.4) at order n in the space of Chebyshev polynomials yields the following simultaneous equations

$$\begin{cases} (\mathcal{I} + aJ)\mathbf{x} - J\mathbf{z} &= \mathbf{f}^1, \\ (\mathcal{I} + bJ)\mathbf{y} &= \mathbf{f}^2, \\ (\mathcal{I} + cJ)\mathbf{z} + J\mathbf{x} &= \mathbf{f}^3. \end{cases} \tag{5.4.5}$$

where $\mathcal{I}$ is the identity matrix of order 3, J is the integration matrix as defined in (5.3.6),

x, y, z are the spectral representation of the unknown functions $[x(t), y(t), z(t)]$ respectively, and similarly $[\mathbf{f}^1, \mathbf{f}^2, \mathbf{f}^3]$ which represent the coefficient vectors of the nonlinear part $[xy, 1-x^2, 0]$ respectively. In other words,

$$\begin{bmatrix} \mathcal{I}+aJ & 0 & -J \\ 0 & \mathcal{I}+bJ & 0 \\ J & 0 & \mathcal{I}+cJ \end{bmatrix} \begin{bmatrix} \mathbf{x} \\ \mathbf{y} \\ \mathbf{z} \end{bmatrix} = \begin{bmatrix} \mathbf{f}^1 \\ \mathbf{f}^2 \\ \mathbf{f}^3 \end{bmatrix}. \tag{5.4.6}$$

This problem is nonlinear, we will apply an iterative method to equation (5.4.6) and the aim is to get the coefficient vector $\underline{c}$ of $u(t) = [x(t), y(t), z(t)]$.
Lets then consider the fix point problem

$$A\underline{c} = \mathbf{f}. \tag{5.4.7}$$

We shall start with an initial guess coming out of the initial condition $[1, 1, 1]$ then get the new $\underline{c}$ by $\mathbf{c} = A^{-1}\mathbf{f}$ where the old $\underline{c}$ is used to compute $\mathbf{f}$ in the iterations. Keeping in mind that the chaotic finance (5.2.1) is also highly nonlinear on some interval, and in order to speed up convergence, we suggest the use of a splitting method on the interval $[0, T]$ into N-subintervals $0 = t_0 < t_1 < ... < t_N = T$ and apply the robust spectral integral method.

The results are implemented for $a = 0.9, b = 0.2, c = 1.2$. Figure 5.4.1 shows the chaotic behaviour of the finance system as expected. The solution functions $x(t), y(t), z(t)$ are plotted in Figure 5.4.2 where a 4-domains decomposition has been used with 8 collocation points per domain.

As we vary the number of collocation points from $n = 4, 8, 16, 32, 64, 128, 256$ and 512, we record in table 5.4.1 the error on each variable x, y and z.

Given that Chebfun returns the solution in 1.05 seconds, we also record the accuracy achieved as the running time increases and with respect to the number of domains (here we consider 1, 2 and 4 subintervals), for a total number of Chebyshev collocation points varying from 256, 512, 1024, 2048 and 4096. Lets also record the error as well as the

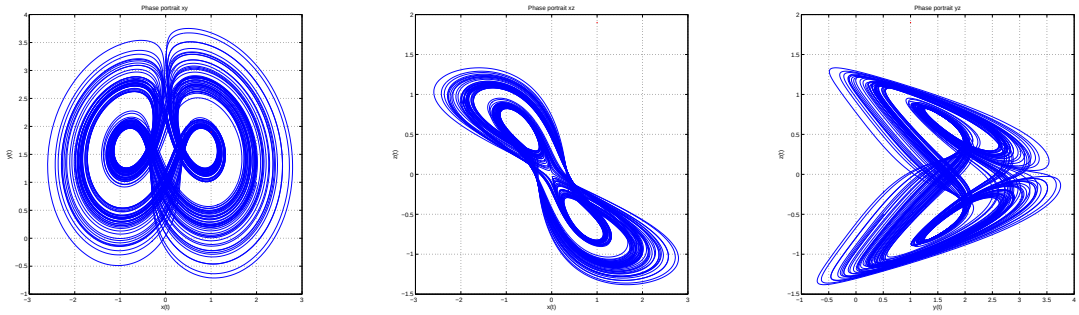

(a) xy-plot (b) xz-plot (c) yz-plot

Figure 5.4.1: Phase portraits for $T = 1000$

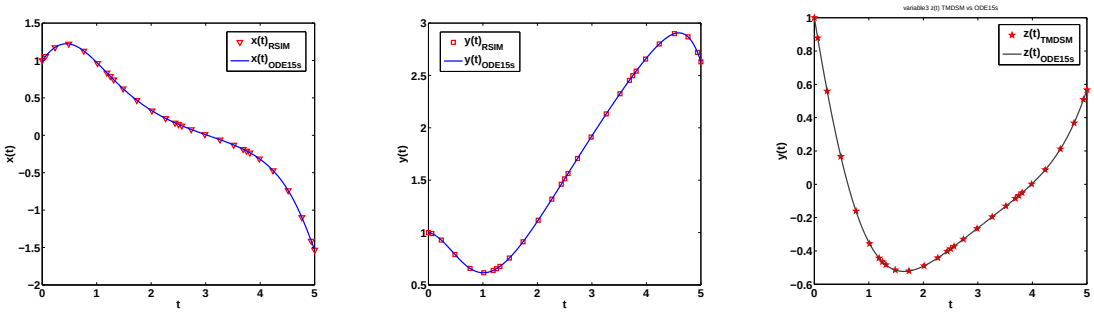

(a) $x(t)$ (b) $y(t)$ (c) $z(t)$

Figure 5.4.2: Plot of the 3 variables for $T = 5$ using 4-domains decomposition

CPU running time in the Table 5.4.2. Figure 5.4.3 shows the efficiency, on one variable, of our method compare to Chebfun in solving the chaotic finance system. The method is reliable on this problem. Clearly the discretization of our interval $[0, T]$ is uniform, that is, $h_N = h = \frac{T}{N}$, where N is the number of domains. In addition we consider $M_N = M$ to be constant since we generate the same number of Chebyshev points in each domain. Moreover, it is not difficult to see that our function f here adheres to the Lipschitz conditions. Therefore we should expect an exponential decay of the error as shown in Figure 5.4.4b where we also considered an additional case of $N = 8$ domains. Table 5.4.2 shows that as the number of collocation points get larger (here $n > 1000$) on each subinterval, the method tends to suffer in terms of rapidity. Indeed matrix A gets very large, making inversion a complicated task. But if the structure of A gets more porous (increase in sparsity) then the spectral method would still be capable of

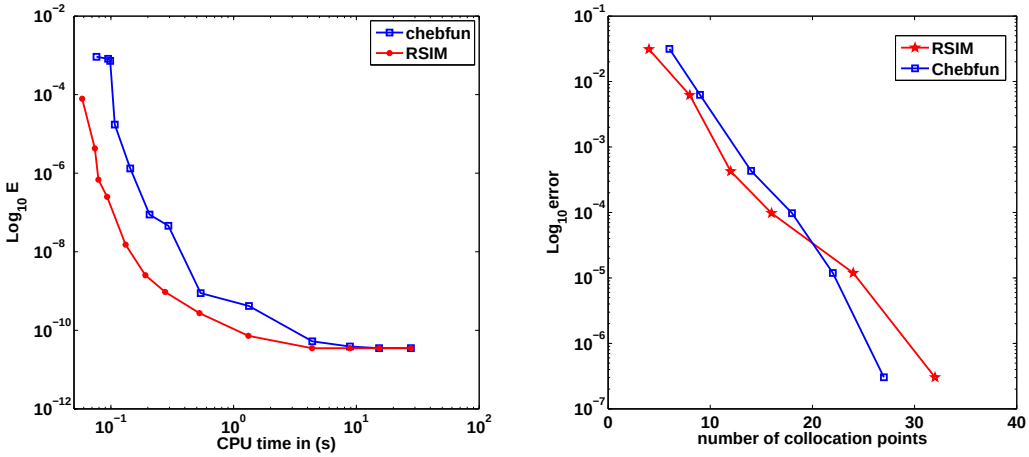

(a) Efficiency (b) Convergence

Figure 5.4.3: Convergence and efficiency RSIM vs Chebfun

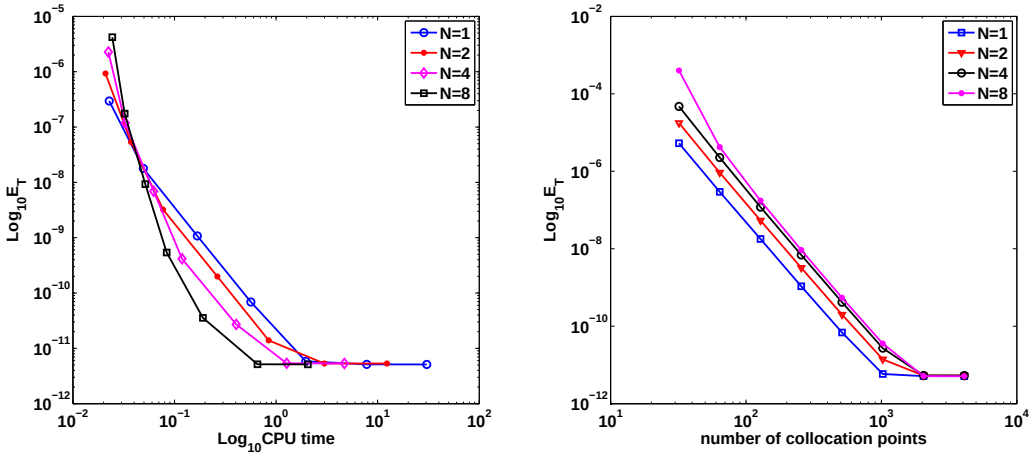

(a) Efficiency (b) Convergence

Figure 5.4.4: Convergence and efficiency as we vary the number of domains on x-variable

	$n=4$	$n=8$	$n=16$	$n=32$	$n=64$	$n=128$	$n=256$	$n=512$
$x(t)$	2.390E-2	4.528E-4	1.992E-5	1.013E-6	5.844E-8	3.501E-9	2.145E-10	1.158E-11
$y(t)$	2.031E-2	4.484E-4	1.673E-5	9.079E-7	5.203E-8	3.139E-9	1.918E-10	1.0752E-11
$z(t)$	6.135E-3	1.001E-4	3.990E-6	2.2074E-7	1.182E-8	7.127E-10	4.361E-11	2.570E-12

Table 5.4.1: Convergence of the error of the variables x, y and z fot $T = 1$ with 1 domain only.

		$n=256$	$n=512$	$n=1024$	$n=2048$	$n=4096$
$N=1$	CPU	0.271	0.746	2.543	10.593	40.02
	Error	6.925E-9	4.304E-10	2.570E-11	3.431E-12	2.814E-12
$N=2$	CPU	0.128	0.344	0.998	3.823	15.508
	Error	1.372E-8	8.429E-10	E-11	4.231E-12	2.961E-12
$N=4$	CPU	0.104	0.174	0.525	1.525	5.451
	Error	3.646E-8	2.189E-9	1.348E-10	9.730E-12	2.762E-12

Table 5.4.2: Convergence and efficiency of RSIM with 1, 2 and 4 domains at $T = 5$.

handling an even larger problem without losing much in accuracy. This explains why in the Table 5.4.2, our algorithm, RSIM, performs faster in larger time scale when splitting is done.

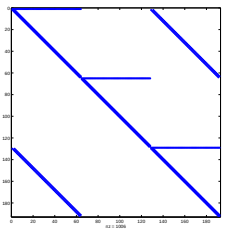

(a) 1-Domain RSIM matrix

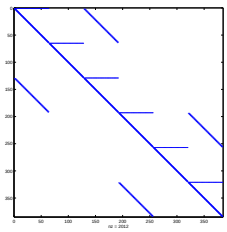

(b) 2-Domain RSIM matrix

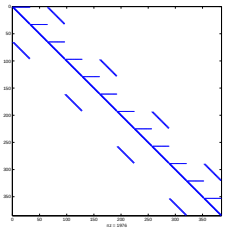

(c) 4-Domain RSIM matrix

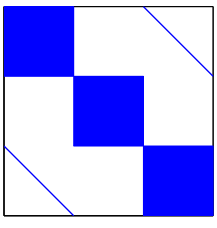

(d) Chebfun matrix

Figure 5.4.5: Plots of the underlying matrix A for 1, 2, and 4-Domain RSIM vs Chebfun matrix

As mentioned earlier, the chaotic finance system is highly sensitive to the initial conditions, which can be a problem for an economical system. Controlling such system is of great importance in order to match a desired way of functioning. This is achieved by means of synchronization.

5.5 Synchronization

This section is devoted to the synchronization mentioned earlier. The sliding mode is applied using two controller parameters. We depart the section by considering our driving system with variables (x, y, z) to be the initial finance system (5.2.1) and let the response system be defined with variables x_s, y_s, z_s in the following way:

$$\begin{cases} \dot{x}_s = z_s + (y_s - a)\, x_s & +u_1(t), \\ \dot{y}_s = 1 - by_s - x_s^2 & +u_2(t), \\ \dot{z}_s = -x_s - cz_s & +u_3(t). \end{cases} \tag{5.5.1}$$

where $u = (u_1, u_2, u_3)$ is a suitable sliding control function to be determined in order to achieve synchronization. The error function from solution $e = (e_1, e_2, e_3)$ is defined by

$$\begin{cases} e_1 = x_s - x, \\ e_2 = y_s - y, \\ e_3 = z_s - z. \end{cases} \tag{5.5.2}$$

The dynamics of the error is thus driven by

$$\begin{cases} \dot{e}_1 &= e_3 - ae_1 + x_s y_s - xy + u_1(t), \\ \dot{e}_2 &= -be_2 - x_s^2 + x^2 + u_2(t), \\ \dot{e}_3 &= -e_1 - ce_3 + u_3(t). \end{cases} \tag{5.5.3}$$

From sliding mode control theory, Kocamaz et al. [56] show that in order to achieve synchronization while maintain the system stable, the required sliding control function

u must satisfy

$$\begin{cases} u_1(t) = -x_s y_s + xy + \nu(t), \\ u_2(t) = x_s^2 - x^2 + \nu(t), \\ u_3(t) = 0, \end{cases} \tag{5.5.4}$$

where $\nu(t) = a_1(x_s - x) - b_1(y_s - y) + c_1(z_s - z) - q\,\text{sign}(-1.75(x_s - x) + 2.75(y_s - y))$ and $a_1 = 1.75(k - a),\ b_1 = 2.75(k - b),\ c_1 = 1.75$, and k, q are some parameters to be adjusted. In other words, sliding mode control achieves synchronisation only requires to act on interest rates and investment demand. Introducing all this back into (5.5.1) we obtain

$$\begin{aligned} \dot{x}_s + (a - a_1)x_s + b_1 y_s - (1 + c_1)z_s &= -a_1 x + b_1 y - c_1 z + xy \\ &- q\,\text{sign}((-1.75(x_s - x) + 2.75(y_s - y)) \\ \dot{y}_s + a_1 x_s + (b_s + b)y_s + c_1 z_s &= -a_1 x + b_1 y - c_1 z + 1 - x^2 \\ &- q\,\text{sign}(-1.75(x_s - x) + 2.75(y_s - y)) \\ \dot{z}_s + x_s + c z_s &= 0. \end{aligned}$$

Applying integration and expressing it in a matrix form as in section 4.4 yields

$$\begin{bmatrix} \mathcal{I} + (a - a_1)J & b_1 J & -(1 + c_1)J \\ -a_1 J & \mathcal{I} + (b + b_1)J & -c_1 J \\ J & 0 & \mathcal{I} + cJ \end{bmatrix} \begin{bmatrix} \mathbf{x} \\ \mathbf{y} \\ \mathbf{z} \end{bmatrix} = \begin{bmatrix} \mathbf{f}^1 \\ \mathbf{f}^2 \\ \mathbf{f}^3, \end{bmatrix} \tag{5.5.5}$$

where $\mathbf{f}^1$ is coefficient vector of $-a_1 x + b_1 y - c_1 z + xy - q\,\text{sign}(-1.75(x_s - x) + 2.75(y_s - y))$ and $\mathbf{f}^2$ is coefficient vector of $-a_1 x + b_1 y - c_1 z + 1 - x^2 - q\,\text{sign}(-1.75(x_s - x) + 2.75(y_s - y))$.

With a driving system starting at initial condition $[1, 2, -0.5]$, and a response system starting with initial condition $[-1, 1.7, 0.5]$, and a time factor varying from 0 to 10, we see from Figure 5.5.1 that synchronization is achieved quite fast from $t = 3.5$ on all three variables x, y, z. In what follows we plot the error dynamics function $e_1 = x_s - x,\ e_2 = y_s - y$ and $e_3 = z_s - z$ in Figure 5.5.2. Again, we have a better

confirmation of that actually from $t = 4$, the two systems behave the same.

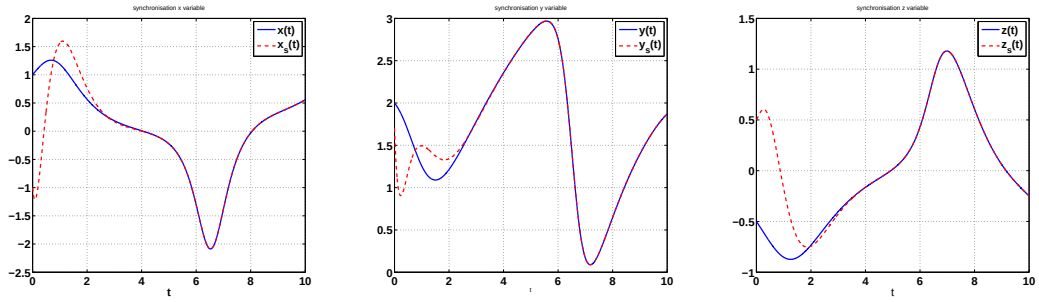

(a) x-variable (b) y-variable (c) z-variable

Figure 5.5.1: Drive and response system behaviour for $k = 5, q = 0.1$ and $0 \leq t \leq 10$

In other words, the controller defined in (5.5.4) is switched at time $t = 4$. Making therefore the chaotic finance system (5.2.1) rapidly controllable.

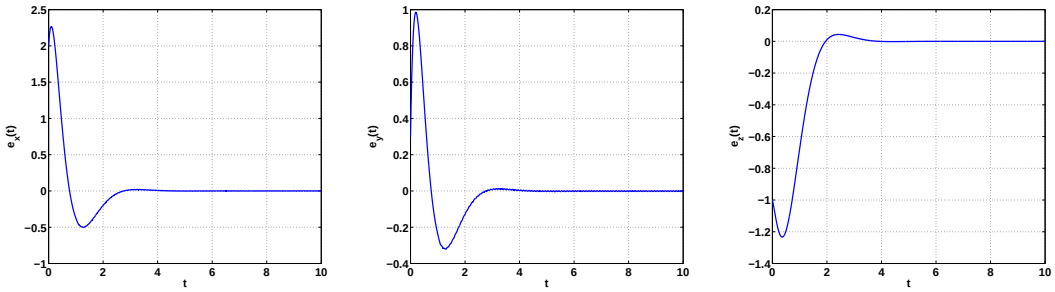

(a) error in the x-variable (b) error in the y-variable (c) error in the z-variable

Figure 5.5.2: Error behaviour for $k = 5$, $q = 0.1$ and $0 \leq t \leq 10$.

5.6 Conclusion

In this chapter, a Chebyshev spectral method has been applied on time multiple domain. The method proves to be robust and efficient for chaotic finance problem. The results are also compared with solutions obtained from other numerical methods in the literature. We achieve good accuracy in very short time as result of using integration in the frequency space. The method also proves to be reliable for synchronization of chaotic finance system. Now that we have seen the advantages of the spectral method

using differentiation on one side and integration on the side, both in the frequency space, it will interesting to compare the efficiency of these approaches specially in problems that are highly sensitive to initial conditions such as hyperchaotic finance systems. We shall explore this topic in details in our next chapter.

Chapter 6

Comparative performance of time spectral methods for solving hyperchaotic finance system

This chapter is a slightly modified version of the article published in *Chaos, Solitons and Fractals: the interdisciplinary journal of Nonlinear Science, and Nonequilibrium and Complex Phenomena*and has been reproduced here with the permission of Elsevier, the copyright holder. This article is available here `https://www.sciencedirect.com/science/article/pii/S0960077921001223?dgcid=author`.This chapter is a slightly modified version of a paper submitted into an accredited journal and still under review.

6.1 Introduction

Nonlinear chaotic systems have attracted many research works in the sense that they can describe the evolution of more complex systems in a reasonable manner. Application of theses systems include the area of physics, control theory, telecommunication artificial neural networks, biological networks, chemical reactor etc. Hyperchaotic system is usually defined as a chaotic system with at least two positive Lyapunov exponents. In the area of economics, the phenomenon of chaos was first discovered in

1985 and later it was found in finance by Ma and Chen [53, 54]. Financial system dynamics have a significant role in micro-economics. This system becomes more and more complicated with economic growth and contains many complex factors such as interest rate, the price of goods, investment demand and stock. Over the past few years, many more hyperchaotic systems have been discovered in the high-dimensional social economical system.

It is without a doubt that an analytical solution for the nonlinear chaotic system is almost unachievable. We shall rely on numerical methods for computation of solutions since the HCFS is actually a dynamical system that is described by a set of nonlinear ODEs.

Countless papers can be found on this literature of numerical methods for differential equations. These methods include finite difference methods (FDM) and variants such as Adams-Bashforth-Moulton methods [102], finite element methods (FEM), homotopy analysis or perturbation methods (HAM/HPM) together with Adomian decomposition [30] etc., and spectral methods. The methods mentionned in first place are very accurate, but computationally costly. Spectral methods, however, have the advantage of being fast converging methods. Their truncation error decays as fast as the global smoothness of the underlying solution permits, their definite integrals are calculated once by the quadrature rule [33].

Various modified and quadrature rules can be found in the literature of spectral methods, including quadrature based on Chebyshev polynomials. Shifted Chebyshev polynomials for instance are used to solve the Klein-Gordon equation, [44]. The method is referred to as Shifted Chebyshev-Tau method. An extension of this method is applied in the case of fractional differential equations [25]. Two years later, Bhrawy [9] introduces an operational matrix to the shifted Chebyshev method to generate an even faster algorithm for fractional integration in the sense that only a small number of shifted Chebyshev polynomials is needed to obtain a satisfactory result.

In a more computational and practical way, Driscoll [27] presents a fast algorithm based on operational matrices in which the matrices have a lower density. The Chebfun

package of Matlab presented by Trefethen [93], is used in the algorithm, as it exploits results from approximation theory, spectral methods, and object-oriented software design. Similarly, another operatorial matrix approach is brought by Trif [94] and introduces the chebpack package that is based on the Chebyshev-Tau method where the focus is more on the spectral space of coefficients rather than the physical space. This approach takes advantage of the spectral properties of Chebyshev polynomials resulting in avoiding full matrices. Actually the obtained matrices are sparse upper triangular and for the particular case of constant coefficient in the system, the matrices become diagonal almost everywhere. Hence a tremendous gain in computation is achieved. We shall use the later technique to construct a spectral method coupled with decomposition method to solve the HCFS, from an integral approach on one hand, and on the other hand using a differential approach.

This chapter is organised as follows, Section 6.2 presents the HCFS, then in Section 6.3 We apply these numerical methods to the HCFS and draw comparisons with solutions obtained from Chebfun. The last section is allocated to the conclusion.

6.2 The hyperchaotic finance system

It has been shown (see Zhao et al. [107]) that four sub-blocks actually drive the dynamics of the finance model: production, money, stocks and labor force. Their interaction is reported by three nonlinear differential equations defining what is termed as the chotic finance system. Technically and more explicitly, the finance system describes the time variation of three main state variable: the interest rate x, the investment demand y and the price index of stock z. The interest rate is an amount expressed as the percentage of the principal by lender to a borrower for an asset. Investment demand can be defined as the desired capital and inventories by firms. The chaotics finance system is expressed as follows:

$$\begin{cases} \dot{x} = z + (y - a)\, x \\ \dot{y} = 1 - by - x^2 \\ \dot{z} = -x - cz \end{cases} \tag{6.2.1}$$

where the parameters a, b, c are respectively the saving, the per-investment cost and the elasticity of the demand [56]. These parameters are all considered to be non-negative and constant. From the chaotic finance system (6.2.1) Yu et al. [106] found that the factors affecting the interest rates are related not only to investment demand and price index but also to the average profit margin. Moreover, the average profit margin and interest rate are proportional. Hence an improved chaotic finance system is constructed by including an additional state variable w that will stand for the average profit margin. The system is now of four dimensional differential equations:

$$\begin{cases} \dot{x} = z + (y - a)x + w, \\ \dot{y} = 1 - by - x^2, \\ \dot{z} = -x - cz, \\ \dot{w} = -d\, xy - ew. \end{cases} \tag{6.2.2}$$

Let us now apply the numerical methods based on spectral Chebyshev methods developed in section 3.3, that will allow us to get solutions of (6.2.2).

6.3 Applications and numerical results on the hyperchaotic finance system

In this section, we apply our method to HCFS and test the convergence, and efficiency of the proposed methods. Since the exact solution is not available we choose the ODE15s with relative and absolute tolerance 10^{-14} to serve as the benchmark solution.

The error we consider E is the maximal error given by:

$$||E|| = ||Sol_{Benchmark} - Sol_{Numerical}||_{\infty}. \tag{6.3.1}$$

In order to apply techniques described in Section 3.3 to the nonlinear hyperchaotic problems stated in Section 6.2. First lets recall the problem (6.2.2) in its initial form

$$\begin{cases} \dot{x} + ax - z - w &= xy, \\ \dot{y} + by &= 1 - x^2, \\ \dot{z} + x + cz &= 0, \\ \dot{w} + ew &= -d\,xy, \end{cases} \tag{6.3.2}$$

which can also be written as:

$$\underline{a}\,u'(t) + B\,u(t) = f(t), \quad t \in [0, T] \tag{6.3.3}$$

where $\underline{a} = (1,1,1,1)$, $u(t) = [x(t), y(t), z(t), w(t)]$, $B = \begin{bmatrix} a & 0 & -1 & -1 \\ 0 & b & 0 & 0 \\ 1 & 0 & c & 0 \\ 0 & 0 & 0 & e \end{bmatrix}$ and $f(t) = (x(t)y(t), 1 - x^2(t), 0, -d\,x(t)y(t))$.

The spectral representation of the (6.3.3) is

$$\begin{bmatrix} D + a\mathcal{I} & 0 & -\mathcal{I} & -\mathcal{I} \\ 0 & D + b\mathcal{I} & 0 & 0 \\ Id & 0 & D + c\mathcal{I} & 0 \\ 0 & 0 & 0 & D + e\mathcal{I} \end{bmatrix} \begin{bmatrix} \mathbf{x} \\ \mathbf{y} \\ \mathbf{z} \\ \mathbf{w} \end{bmatrix} = \begin{bmatrix} \mathbf{f}^1 \\ \mathbf{f}^2 \\ \mathbf{f}^3 \\ \mathbf{f}^4 \end{bmatrix} \tag{6.3.4}$$

where **x, y, z, w** are the spectral representation of the unknown functions $[x(t), y(t), z(t), w(t)]$ respectively, and similarly $[\mathbf{f}^1, \mathbf{f}^2, \mathbf{f}^3, \mathbf{f}^4]$ which represent the coefficient vectors of the nonlinear part $[xy, 1 - x^2, 0, dxy]$ respectively.

On the other hand we can approach the hyperchaotic problem by integration first then apply Chebychev approximation to the resulting integral problem.

It is not difficult to see that the Chebyshev approximation of problem (5.4.4) at order n in the space of Chebyshev polynomials yields the following simultaneous equations

$$\begin{cases} (\mathcal{I}+aJ)\mathbf{x} - J\mathbf{z} - J\mathbf{w} &= \mathbf{f}^1, \\ (\mathcal{I}+bJ)\mathbf{y} &= \mathbf{f}^2, \\ (\mathcal{I}+cJ)\mathbf{z} + J\mathbf{x} &= \mathbf{f}^3, \\ (\mathcal{I}+eJ)\mathbf{w} &= \mathbf{f}^4, \end{cases} \tag{6.3.5}$$

where **x, y, z, w** are defined as above, and similarly $[\mathbf{f}^1, \mathbf{f}^2, \mathbf{f}^3, \mathbf{f}^4]$ which represent the coefficient vectors of the integral of the nonlinear part $[xy, 1-x^2, 0, dxy]$ respectively. In other words,

$$\begin{bmatrix} \mathcal{I}+aJ & 0 & -J & -J \\ 0 & \mathcal{I}+bJ & 0 & 0 \\ J & 0 & \mathcal{I}+cJ & 0 \\ 0 & 0 & 0 & \mathcal{I}+eJ \end{bmatrix} \begin{bmatrix} \mathbf{x} \\ \mathbf{y} \\ \mathbf{z} \\ \mathbf{w} \end{bmatrix} = \begin{bmatrix} \mathbf{f}^1 \\ \mathbf{f}^2 \\ \mathbf{f}^3 \\ \mathbf{f}^4 \end{bmatrix} \tag{6.3.6}$$

The two approaches generates nonlinear problem, we will apply an iterative method to equations (6.3.6) and (6.3.4). The aim is to get the coefficient vector $\underline{c}$ of $u(t) = [x(t), y(t), z(t)]$.

Lets then consider the fix point problem

$$A\underline{c} = \mathbf{f}. \tag{6.3.7}$$

We shall start with an initial guess coming out of the initial condition then get the new $\underline{c}$ by $\mathbf{c} = A^{-1}\mathbf{f}$ where the old $\underline{c}$ is used to compute $\mathbf{f}$ in the iterations. Keeping in mind that the chaotic finance (6.2.2) is also highly nonlinear on some interval, and in order to speed up convergence we suggest the use of a splitting method on the interval $[0, T]$ into N-domains $0 = t_0 < t_1 < ... < t_N = T$ and apply the spectral methods.

The results are implemented for $a = 0.9, b = 0.2, c = 1.2, d = 0.2, e = 0.17$. Figure 6.3.1 shows the phase portraits between variables for a long time $T = 200$. They both exhibit chaos as excected.

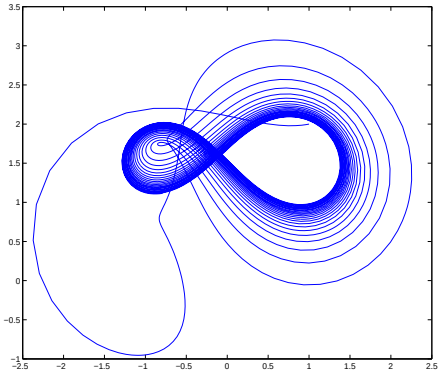

(a) Phase portrait xy

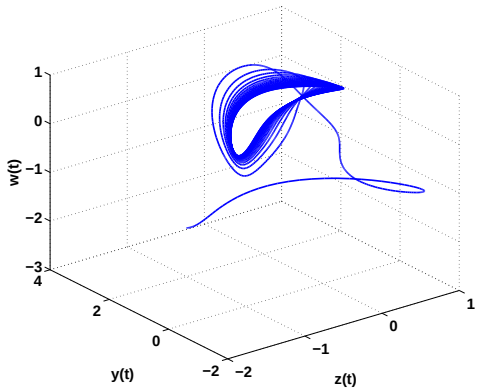

(b) Phase portrait yzw

Figure 6.3.1: Phase portraits 2D and 3D

The solution functions $x(t), y(t), z(t), w(t)$ are plotted in Figure 6.3.2 where a 3 domain decomposition have been used with 16 collocation points per domain and $T = 5$. It is clear, the numerical solutions from both spectral approaches match the benchmark solution from ODE15s.

We go on into investigating the effect of n and N on the decay error. Figure 6.3.3a shows that employing more collocation points on a domain enhances the precision of the numerical solution both from integration as well as differentiation method. It is also remarquable to see that while it takes close 80 points for Chebfun to reach an accuracy of 10^{-4}, the integral and differentiation spectral methods only require 20 points to achieve same accuracy. However the later methods tend to lose this quality as the number of points gets larger (here $n = 120$) as compare to Chebfun. This makes us consider a domain decomposition of the interval $[0, T]$.

However, better accuracy can also bring along a cost in time. Figure 6.3.3e presents the efficiency of the three methods. From the reading of that graph one can see that

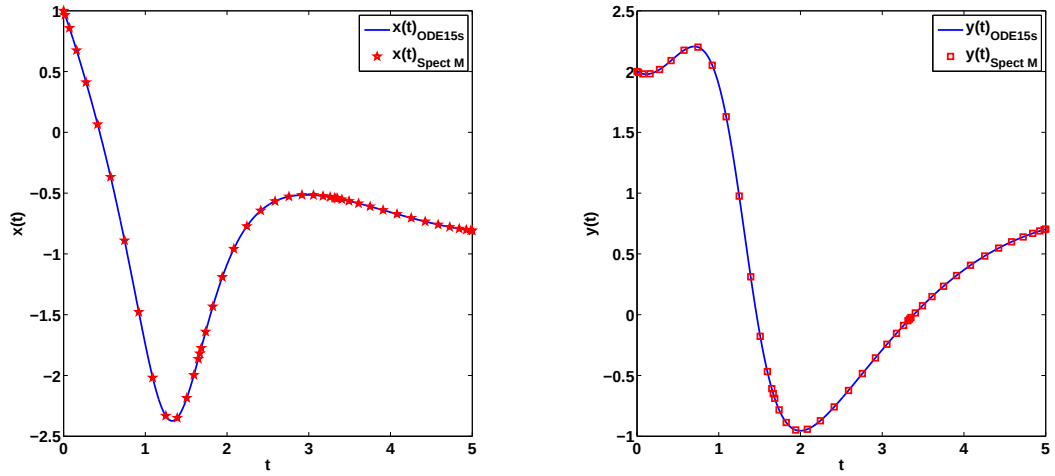

(a) $x(t)$ (b) $y(t)$

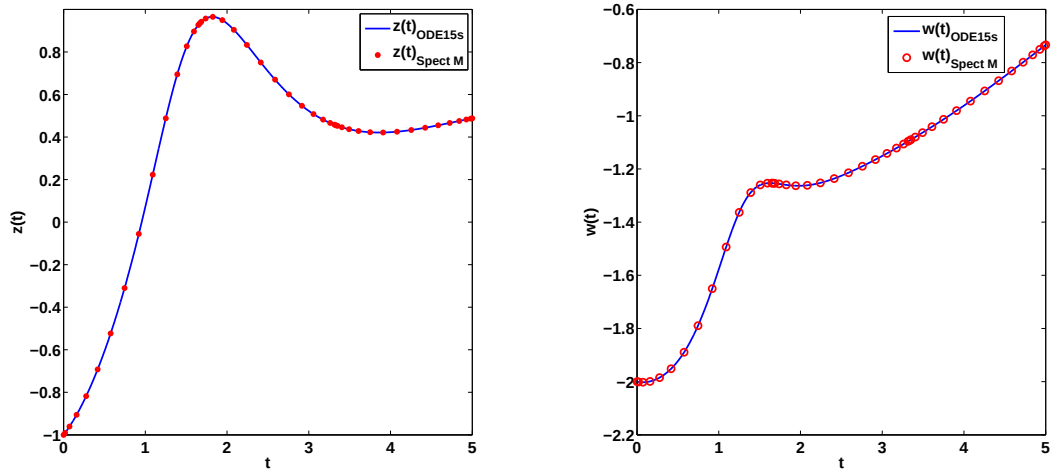

(c) $z(t)$ (d) $w(t)$

Figure 6.3.2: Plot of x, y, z, w variables using 3 domains and 16 collocation points and $T = 5$

the spectral integral method outperforms better than the other two methods on the hyperchaotic finance system for time $T = 5$. The reason for such is mainly due to the level of sparcity of the matrices generated by the schemes. Figure 6.3.5 shows the sparcity structures of matrices generated for each method. The integral method has a matrix structure more porous than others, giving it the advantage to be invertible faster than the matrix from differentiation method which is upper triangular, and also

matrix from chebfun which is is full.

Another point to consider is the factor T. It is worth noting that during the course of our simulations, the differentiation method starts malperforming when the size of the domain gets greater than 2 and same remark would apply to the integral method but for $T > 4$. For this additional reason, as T gets larger, we shall decompose our interval $[0, T]$ into multiple domains. The same remark also holds for Chebfun, it degenerates whenever $T > 11$ as shown in Figure 6.3.3d. The remedy is the same, one has to consider decomposing the intervals into sub-intervals. This turns out also to produce improvement in the CPU running time, (see figure 6.3.4). In all cases, still the integral method performs faster than the differentiation method.

As we vary the total number of collocation points from $n = 32, 64, 128, 256, 512, 1024, 2048$ and 4096, the error on each variable x, y, z and w.

Figure 6.3.4 shows that as the number of collocation points get larger (here $n >$ 1000) on each subinterval, the methods tend to suffer in terms of rapidity. Indeed matrix A gets very large, making inversion a complicated task. But if the structure of A gets more porous (increase in sparsity) then the spectral methods would still be capable of handling an even larger problem without losing much in accuracy. For instance, one can see that with the differentation approach, it takes 1320s ie. 23min to obtain an error of order 10^{-12} using one domain but with 8 domain decomposition the algorithm will take less that 2min using differention method and less than 1min using the integral method.

We look at the influence of number of domains N and the time T as it increases maintaining the number of collocation point n constant equal 64. Figure 6.3.6 shows that the error remains the same no matter how big is T, as long as the domain sizes are enough to allow for the spectral method to run on each domain. The number of domains N does not influence the error but helps in speeding up the algorithm.

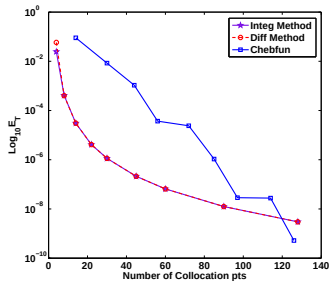

(a) Error versus n for $T = 2$ $N = 1$

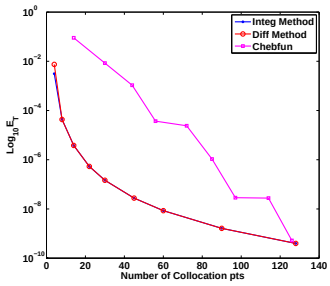

(b) Error versus n for $T = 2$ $N = 2$

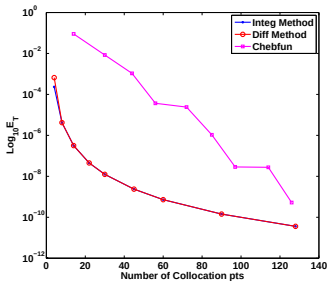

(c) Error versus n for $T = 2$ $N = 4$

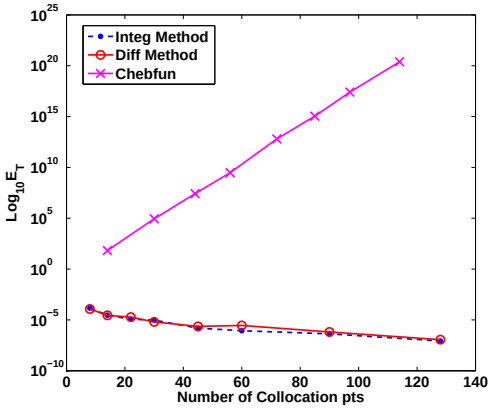

(d) Error versus n for $T = 11$ $N = 4$

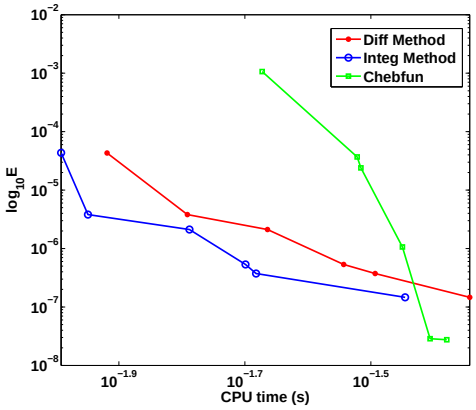

(e) Efficiency

Figure 6.3.3: Convergence and efficiency of the three methods a we vary the number of collcation points

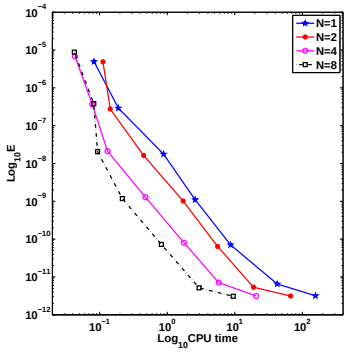

(a) Efficiency with integration method

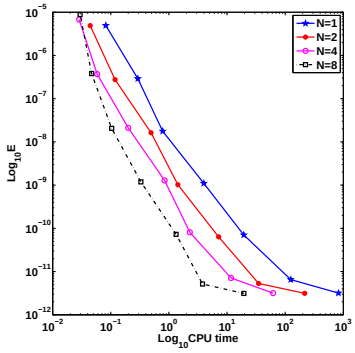

(b) Efficiency with differentiation method

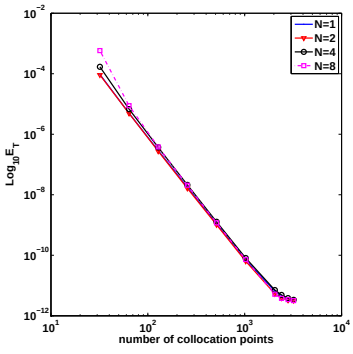

(c) Convergence of integration/differention method

Figure 6.3.4: Efficiency and convergence of integral and differentiation method as we vary the number of domains

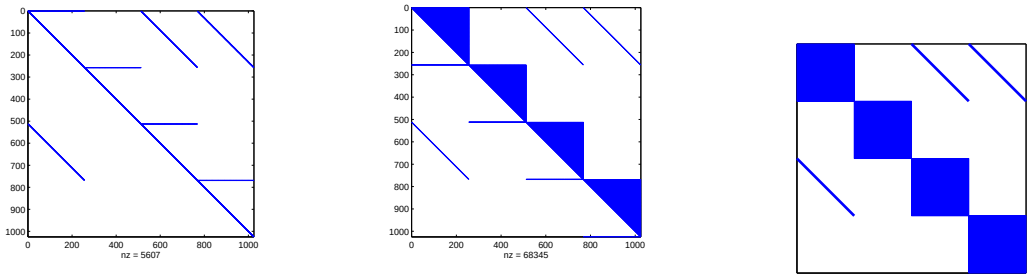

(a) 1-Domain Integration matrix (b) 1-Domain Differentiation matrix (c) Chebfun matrix

Figure 6.3.5: Plots of the underlying matrix A of all three methods.

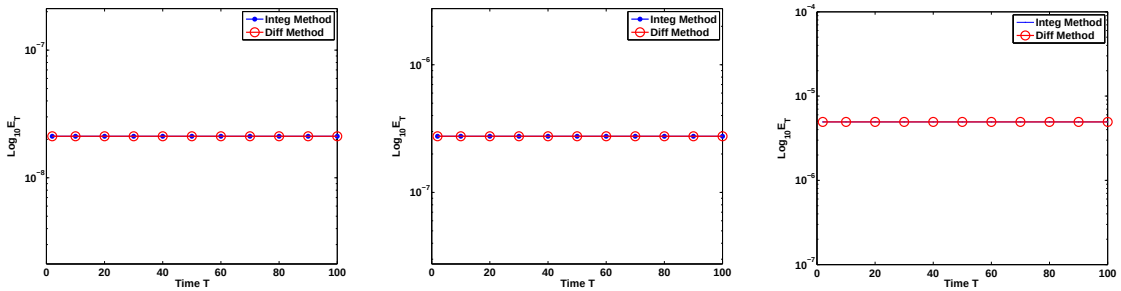

(a) $0 \leq T \leq 100, N = 200$ ie. h=0.5 (b) $0 \leq T \leq 100, N = 100$ ie. $h = 1$ (c) $0 \leq T \leq 100, N = 50$ i.e h=2

Figure 6.3.6: Plots of error as T increases to 100 and $n = 64$, for different number of domains

6.4 Conclusion

In this chapter, a Chebyshev spectral method has been applied on time multiple domain using differentiation matrix and also using integration approach. The methods prove to be robust with the integral approach showing to be more efficient for hyperchaotic finance problem than the method from differential approach. The results are also compared with solutions obtained from other numerical methods in the literature to confirm reliabily of the solutions. The spectral methods presented here are simple and accurate for handling even more complicated ODEs, however when it comes to fractional cases, it will be interesting to see how can the method perform on such problem. This is the subject of the next coming chapter.

Chapter 7

Fractional spectral integral methods for valuing cryptocurrency asset flow modeled by fractional differential equations

This chapter is a slightly modified version of a paper submitted into an accredited journal and still under review.

7.1 Introduction

Recently the notion of cryptocurrency has become increasingly popular. A cryptocurrency is essentially a type of digital asset used as money in a sense of the Austrian school of economics, i.e. money emerges from a competition of medium of exchanges [12, 92]. A cryptocurrency value is dictated by the supply and demand in a free economy where the intervention of any entity or government is not possible in the issuance of its new units as to opposed fiat currencies that follow the Keynesian school of economics, i.e. a governmental organization can have a positive effect on an economy, especially when

it begins to slow down or take a hit [46, 89]. The backbone technology underpinning a cryptocurrency is the blockchain. It is a distributed public ledger that records all the transactions since inception in a safe, secure, verifiable and non-editable manner [3]. Newly issued units of a cryptocurrency is realized through a process called mining. Miners verify transactions in a block by solving of complex hard mathematical process which requires an enormous amount of computing power. This is known as the proof of work. During this process, the most competitive miner receives mining rewards and transactions fees. This is how new coins are issued [63]. Bitcoin uses the proof of work verification process to ensure the integrity of the system. There exists other types of verification processes such as the proof of stake, the delegated proof of stake, the proof of authority, etc. [10, 85].

A lot of research has been carried out to gain insights into the dynamics of the bitcoin price. However most of them focuses on time series modelling [88]. Bitcoin prices and derivatives are barely studied from modelling point of view. Some papers dealing with option pricing are available but an extensive empirical analysis is missing. Additional literature on pricing is provided by Madan et al. [63]. A dynamical approach instead is carried by Caginalp [15] to analyse stability of cryptocurrency markets. The model describes a system of nonlinear ordinary differential equations.

However, due to high variability in the dataset, total differentiation can in some instance leave some challenges in the degree of the accuracy of the model and by using fractional differentiation, the accuracy on pricing models may be improved. We extend the study of the model proposed by Caginalp [15] to fractional differential equations (FDE). Fractional derivatives are unfortunately not unique. The classical ones are the Rieman-Liouville fractional derivatives and the Caputo fractional derivative [77]. One challenge with classical fractional calculus is to handle nonlinear phenomena [17, 29]. Various fractional derivative operators have been introduced recently among them, the Atangana-Baleanu (AB) fractional derivative. Fractional derivatives have been tested with success in many fields including chaotic behavior, epidemiology [5, 8, 49]. Since our cryptocurrency model also is valid on a short period of time, singularities are not

observed. Hence a Caputo fractional operator is preferred in order to facilitate the introduction of fractional integration. A fractional dynamical approach for cryptocurrency in the Caputo sense is therefore proposed.Attempts to solve FDEs has been an ongoing active topic of research. There are several analytical methods such as Adomian decomposition methods, homotopy- perturbation methods, variational iteration method and homotopy Analysis methods [32, 66, 80, 105]. In general, most FDEs do not have exact analytical solutions, so approximations and numerical techniques must be used. Most works developed in numerical methods for solving FDEs have focused on lower (or classical) methods which include the class of finite difference and finite element methods. These methods have shown a slow convergence.

Higher order (or spectral) methods, however, have the advantage of being fast converging methods. Though only sparely explored in the context of fractional differential equations, high order methods have the potential to reduce computational cost by allowing the use of fewer points, while achieving the same accuracy as that of lower order methods [20]. In this chapter we intend to solve the fractional dynamical system governing the price process of cryptocurrency by means of spectral method, following the footsteps of [67, 94] with an extension to the three dimensional problem. More precisely the Caputo fractional operator is used for handling fractional differentiation.

This chapter is organised as follows. Section **??** presents some basic concepts of fractional integrals derivatives. In Section 7.3, we introduce the fractional spectral integral method that will be used, then we apply this to the cryptocurrency problem in Section 7.4. In the same section we present results and conduct an error analysis. The last section is devoted to the conclusion.

7.2 Quick review of fractional operators

We first recall Euler's Gamma function from Equation (2.2.1).

$$\Gamma(x) := \int_0^{+\infty} t^{x-1}e^{-t} \tag{7.2.1}$$

Assuming that a function $f(x)$ is well defined where $x > 0$, we can form the definite integral from 0 to x. The fractional integral of order α of f is

$$(J^\alpha f)(x) = \frac{1}{\Gamma(\alpha)} \int_0^x (x-t)^{\alpha-1} f(t)dt. \tag{7.2.2}$$

and the he Riemann-Liouville fractional order derivative of f is defined as the m^{th} derivative of the fractional integral of order $m - q$. That is:

$${}^{RL}_{a}D^q_t f(t) = \frac{d^m}{dt^m}\left[\frac{1}{\Gamma(m-q)} \int_a^t (t-\tau)^{m-q-1} f(\tau)d\tau\right], \qquad m = [q] + 1. \tag{7.2.3}$$

For all $a < t < T$

The Caputo frsctional derivative on the other hand is defined as the fractional integral of the m^{th}-derivative, That is:

$${}^{C}_{a}D^q_t f(t) = \frac{1}{\Gamma(m-q)} \int_a^t \frac{f^{(m)}(\tau)}{(t-\tau)^{q+1-m}} d\tau, \qquad m-1 \leq q < m \tag{7.2.4}$$

With the Caputo derivative we recover the fact that the derivative of a constant function is indeed zero, however we have to pay the price that f has to be m-differentiable. The following relations shows the equivalence between the Riemann-Liouville and the Caputo fractional derivatives:

$${}^{RL}_{a}D^\alpha f(t) = {}^{C}_{a}D^\alpha f(t) + \sum_{k=0}^{m-1} \frac{t^{k-\alpha}}{\Gamma(k-\alpha+1)} f^{(k)}(0^+), \tag{7.2.5}$$

Consequently,

$${}^{RL}_{a}D^\alpha f(t) := D^m J^{m-\alpha} f(t) \neq J^{m-\alpha} D^m f(t) := {}^{C}_{a}D^\alpha f(t), \tag{7.2.6}$$

unless the function $f(t)$ along with its first $m-1$ derivatives vanishes at $t = 0^+$.

7.3 Chebyshev approximation and fractional integral matrix operator

We recall the definition of the fractional integral in (7.2.2)

$$J^q f(x) = \frac{1}{\Gamma(q)} \int_0^x (x-t)^{q-1} f(t) dt. \tag{7.3.1}$$

Let us consider a function $f : [0, b] \to \mathbb{R}$, with the Chebyshev approximation:

$$f(x) = \sum_{k=0}^{n-1} c_k T_k(\alpha x + \beta), \quad \alpha = \frac{2}{b}, \quad \beta = -1. \tag{7.3.2}$$

Note that $c = (c_0, c_1, \ldots, c_n)$ is its spectral representation. The fractional integral of order q of the function f at any collocation point x_k is:

$$\begin{aligned} J^q f(x_j) &= \frac{1}{\Gamma(q)} \int_0^{x_j} (x_j - t)^{q-1} \sum_{k=0}^{n-1} c_k T_k(\alpha t - 1) dt \\ &= \sum_{k=0}^{n-1} c_k \int_0^{x_j} (x_j - t)^{q-1} T_k(\alpha t - 1) dt \\ &= \sum_{k=0}^{n-1} c_k I_k(x_j) \end{aligned}$$

where

$$I_k(x_j) = \int_0^{x_j} (x_j - t)^{q-1} T_k(\alpha t - 1) dt. \tag{7.3.3}$$

Thus the physical representation of the fractional integral of f on the entire interval $[0, b]$ is:

$$\begin{aligned} \underline{v}(x) = J^q f(x) &= (J^q f(x_0), J^q f(x_1), ..., J^q f(x_n)) \\ \left(\sum_{k=0}^{n} \tilde{c}_k T_k(x_0), ..., \sum_{k=0}^{n} \tilde{c}_k T_k(x_n) \right) &= \left(\sum_{k=0}^{n} c_k I_k(x_0), ..., \sum_{k=0}^{n} c_k I_k(x_n) \right) \end{aligned}$$

The above relation implies the existence of a matrix I such that

$$\begin{aligned} T\,\tilde{c} &= I\,c \\ \tilde{c} &= T^{-1} I\,c \end{aligned}$$

where $\tilde{c}$ is the spectral representation of the fractional integral of f, the matrix I is defined as follows

$$I = (I_{kj}), \quad I_{kj} = I_k(x_j), \quad i, j = 1, 2, ..., n \tag{7.3.4}$$

$I_k(x_j)$ being defined as in (7.3.3). Consequently the physical representation of the fractional integral operator is $I \cdot T^{-1}$ and the spectral representation of the fractional integral operator is $T^{-1}I$. It remains therefore to compute the matrix I. To this extend we have the following lemma, see also [72, 95].

Lemma 29. *[95] Let f be a continuous function defined on [0,b] and vanishing at 0, and define $I_k(x)$ as in (7.3.3). Then*

$$\begin{aligned} I_0(x) &= \frac{x^{1-q}}{1-q}/2, \\ I_1(x) &= \frac{\alpha x^{2-q}}{(2-q)(1-q)} - \frac{x^{1-q}}{k(1-q)}, \\ I_2(x) &= \frac{4\alpha^2 x^{3-q}}{(3-q)(2-q)(1-q)} - \frac{4\alpha x^{2-q}}{(2-q)(1-q)} + \frac{x^{1-q}}{1-q} \end{aligned}$$

and

$$\left(1 + \frac{1-q}{k}\right) \cdot I_k(x) = 2(\alpha x - 1) \cdot I_{k-1}(x) + \left(\frac{1-q}{k-2} - 1\right) \cdot I_{k-2}(x) - \frac{2(-1)^k}{k(k-2)} x^{1-q}$$

Proof. [95] We are interested in computing the following integral

$$I_k(x) = \int_0^x \frac{T_k(\alpha t - 1)}{(x-t)^{q-1}} dt \tag{7.3.5}$$

We have

$$\int_0^x \frac{1}{(x-t)^{1-q}}dt = \frac{x^q}{2q} \tag{7.3.6}$$

$$\int_0^x \frac{t}{(x-t)^{1-q}}dt = \frac{x^{q+1}}{q(q+1)} \tag{7.3.7}$$

$$\int_0^x \frac{t^2}{(x-t)^{1-q}}dt = \frac{2x^{q+2}}{q(q+1)(q+2)} \tag{7.3.8}$$

Thus

$$I_0(x) = \int_0^x \frac{1}{(x-t)^{1-q}}dt = \frac{x^q}{2q} \tag{7.3.9}$$

$$\begin{aligned} I_1(x) &= \int_0^x \frac{(\alpha t-1)}{(x-t)^{1-q}}dt \\ &= \alpha\int_0^x \frac{t\,dt}{(x-t)^{1-q}}dt + \int_0^x \frac{dt}{(x-t)^{1-q}} \\ &= \alpha\frac{x^{q+1}}{q(q+1)} - \frac{x^q}{2q} \end{aligned} \tag{7.3.10}$$

$$\begin{aligned} I_2(x) &= \int_0^x \frac{2(\alpha t-1)^2-1}{(x-t)^{1-q}}dt = 2\alpha^2\int_0^x \frac{t^2dt}{(x-t)^{1-q}} - 4\alpha\int_0^x \frac{t\,dt}{(x-t)^{1-q}} \\ &+ \int_0^x \frac{1}{(x-t)^{1-q}}dt \\ &= 4\alpha^2\frac{x^{q+2}}{q(q+1)(q+2)} - 4\alpha\frac{x^{q+2}}{q(q+1)} + \frac{x^q}{q} \end{aligned} \tag{7.3.11}$$

Using the recurrence relation in (**??**) we get the following

$$I_k(x) = \int_0^x \frac{T_k(\alpha t-1)}{(x-t)^q}dt = \int_0^x \frac{2(\alpha t-1)T_{k-1}(\alpha t-1) - T_{k-2}(\alpha t-1)}{(x-t)^q}dt \tag{7.3.12}$$

$$\begin{aligned} &= 2\alpha\int_0^x \frac{tT_{k-1}(\alpha t-1)}{(x-t)^{1-q}}dt - 2\int_0^x \frac{T_{k-1}(\alpha t-1)}{(x-t)^{1-q}}dt - \int_0^x \frac{T_{k-2}(\alpha t-1)}{(x-t)^{1-q}}dt \\ &= 2\alpha\left[t\int_0^x \frac{T_{k-1}(\alpha t-1)}{(x-t)^{1-q}}dt\right]_{t=0}^{t=x} - 2\alpha\int_0^x \frac{T_{k-1}(\alpha t-1)}{(x-t)^{1-q}}dt - 2I_{k-1}(x) - I_{k-2}(x) \\ &= 2\alpha x I_{k-1}(x) - 2\alpha\int_0^x \frac{T_{k-1}(\alpha t-1)}{(x-t)^{1-q}}dt - 2I_{k-1}(x) - I_{k-2}(x). \end{aligned} \tag{7.3.13}$$

On the other hand,

$$\begin{aligned}
\tilde{I}_{k-1}(x) &= \int_0^x (x-t)^q T_{k-1}(\alpha t-1)dt \\
&= \int_0^x (x-t)^q \left[\frac{T_k'(\alpha t-1)}{2k} - \frac{T_{k-2}'(\alpha t-1)}{2(k-2)}\right] dt \\
&= \frac{1}{2k}\int_0^x (x-t)^q T_k'(\alpha t-1)dt - \frac{1}{2(k-2)}\int_0^x (x-t)^q T_{k-2}'(\alpha t-1)dt \\
&= \frac{1}{2k}\left\{\left[\frac{1}{\alpha}(x-t)^q T_k(\alpha t-1)\right]_{t=0}^{t=x} + \int_0^x \frac{q}{\alpha}(x-t)^{q-1} T_k(\alpha t-1)dt\right\} \\
&- \frac{1}{2(k-2)}\left\{\left[\frac{1}{\alpha}(x-t)^q T_{k-2}(\alpha t-1)\right]_{t=0}^{t=x} + \int_0^x \frac{q}{\alpha}(x-t)^{q-1} T_{k-2}(\alpha t-1)dt\right\} \\
&= \frac{1}{2k}\left[-\frac{x^q}{\alpha}T_k(-1)\right] + \frac{q}{2k\alpha}\int_0^x (x-t)^{q-1} T_k(\alpha t-1)dt \\
&\quad -\frac{1}{2(k-2)}\left[-\frac{x^q}{\alpha}T_{k-2}(-1)\right] - \frac{q}{2\alpha(k-2)}\int_0^x (x-t)^{q-1} T_{k-2}(\alpha t-1)dt \\
&= \frac{x^q}{2\alpha}\left[\frac{T_{k-2}(-1)}{k-2} - \frac{T_k(-1)}{k}\right] + \frac{q}{2k\alpha}\int_0^x (x-t)^{q-1} T_k(\alpha t-1)dt \\
&\quad -\frac{q}{2\alpha(k-2)}\int_0^x (x-t)^{q-1} T_{k-2}(\alpha t-1)dt \\
&= \left[\frac{(-1)^{k-2}}{k-2} - \frac{(-1)^k}{k}\right]\frac{x^q}{2k\alpha} + \frac{q}{2k\alpha}I_k(x) - \frac{q}{2\alpha(k-2)}I_{k-2}(x) \\
&= \frac{(-1)^k x^q}{\alpha k(k-2)} + \frac{q}{2k\alpha}I_k(x) - \frac{q}{2\alpha(k-2)}I_{k-2}(x).
\end{aligned}$$

Therefore

$$\begin{aligned}
I_k(x) &= -2\alpha\left[\frac{(-1)^k x^q}{\alpha k(k-2)} + \frac{q}{2k\alpha}I_k(x) - \frac{q}{2\alpha(k-2)}I_{k-2}(x)\right] \\
&+ 2(\alpha x-1)I_{k-1}(x) - I_{k-2}(x) \\
&= \frac{-2(-1)^k x^q}{k(k-2)} - \frac{q}{k}I_k(x) + \frac{q}{k-2}I_{k-2}(x) + 2(\alpha x-1)I_{k-1}(x) - I_{k-2}(x) \\
\left(1+\frac{q}{k}\right)I_k &= 2(\alpha x-1)I_{k-1}(x) + \left(\frac{q}{k-2}-1\right)I_{k-2}(x) - \frac{2(-1)^k x^q}{k(k-2)}.
\end{aligned}$$

□

Consequently let $0 < q_0 < q_1 < ... < q_m$, and consider a general multiple order

fractional differential equation $\mathcal{A}u = f$ of order q_m with constant coefficients. Suppose the fractional differential operator can be written as $\mathcal{A} = L + \mathcal{N}$ where L and $\mathcal{N}$ are respectively the linear part and the nonlinear part, then the equation can be written as

$$\begin{aligned} Lu(t) + \mathcal{N}u(t) &= f(t) && (7.3.14) \\ \sum_{k=0}^{m} D^{q_k} u(t) &= -\mathcal{N}u(t) + f(t) && (7.3.15) \end{aligned}$$

Taking fractional integral of order q_m to (7.3.15) and applying relation (7.2.6) we get:

$$\sum_{k=0}^{m} J^{q_m - q_k} u(t) = J^{q_m} \left[-\mathcal{N}u(t) + f(t) \right]. \tag{7.3.16}$$

The above equation can be represented in the frequency space as:

$$\begin{aligned} \sum_{k=0}^{m} \mathbf{J}^{q_m - q_k} \underline{c} &= -\mathbf{n} + \tilde{\mathbf{f}} \\ \mathbf{A}\,\underline{c} &= \mathbf{f} && (7.3.17) \\ \text{implying} \qquad \underline{c} &= \mathbf{A}^{-1}(\mathbf{f}) \end{aligned}$$

for some $\mathbf{A} = \sum_{k=0}^{m} \mathbf{J}^{q_m - q_k}$; where $\mathbf{n}, \tilde{\mathbf{f}}$ are the spectral representation of $J^{q_m}\mathcal{N}u$ and $J^{q_m} f$ respectively, and $\mathbf{f} = -\mathbf{n} + \tilde{\mathbf{f}}$.

7.4 Application and numerical results

In this section, we apply our fractional spectral integral method (FSIM) to problems in cryptocurrency world. We also test the convergence of our proposed method against existing fde12 method [36, 37]. Whenever the analytical solution is not found, we choose our FSIM with relative tolerance 10^{-14} (that is 2000 collocation points) as the

benchmark solution. The error E is the maximal error given by

$$||E|| = ||Sol_{Benchmark} - Sol_{Numerical}||_{\infty}. \tag{7.4.1}$$

All the numerical simulations are performed on a processor Intel core I5, 8th Gen.

7.4.1 Benchmark problem

Here we consider the following system of fractional differential equation [103]

$$\begin{cases} D^{q_1}x(t) &= \sqrt{t} + \sqrt[6]{(y(t)-0.5)(z(t)-0.3)}, \\ D^{q_2}y(t) &= \Gamma(2.2), \\ D^{q_3}z(t) &= \frac{\Gamma(2.8)}{\Gamma(2.2)}, \end{cases} \tag{7.4.2}$$

with $q_1 = 0.5$ $q_2 = 0.2$ and $q_3 = 0.6$ together with initial condition: $x(0) = 1, y(0) = 0.5$ and $z(0) = 0.3$, for which the exact solution is found to be $x(t) = t+1, y(t) = t^{1.2}, z(t) = t^{1.8} + 0.3$.

Applying our method and comparing with the exact solution we get the following plot for the solutions x, y, z in Figure 7.4.1. This plot shows that the numerical solution from (FSIM) and the exact solution are in good agreement.

We also run a comparison with another already existing numerical method, here fde12 which is based on Taylor expension approximation.
As we vary the number of collocation points on the FSIM we record in Figure 7.4.1d the evolution of the error dynamics on the variable z. The log-log graph shows an exponential decay of the error which is expected from a spectral method. The same result holds also for the variables x and y.

7.4.2 Cryptocurrency model

The behaviour of the cryptocurrency price dynamics in the market is based on some key factors:

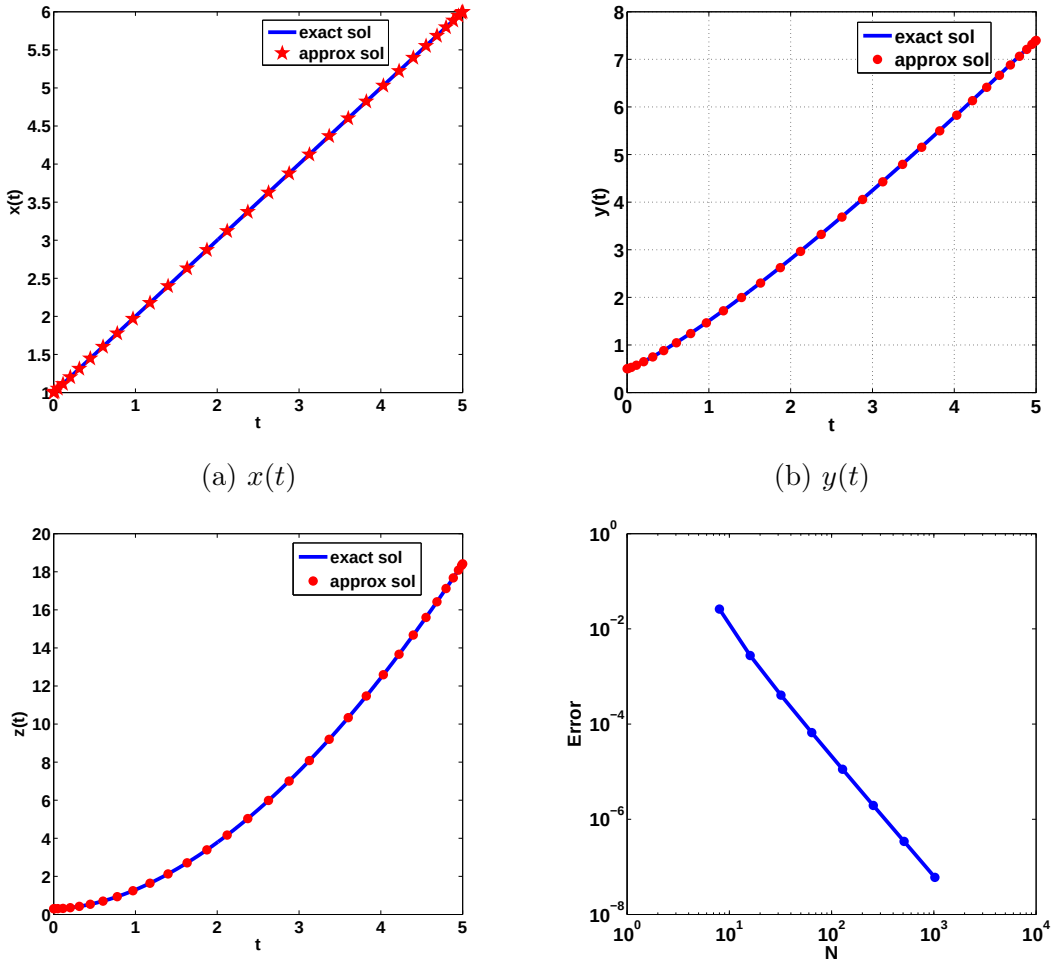

(a) $x(t)$ (b) $y(t)$

(c) $z(t)$ (d) Convergence

Figure 7.4.1: Plot of the variables x, y, z for $T = 5$ and $N = 32$ collocation points and convergence

- $P(t)$: The market price of cryptocurrency.
- $L(t)$: The Liquidity price at time t.
- $\zeta_1(t)$: The trend-based component of investor preference at time t.

Caginalp [15] proposed a dynamical system based on asset flow differential equation to describe the behaviour of those three variables in the market as :

$$\begin{cases} \tau_0 \frac{dP}{dt} &= (1+2\zeta_1)L - P, \\ c_0 \frac{dL}{dt} &= 1 - L + q(1+2\zeta_1)L - qP, \\ c_1 \frac{d\zeta_1}{dt} &= q_1(1+2\zeta_1)\frac{L}{P} - q_1 - \zeta_1. \end{cases} \tag{7.4.3}$$

The system admits only one equilibrium point obtained for $L = P$ and $\zeta_1 = 0$.
It is known that integer order derivative may fail to take into consideration the history of the system and fails to address some technical issues describing this system. For this reason, let substitute the integer derivative by a Caputo fractional derivatives into the system, we get:

$$\begin{cases} \tau_0 {}_0^c D_t^{\alpha_1} P &= (1+2\zeta_1)L - P, \\ c_0 {}_0^c D_t^{\alpha_2} L &= 1 - L + q(1+2\zeta_1)L - qP, \\ c_1 {}_1^c D_t^{\alpha_3} \zeta_1 &= q_1(1+2\zeta_1)\frac{L}{P} - q_1 - \zeta_1. \end{cases} \tag{7.4.4}$$

Taking fractional integrals appropriately for each equation in the system and using (7.2.6) we get

$$\begin{cases} \tau_0 P = J^{\alpha_1}(1+2\zeta_1)L - J^{\alpha_1} P, \\ c_0 L = J^{\alpha_2}(1 - L + q(1+2\zeta_1)L - qP), \\ c_1 \zeta_1 = J^{\alpha_3}(q_1(1+2\zeta_1)\frac{L}{P} - q_1 - \zeta_1). \end{cases} \tag{7.4.5}$$

Equation (7.4.2) is a 3 dimensional system of nonlinear ordinary fractional integral equations. It can be written as:

$$Au + Nu = f \tag{7.4.6}$$

Using our Fractional Spectral Integral Method described in section 3, we transport the equation in the frequency space and it becomes

$$\mathbf{A}\underline{c} = \mathbf{f} \tag{7.4.7}$$

where $\underline{c}$ and $\mathbf{f}$ are spectral representations of the unknown solution vector $u = (P, L, \zeta_1)$ and the nonlinear part $f - Nu$, respectively. In addition, the matrix $\mathbf{A}$ is of the form:

$$\mathbf{A} = \begin{bmatrix} \tau_0\mathcal{I} + J^{\alpha_1} & -J^{\alpha_1} & 0 \\ qJ^{\alpha_2} & c_0\mathcal{I} + (1-q)J^{\alpha_2} & 0 \\ 0 & 0 & c_1\mathcal{I} + J^{\alpha_3} \end{bmatrix}$$

where $\mathcal{I}$ is the identity matrix and J is the integral matrix as defined in (7.3.4). The nonlinear part will write as:

$$N = \begin{bmatrix} 2J^{\alpha_1}\zeta_1 L \\ J^{\alpha_2}(1 + 2q\zeta_1 L) \\ J^{\alpha_3}\left(q_1(1+2\zeta_1)\frac{L}{P} - q_1\right) \end{bmatrix}.$$

We run the algorithm for the following set of parameters $\tau_0 = 1.8,\ c_0 = 1,\ q_0 = 0.75,\ q_1 = -2.5,\ c_1 = 1$; considering an initial solution to be $P(0) = 1.8,\ L(0) = 0.8,\ \zeta_1(0) = -0.1$, and $\alpha_1 = 0.5, \alpha_2 = 0.7, \alpha_3 = 0.9$. We compare the results with the solution from fde12 method. The solutions are plotted in Figure 7.4.2 for the variables $x(t), y(t), z(t)$.

A long run behaviour of the solutions is plotted in Figure 7.4.3a together with a phase plane $PL, P\zeta_1$ and $L\zeta_1$ in Figure 7.4.3b, Figure 7.4.3c and Figure 7.4.3d respectively. These plots confirm the stability analysis announced earlier and that is, there is no chaotic behaviour observed in the cryptocurrency pricing problem, see also [78] for more on the stability analysis.

Looking at the effect of varying the fractional order of differentiation, Figure 7.4.4 shows that as $\alpha \to 1$ the solution of the fractional differential equation converges to

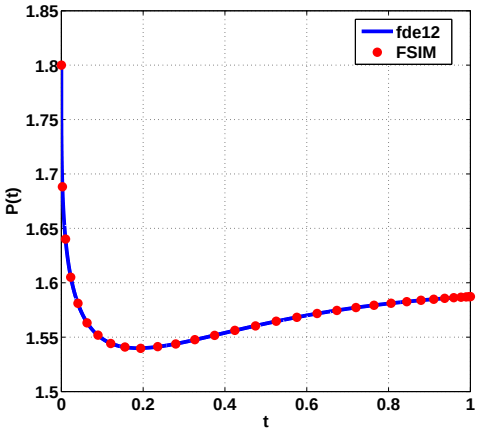

(a) $P(t)$

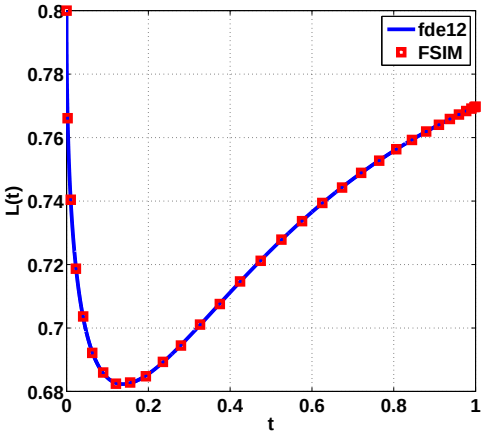

(b) $L(t)$

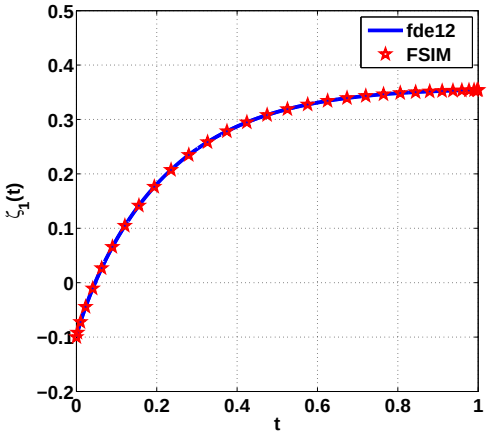

(c) $\zeta_1(t)$

Figure 7.4.2: Plot of the variables P, L, ζ_1 for $T = 1$, $N = 32$ collocation points and $h = 10^{-5}$ for the fde12 method

the solution of the ordinary differential equation. In addition, the numerical results demonstrate that a decrease in the derivative order is associated with a decrease in the minimum value of P and L and in the maximum value of ζ_1.

We investigate the convergence and efficiency of the method compared to fde12 method. Figure 7.4.4e confirms the fast convergence of the spectral method. Indeed it only takes 32 points and 512 points to already reach accuracy of order 10^{-3} and 10^{-7} respectively while it would necessitate respectively 1000 and 100,000 points to achieve the same order of accuracy for the fde12 method. In terms of efficiency, Figure

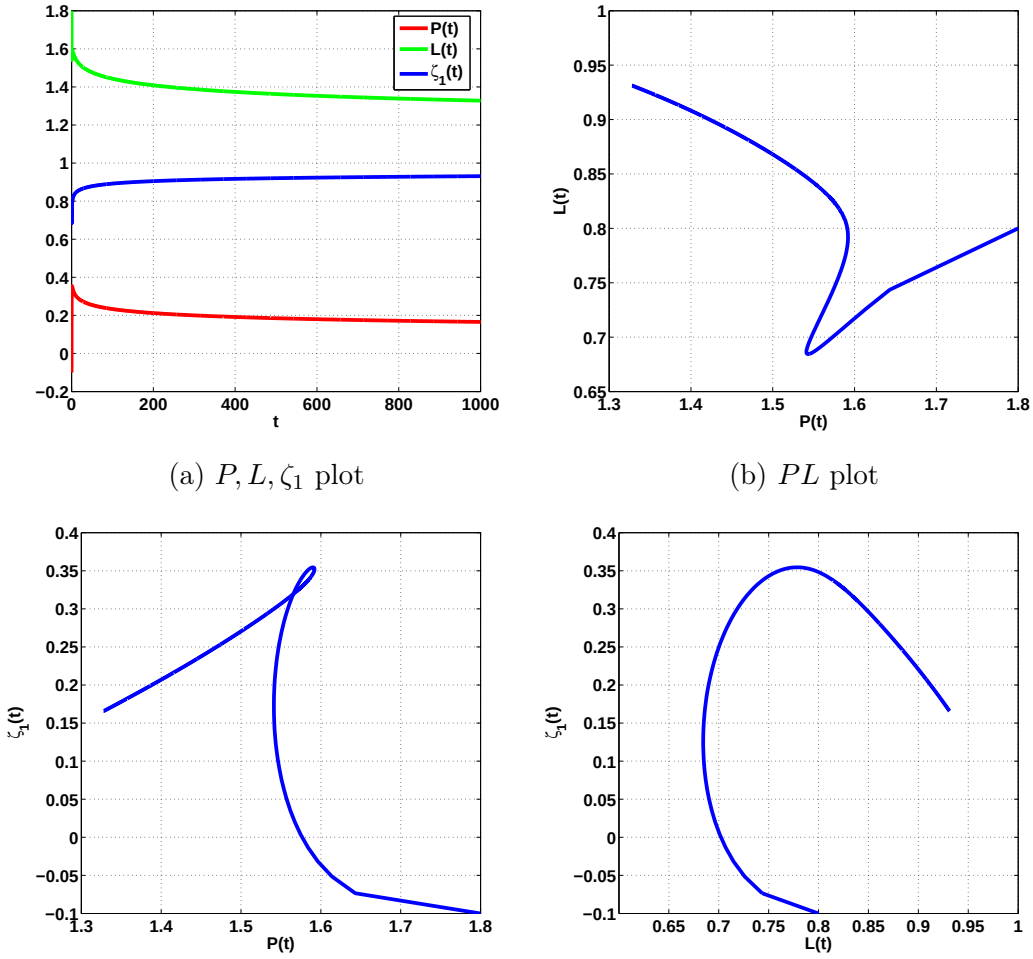

(a) P, L, ζ_1 plot

(b) PL plot

(c) $P\zeta_1$ plot

(d) $L\zeta_1$ plot

Figure 7.4.3: Phase planes for large $T = 1000$

7.4.4d shows that fde12 method takes 1.7s to achieve accuracy order 10^{-4} whereas our spectral method covers this same accuracy within 0.2s. In addition, it becomes a mission for the fde12 to reach higher order of accuracy since the number of unkowns becomes extremely large.

7.5 Conclusion

In this chapter we have presented a spectral integral method to numerically solve systems of FDEs especially in the case of cryptocurrency models where the problem

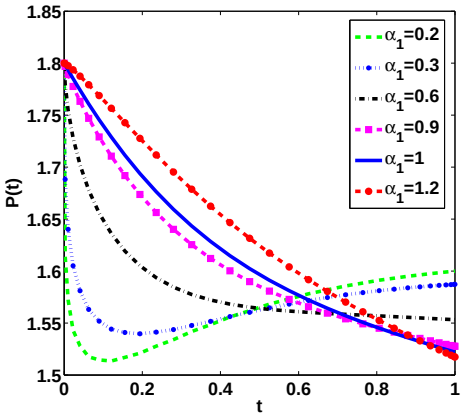

(a) $P(t)$ for $\alpha_2 = 0.5$, $\alpha_3 = 0.9$

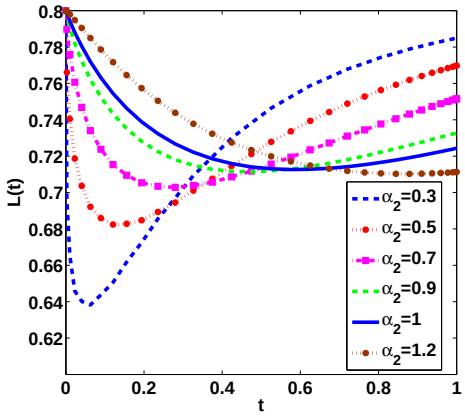

(b) $L(t)$ for $\alpha_1 = 0.3$, $\alpha_3 = 0.9$

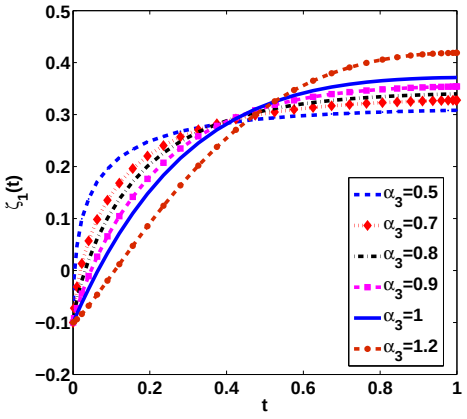

(c) $\zeta_1(t)$ for $\alpha_2 = 0.3$, $\alpha_2 = 0.5$

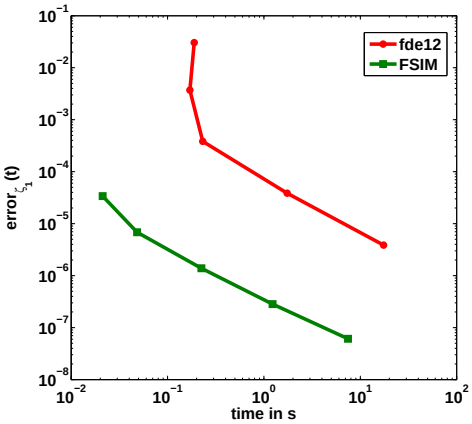

(d) Efficiency

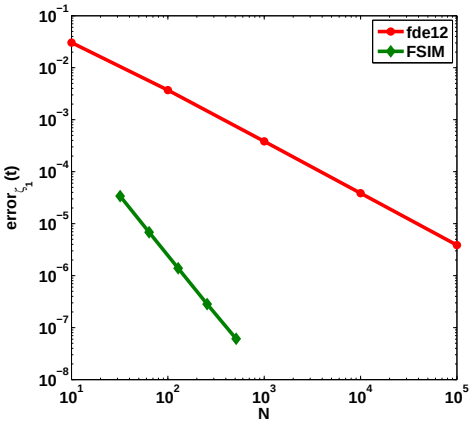

(e) Convergence

Figure 7.4.4: Plot of the variables x, y, z for $T = 1$

involves multiple orders of FDE. The result from error analysis shows that our method maintains its spectral convergence. An efficiency analysis was also conducted against an existing method, here the fde12 and results are satisfactory. For further application it would be interesting to couple our method with a spliting method in order to deal large time scale FDEs. Also see how the method can be adjusted in the case of problems with kernels that would require Atanga-Baleanu fractional derivatives in the modeling instead of the Caputo derivative.

Chapter 8

Conclusion and Future Perspectives

8.1 Conclusion

We have designed a spectral method that accommodates problems of various type in finance. These problems result into solving systems of ODEs. The proposed numerical method presents an operatorial matrix based on chebyshev polynomials with solutions in the frequency domain instead of the physical domain as most actual numerical methods do.

For large time scale ODEs, a discretization of the time is applied allowing thus the spectral method to converge not only on the subdomains but also globally. In the sequel, two approaches are implemented: The differential approach on one side, resulting into triangular matrices and the integral approach on the other side resulting in band matrices which become diagonal when the problem involves constant coefficients. In both cases the matrices are spares reducing tremendously the amount of calculations. A comparison is run on hyperchaotic problems and results tend favoured the integral approach in terms of efficiency.

We also apply our method to fractional cryptocurrency problems. From a dynamical approach, the problem yields a system of fractional differential equations of multiple orders. In this framework the spectral integral method is redesigned to handle such problems.

Most importantly, our designed spectral methods show robustness and fast con-

vergence when compared to existing well known Matlab numerical packages that are available, we mention ODE15s, Chebfun [93], DMS [101] and for fractional case we mention fde12 [37].

8.2 Future Perspectives

The results obtained in this thesis and challenges encountered during the process, have lead to numerous research questions which require further investigation. Some of them are listed below.

- To further extend the method to stochastic differential equations and partial integro-differential equations

- To further investigate fractional problems with singularities.

Bibliography

[1] Mohammed Salah Abd-Elouahab, Nasr-Eddine Hamri, and Junwei Wang. Chaos control of a fractional-order financial system. *Mathematical Problems in Engineering*, 2010, 2010.

[2] Niels Abel. Solution de quelques problèmes à l'aide d'intégrales définies. *Oeuvres*, 1:11–27, 1881.

[3] Kelly Aedan and Blum Derek. *The Complete Step by Step Guide to Cryptocurrency Trading and Investing*. CryptoMeister.io.

[4] Torben G Andersen, Luca Benzoni, and Jesper Lund. Stochastic volatility, mean drift, and jumps in the short-term interest rate. *Northwestern University, Chicago*, 2004.

[5] Abdon Atangana and Dumitru Baleanu. New fractional derivatives with nonlocal and non-singular kernel: theory and application to heat transfer model. *arXiv preprint arXiv:1602.03408*, 2016.

[6] ESMAEIL Babolian and MM Hosseini. A modified spectral method for numerical solution of ordinary differential equations with non-analytic solution. *Applied Mathematics and Computation*, 132(2):341–351, 2002.

[7] Dumitru Baleanu and Arran Fernandez. On some new properties of fractional derivatives with mittag-leffler kernel. *Communications in Nonlinear Science and Numerical Simulation*, 59:444–462, 2018.

[8] Dumitru Baleanu, B Shiri, HM Srivastava, and M Al Qurashi. A chebyshev spectral method based on operational matrix for fractional differential equations involving non-singular mittag-leffler kernel. *Advances in Difference Equations*, 2018(1):353, 2018.

[9] AH Bhrawy and AS Alofi. The operational matrix of fractional integration for shifted chebyshev polynomials. *Applied Mathematics Letters*, 26(1):25–31, 2013.

[10] G BitFury. Proof of stake versus proof of work. *White paper, Sep*, 2015.

[11] T Björk. *Arbitrage Theory in Continuous Time*. Oxford University Press, second edition, 2004.

[12] Peter J Boettke. Austrian school of economics. *Concise Encyclopedia of Economics*, 2008.

[13] WILLIAM Bourke, Bryant McAvaney, KAMAL Puri, and R Thurling. Global modeling of atmospheric flow by spectral methods. *Methods in computational physics*, 17:267–324, 1977.

[14] John P Boyd. *Chebyshev and Fourier spectral methods*. Courier Corporation, 2001.

[15] Carey Caginalp. A dynamical systems approach to cryptocurrency stability. *arXiv preprint arXiv:1805.03143*, 2018.

[16] Claudio Canuto, M Yousuff Hussaini, Alfio Quarteroni, A Thomas Jr, et al. *Spectral methods in fluid dynamics*. Springer Science & Business Media, 2012.

[17] Michele Caputo. Linear models of dissipation whose q is almost frequency independentâĂŤii. *Geophysical Journal International*, 13(5):529–539, 1967.

[18] Michele Caputo and Mauro Fabrizio. A new definition of fractional derivative without singular kernel. *Progr. Fract. Differ. Appl*, 1(2):1–13, 2015.

[19] Changzhong Chen, Tao Fan, and Bangrong Wang. Inverse optimal control of hyperchaotic finance system. *World Journal of Modelling and Simulation*, 10(2): 83–91, 2014.

[20] Feng Chen, Qinwu Xu, and Jan S Hesthaven. A multi-domain spectral method for time-fractional differential equations. *Journal of Computational Physics*, 293: 157–172, 2015.

[21] R Cont and P Tankov. *Financial Modeling With Jump Processes*. Chapman and Hall/CRC, 2004.

[22] Germund Dahlquist and Ake Bjorck. *Numerical Methods in Scientific Computing: Volume 1*, volume 103. Siam, 2008.

[23] Shijie Deng. *Stochastic models of energy commodity prices and their applications: Mean-reversion with jumps and spikes*. University of California Energy Institute Berkeley, 2000.

[24] Juan Ding, Weiguo Yang, and Hongxing Yao. A new modified hyperchaotic finance system and its control. *International Journal of Nonlinear Science*, 8(1): 59–66, 2009.

[25] EH Doha, AH Bhrawy, and SS Ezz-Eldien. A chebyshev spectral method based on operational matrix for initial and boundary value problems of fractional order. *Computers & Mathematics with Applications*, 62(5):2364–2373, 2011.

[26] JJ Dongarra, B Straughan, and DW Walker. Chebyshev tau-qz algorithm methods for calculating spectra of hydrodynamic stability problems. *Applied Numerical Mathematics*, 22(4):399–434, 1996.

[27] Tobin A Driscoll. Automatic spectral collocation for integral, integro-differential, and integrally reformulated differential equations. *Journal of Computational Physics*, 229(17):5980–5998, 2010.

[28] D Duffie, J Pan, and K Singleton. Transform analysis and asset pricing for affine jump-diffusions. *Econometrica*, (68):1343–1376, 2000.

[29] Baleanu Dumitru, Diethelm Kai, and Scalas Enrico. *Fractional calculus: models and numerical methods*, volume 3. World Scientific, 2012.

[30] Bonyah Ebenezer, OT Kolebaje, and Kwasi Awuah-Werekoh. Using multistage laplace adomian decomposition method to solve chaotic financial system. *Journal of Advances in Mathematics and Computer Science*, pages 1–14, 2016.

[31] Matthias Ehrhardt and Ronald E Mickens. A fast, stable and accurate numerical method for the black–scholes equation of american options. *International Journal of Theoretical and Applied Finance*, 11(05):471–501, 2008.

[32] AMA El-Sayed, IL El-Kalla, and EAA Ziada. Analytical and numerical solutions of multi-term nonlinear fractional orders differential equations. *Applied Numerical Mathematics*, 60(8):788–797, 2010.

[33] Gamal N Elnagar and M Kazemi. Chebyshev spectral solution of nonlinear volterra-hammerstein integral equations. *Journal of computational and applied mathematics*, 76(1):147–158, 1996.

[34] Clive AJ Fletcher. Computational galerkin methods. In *Computational galerkin methods*, pages 72–85. Springer, 1984.

[35] Bengt Fornberg and Tobin A Driscoll. A fast spectral algorithm for nonlinear wave equations with linear dispersion. *Journal of Computational Physics*, 155 (2):456–467, 1999.

[36] Roberto Garrappa. Short tutorial: solving fractional differential equations by matlab codes. *Department of Mathematics University of Bari, Italy*, 2014.

[37] Roberto Garrappa. Numerical solution of fractional differential equations: A survey and a software tutorial. *Mathematics*, 6(2):16, 2018.

[38] Călin Ioan Gheorghiu. *Spectral methods for differential problems*. Casa Cărţii de Ştiinţă Cluj-Napoca, 2007.

[39] Rudolf Gorenflo. Fractional calculus: some numerical methods. *Courses and lectures-international centre for mechanical sciences*, pages 277–290, 1997.

[40] Rudolf Gorenflo and Francesco Mainardi. Fractional calculus. In *Fractals and fractional calculus in continuum mechanics*, pages 223–276. Springer, 1997.

[41] David Gottlieb and Steven A Orszag. *Numerical analysis of spectral methods: theory and applications*. SIAM, 1977.

[42] Ben-Yu Guo, Zhong-Qing Wang, Hong-Jiong Tian, and Li-Lian Wang. Integration processes of ordinary differential equations based on laguerre-radau interpolations. *Mathematics of Computation*, 77(261):181–199, 2008.

[43] Benyu Guo. *Spectral methods and their applications*. World Scientific, 1998.

[44] Nejla Gurefe, Emine Gokcen Kocer, and Yusuf Gurefe. Chebyshev-tau method for the linear klein-gordon equation. *International Journal of Physical Sciences*, 7(43):5723–5728, 2012.

[45] Houde Han and Xiaonan Wu. A fast numerical method for the black–scholes equation of american options. *SIAM Journal on Numerical Analysis*, 41(6):2081–2095, 2003.

[46] FA Hayek. The mythology of capital. *The Quarterly Journal of Economics*, 50 (2):199–228, 1936.

[47] S.L. Heston. A closed-form solution for options with stochastic volatility with applications to bond and currency options. *The Review of Financial Studies*, 6 (2):327–343, 1993.

[48] M Hiegemann. Chebyshev matrix operator method for the solution of integrated forms of linear ordinary differential equations. *Acta mechanica*, 122(1-4):231–242, 1997.

[49] Jordan Hristov. On the atangana–baleanu derivative and its relation to the fading memory concept: the diffusion equation formulation. In *Fractional Derivatives with Mittag-Leffler Kernel*, pages 175–193. Springer, 2019.

[50] Shirley J Huang and Jun Yu. On stiffness in affine asset pricing models. *Available at SSRN 676203*, 2004.

[51] Shirley Jun Ying Huang. Implementation of general linear methods for stiff ordinary differential equations. *The University of Auckland, New Zealand*, 2005.

[52] M Yousuff Hussaini and Thomas A Zang. Spectral methods in fluid dynamics. *Annual review of fluid mechanics*, 19(1):339–367, 1987.

[53] Y. Chen J. Ma. Study for the bifurcation topological structure and the global complicated character of a kind of non-linear finance system (ii). *Applied Mathematics and Mechanics*, 22.

[54] Y. Chen J. Ma. Study for the bifurcation topological structure and the global complicated character of a kind of non-linear finance system (i). *Applied Mathematics and Mechanics*, 22(11):1240–âĂŞ1251, 2001.

[55] Anatoliĭ Kilbas. *Theory and applications of fractional differential equations*.

[56] Uğur Erkin Kocamaz, Alper Göksu, Harun Taşkın, and Yılmaz Uyaroğlu. Synchronization of chaos in nonlinear finance system by means of sliding mode and passive control methods: a comparative study. *Information Technology and Control*, 44(2):172–181, 2015.

[57] Dimitri Komatitsch and Jeroen Tromp. Introduction to the spectral element

method for three-dimensional seismic wave propagation. *Geophysical journal international*, 139(3):806–822, 1999.

[58] Sylvestre Francois Lacroix. *Traite'du calcul differentiel et du calcul integral, par SF Lacroix: Du calcul differentiel!* chez JBM Duprat, 1797.

[59] Karl Larsson and Marcus Nossman. Jumps and stochastic volatility in oil prices: Time series evidence. *Energy Economics*, 33(3):504–514, 2011.

[60] MIHAILO P Lazarević, MILAN R Rapaić, TOMISLAV B Šekara, V Mladenov, and N Mastorakis. Introduction to fractional calculus with brief historical background. In *Chapter in book:âĂIJAdvanced Topics on Applications of Fractional Calculus on Control Problems, System Stability and Modeling*, pages 3–16. WSAES Press, 2014.

[61] Fei Liu, Xingde Ye, and Xinghua Wang. Efficient chebyshev spectral method for solving linear elliptic pdes using quasi-inverse technique. *Numerical Mathematics: Theory, Methods and Applications*, 4(02):197–215, 2011.

[62] Heping Ma. Chebyshev–legendre spectral viscosity method for nonlinear conservation laws. *SIAM Journal on Numerical Analysis*, 35(3):869–892, 1998.

[63] Dilip B Madan, Sofie Reyners, and Wim Schoutens. Advanced model calibration on bitcoin options. *Digital Finance*, 1(1-4):117–137, 2019.

[64] John C Mason and David C Handscomb. *Chebyshev polynomials*. CRC press, 2002.

[65] Alexey Mikhaylov. Cryptocurrency market analysis from the open innovation perspective. *Journal of Open Innovation: Technology, Market, and Complexity*, 6(4):197, 2020.

[66] Claude Rodrigue Bambe Moutsinga, Edson Pindza, and Eben Mare. Homotopy

perturbation transform method for pricing under pure diffusion models with affine coefficients. *Journal of King Saud University-Science*, 30(1):1–13, 2018.

[67] Claude Rodrigue Bambe Moutsinga, Edson Pindza, and Eben Maré. A robust spectral integral method for solving chaotic finance systems. *Alexandria Engineering Journal*, 59(2):601–611, 2020.

[68] Edgard Ngounda, Kailash C Patidar, and Edson Pindza. Contour integral method for european options with jumps. *Communications in Nonlinear Science and Numerical Simulation*, 18(3):478–492, 2013.

[69] Keith Oldham and Jerome Spanier. *The fractional calculus theory and applications of differentiation and integration to arbitrary order*. Elsevier, 1974.

[70] D Omale, PB Ojih, and MO Ogwo. Mathematical analysis of stiff and non-stiff initial value problems of ordinary differential equation using matlab. *International journal of scientific & engineering research*, 5(9):49–59, 2014.

[71] Ju H Park. Chaos synchronization of a chaotic system via nonlinear control. *Chaos, Solitons & Fractals*, 25(3):579–584, 2005.

[72] Robert Piessens and Maria Branders. Numerical solution of integral equations of mathematical physics, using chebyshev polynomials. *Journal of Computational Physics*, 21(2):178–196, 1976.

[73] E Pindza, KC Patidar, and E Ngounda. Robust spectral method for numerical valuation of european options under merton's jump-diffusion model. *Numerical Methods for Partial Differential Equations*, 30(4):1169–1188, 2014.

[74] Edson Pindza, Kailash C Patidar, and Edgard Ngounda. Implicit-explicit predictor-corrector methods combined with improved spectral methods for pricing european style vanilla and exotic options. *Electronic Transactions on Numerical Analysis*, 40:268–293, 2013.

[75] Edson Pindza, Francis Youbi, Eben Maré, and Matt Davison. Barycentric spectral domain decomposition methods for valuing a class of infinite activity lévy models. *Discrete & Continuous Dynamical Systems-S*, 12(3):625–643, 2019.

[76] R. B. Platte and N. Trefethen. Chebfun: A new kind of numerical computing. *Progress in Industrial Mathematics at ECMI 2008. Mathematics in Industry*, (15):69–87, 2010.

[77] Igor Podlubny. *Fractional differential equations: an introduction to fractional derivatives, fractional differential equations, to methods of their solution and some of their applications*. Elsevier, 1998.

[78] Din Prathumwan, Wannika Sawangtong, and Panumart Sawangtong. An analysis on the fractional asset flow differential equations. *Mathematics*, 5(2):33, 2017.

[79] Humberto Rafeiro and Stefan Samko. Fractional integrals and derivatives: mapping properties. *Fractional Calculus and Applied Analysis*, 19(3):580–607, 2016.

[80] S Saha Ray and RK Bera. Solution of an extraordinary differential equation by adomian decomposition method. *Journal of Applied mathematics*, 2004(4): 331–338, 2004.

[81] Theodore J Rivlin. *Chebyshev polynomials: from approximation theory to algebra and number theory*. Dover Publications, 2020.

[82] Bertram Ross. The development of fractional calculus 1695–1900. *Historia Mathematica*, 4(1):75–89, 1977.

[83] Aceng Sambas, Mustafa Mamat, Ayman Ali Arafa, Gamal M Mahmoud, Mohamad Afendee Mohamed, and WS Sanjaya. A new chaotic system with line of equilibria: dynamics, passive control and circuit design. *International Journal of Electrical & Computer Engineering (2088-8708)*, 9, 2019.

[84] Simon S.Clift and Peter A.Forsyth. Numerical solution of two asset jump diffusion models for option valuation. *Applied Numerical Mathematics*, (58):743–782, 2008.

[85] Sothearath Seang, Dominique Torre, et al. Proof of work and proof of stake consensus protocols: a blockchain application for local complementary currencies. *France: Universite Cote d'Azur-GREDEG-CNRS. Str*, 3(4), 2018.

[86] Jie Shen, Tao Tang, and Li-Lian Wang. *Spectral methods: algorithms, analysis and applications*, volume 41. Springer Science & Business Media, 2011.

[87] Jie Shen, Tao Tang, and Li-Lian Wang. *Spectral methods: algorithms, analysis and applications*, volume 41. Springer Science & Business Media, 2011.

[88] Eduard Silantyev. Order flow analysis of cryptocurrency markets. *Digital Finance*, 1(1-4):191–218, 2019.

[89] H Soto de Jesus. The austrian school market order and entrepreneurial creativity, 2008.

[90] Karel J.in 't Hout and Jari Toivanen. Adi schemes for valuing european options under the bates model. *Applied Numerical Mathematics*, (130):1343–1376, 2018.

[91] B. Taruvinga, B. Kang, and C.S. Nikitopoulos. Quantitative finance research centre, university of technology, sydney. *Applied Numerical Mathematics*, (394): 1–43, 2018.

[92] Thomas C Taylor. *An introduction to Austrian economics*. Ludwig von Mises Institute, 1980.

[93] Lloyd N Trefethen. *Spectral methods in MATLAB*, volume 10. Siam, 2000.

[94] Damian Trif. Matrix based operatorial approach to differential and integral problems. In *MATLAB-A Ubiquitous Tool for the Practical Engineer*. IntechOpen, 2011.

[95] Damian Trif. Operatorial tau method for fractional differential equations. *J. Math. Comput. Sci.*, 4(2):148–166, 2014.

[96] Sundarapandian Vaidyanathan. Global chaos synchronisation of identical li-wu chaotic systems via sliding mode control. *International Journal of Modelling, Identification and Control*, 22(2):170–177, 2014.

[97] Sundarapandian Vaidyanathan, Sifeu Takougang Kingni, Aceng Sambas, Mohamad Afendee Mohamed, and Mustafa Mamat. A new chaotic jerk system with three nonlinearities and synchronization via adaptive backstepping control. *International Journal of Engineering & Technology*, 7(3):1936–1943, 2018.

[98] Sundarapandian Vaidyanathan, Aceng Sambas, and Mustafa Mamat. A new chaotic system with axe-shaped equilibrium, its circuit implementation and adaptive synchronization. *Archives of Control Sciences*, 28, 2018.

[99] Sundarapandian Vaidyanathan, Leutcho Gervais Dolvis, Kengne Jacques, Chang-Hua Lien, and Aceng Sambas. A new five-dimensional four-wing hyperchaotic system with hidden attractor, its electronic circuit realisation and synchronisation via integral sliding mode control. *International Journal of Modelling, Identification and Control*, 32(1):30–45, 2019.

[100] Zhong-qing Wang and Jun Mu. A multiple interval chebyshev-gauss-lobatto collocation method for ordinary differential equations. *Numerical Mathematics: Theory, Methods and Applications*, 9(4):619–639, 2016.

[101] J.A. Weideman and S.C. Reddy. A matlab differentiation matrix suite. *ACM Transactions on Mathematical Software (TOMS)*, 26(4):465–519, 2000.

[102] Baogui Xin and Yuting Li. 0-1 test for chaos in a fractional order financial system with investment incentive. In *Abstract and Applied Analysis*, volume 2013. Hindawi, 2013.

[103] Dingyü Xue and Lu Bai. Benchmark problems for caputo fractional-order ordinary differential equations. *Fractional Calculus and Applied Analysis*, 20(5): 1305–1312, 2017.

[104] Mingzheng Yang, Bing Cai, and Guoliang Cai. Projective synchronization of a modified three-dimensional chaotic finance system. *International Journal of Nonlinear Science*, 10(1):32–38, 2010.

[105] Shuiping Yang, Aiguo Xiao, and Hong Su. Convergence of the variational iteration method for solving multi-order fractional differential equations. *Computers & Mathematics with Applications*, 60(10):2871–2879, 2010.

[106] Haojie Yu, Guoliang Cai, and Yuxiu Li. Dynamic analysis and control of a new hyperchaotic finance system. *Nonlinear Dynamics*, 67(3):2171–2182, 2012.

[107] Xiaoshan Zhao, Zhenbo Li, and Shuang Li. Synchronization of a chaotic finance system. *Applied Mathematics and Computation*, 217(13):6031–6039, 2011.

[108] Song Zheng, Gaogao Dong, and Qinsheng Bi. Adaptive modified function projective synchronization of hyperchaotic systems with unknown parameters. *Communications in Nonlinear Science and Numerical Simulation*, 15(11):3547–3556, 2010.

[109] Wuming Zhu and David A. Kopriva. A spectral element approximation to price european options. ii. the black-scholes model with two underlying assets. *Journal of Scientific Computing*, (39):323âĂŞ339, 2009.